INSIGHTS INTO ORGANIC MATTER AND REDOX CONTROLS ON WETLAND ARSENIC SPECIATION AND BIOAVAILABILITY

A Dissertation

Presented to the Faculty of the Graduate School

of Cornell University

In Partial Fulfillment of the Requirements for the Degree of

Doctor of Philosophy

by

Lena Abu-Ali

December 2022

INSIGHTS INTO ORGANIC MATTER AND REDOX CONTROLS ON WETLAND ARSENIC SPECIATION AND BIOAVAILABILITY

Lena Abu-Ali, Ph. D.

Cornell University 2022

Arsenic (As) is a toxic metalloid that occurs naturally in the Earth's crust. As is an oxyanion-forming element that exists in several inorganic and organic forms in the environment, which have different toxicities to both humans and plants. Rice paddies and wetlands are of particular interest for As contamination due to their reducing redox conditions that promote As release and mobility. Managing As in contaminated soils as well as its speciation is crucial for protecting human and environmental health. This research seeks to expand on established principles of As mobility, with a focus on the understudied and unique pore water chemical conditions of wetlands. Three research projects were designed to support the goal of exploring organic matter and redox controls on As speciation and bioavailability. The objectives of the first project were to quantify As(III) binding to dissolved organic matter (DOM), evaluate the role of organic sulfur in As(III)-DOM binding, and determine the impacts of As(III)-DOM binding to bioavailability to microorganisms. The results of this work revealed significant binding of As(III) to DOM at environmentally relevant As/dissolved organic carbon ratios, and that the organic sulfur content of DOM was highly correlated with levels of As(III)-DOM complexation. The second project evaluated a two-year field study on the effect of rice cultivars vs irrigation practices on the concentration and speciation of As in addition to the micronutrient content. Linear mixed-effects (LME) models indicated that cultivar selection

and alternate wetting and drying (AWD) are important controls on rice grain chemical composition, AWD was found to be most effective at reducing the organic As pool, and interannual variability was significant for trace elements. The final research project investigated the effect of AWD on As demethylation in soil microcosm experiments and benchtop batch reactors. Pore water concentrations of both inorganic and organic As were decreased by AWD, and the addition of nitrate correlated with a decrease in dimethyl arsenic acid (DMA). The results of these three research projects offer new insights into the complex, under-explored biogeochemical reactions controlling As fate in dynamic wetland environments, informing best practices for agriculture and remediation.

BIOGRAPHICAL SKETCH

Lena Abu-Ali was born in Nablus, Palestine in 1995. She moved to Gary, Indiana, USA at the age of 3. Following her schoolwork at Andrean High School in 2013, she entered Purdue University. Her first experience with research as an undergraduate was under the mentorship of Dr. Whelton in Environmental & Ecological Engineering. During her junior and senior years, she did research with Drs. Michael Mashtare and Linda S. Lee in the Department of Agronomy. Her interest in environmental organic chemistry and contaminant fate & transport was nurtured in graduate-level coursework at Purdue. Lena received a Bachelor of Science in Environmental & Ecological Engineering in May 2017. In August 2017, she entered the Civil & Environmental Engineering program at Cornell University.

“The Road goes ever on and on

Down from the door where it began.

Now far ahead the Road has gone,

And I must follow, if I can,

Pursuing it with eager feet,

Until it joins some larger way

Where many paths and errands meet.

And whither then? I cannot say”

— J.R.R. Tolkien

ACKNOWLEDGMENTS

First and foremost, I would like to thank my advisor and mentor Dr. Matt Reid for his academic training, thoughtful and thorough feedback on all aspects of research, and incredible patience in guiding a student who was often unsure of herself. I was far from a perfect graduate student and am grateful that Matt recognized when I needed to be given an extra push. His dedication and high standards have made me into a capable scientist, and went as far as spending several days in the 90° Arkansas heat making sure that every aspect of an experiment was just right. I am grateful to join his growing academic family.

I would like to thank my committee members Drs. Carmen Martinez and Johannes Lehmann for the insightful feedback and help throughout the candidacy process. Their criticisms and questions have strengthened my ability to think on my feet and consider the multidisciplinary aspects of my work.

Thank you to all of the collaborators that I have had the honor of working with at this early stage of my career: Drs. Jai Rohila and Anna McClung of USDA, Drs. Angelia Seyfferth and Matt Limmer of the University of Delaware, Drs. Ben Runkle and Beatriz Moreno-Garcia of the University of Arkansas, and Dr. Bruce Ravel of Brookhaven National Laboratory. The opportunity to interface with so many excellent examples of leadership has been wonderful.

Many thanks to Drs. Scott Maguffin and Phil McGuire of the Reidsearch group, who have guided me since my first day in the lab and inspired me to do my best; thank you to Hyun, Anita, Yi, Simiao, Xuhui, Zihao, Jess, Jessica, and Jenna for being great labmates and helping me whenever I needed last-minute samples run or help changing a heavy gas tank.

Thanks to the staff in Hollister who provided various support throughout my time in CEE: Beth Korson, Melissa Totman, and Tania Sharpsteen.

I would like to thank my family for always providing me with care, comfort, and a home back in Indiana: Mom, Samir, Dianna, Dimitri, and Nadia. I'll never forget checking

my phone from the middle of a rice field to hear the amazing news that my niece was born. I'm very lucky to have a family that has always believed in me.

Thank you to Dan, who has been my biggest supporter every single day of this journey, from giving me rides to and from work, to listening to all my frustrations and joys, and always encouraging me to be the best that I can be. His promise to read my entire completed dissertation was a great motivator, and his dedication and love has kept me going.

Lastly, I'd like to thank my amazing friends for keeping me sane the past five years: Hannah, Ruben, Casey, Paige, Carrie, Jingyi, Marika, Corey, and so many others. The biggest thanks goes to Spencer Moller, who I am forever grateful to have met in graduate school. Thank you for always being by my side and believing in me.

TABLE OF CONTENTS

LIST OF FIGURES

LIST OF TABLES

CHAPTER 1: Introduction

Background

Arsenic (As) is a naturally occurring metalloid and non-threshold human carcinogen listed as the number one substance on the Agency for Toxic Substance and Disease Registry's Substance Priority List for 2019. Found widespread in the Earth's crust, As is most often found as a drinking water contaminant (Rawson et al., 2016), a by-product of mining and industrial applications (Lim et al., 2009), and as a bioavailable element in crops grown in polluted soil (Schoof et al., 1999). In a bulletin to the World Health Organization, groundwater contamination by As in Bangladesh has been named the "largest mass poisoning of a population in history," exposing millions to unsafe levels of As causing long-term health effects such as skin cancer (Smith et al., 2000). Additionally, ingestion of As by way of rice, a dietary staple for billions, has been identified as a major exposure pathway that may lead to increased cancer risk (Li et al., 2011; Davis et al., 2017). Creating engineered solutions for As exposure requires a deep understanding of porewater physical, chemical, and biological processes that influence As speciation and bioavailability.

While drinking water remediation techniques have been well-studied, the interactions between As and carbon in carbon-rich wetland environments such as rice paddies are relatively under-studied yet are crucial to managing these systems for increasing regulations around As in rice products. It is well-known that As(III) forms complexes with thiol-containing functional groups in proteins and biomolecules, but interactions of As(III) with thiol moieties in natural organic matter (NOM), and how this impacts As bioavailability, are not yet well-understood. Additionally, increased attention

is being given to alternate irrigation strategies in rice paddies as a way to alleviate plant As uptake. Strategies such as alternate wetting and drying (AWD), which involve periodically draining fields that are usually continuously flooded, have proven to decrease grain As concentrations. However, considerable questions remain as to the optimal timing, duration, and frequency of these drying events. Moreover, these drying events may increase plant uptake of unfavorable elements in contaminated soils such as cadmium (Cd) and accelerate the release of potent greenhouse gases such as nitrous oxide (N_2O) (Balaine et al., 2019). Some studies show that AWD reduces total As but is less effective at reducing the concentrations of inorganic As (iAs), which are the more toxic species. Therefore, a thorough exploration of field-scale experiments is needed to effectively manage rice paddies for the most favorable outcome.

This research aims to improve our understanding of the As transformations that take place in the dynamic, carbon-rich environment of wetlands by employing experiments across physical scales: (1) laboratory-scale experiments focused on quantifying As-DOM interactions, (2) large field scale experiments testing the impact of irrigation strategy and cultivar on rice-grain As concentration and speciation, and (3) a meso-scale soil incubation study evaluating the effects of alternate irrigation strategies on porewater As speciation. Insights from molecular-scale chemistry, soil incubation studies, and full field-scale experiments will provide a characterization of the system across multiple scales. The results of this work will not only broaden our knowledge of critical porewater chemical processes but also provide relevant, immediate recommendations for agricultural management practices.

Arsenic Speciation

Arsenic (As) is a metalloid element that occurs naturally in the Earth's crust in several minerals. As has both inorganic and organic species. Environmentally, inorganic As exists in one of two forms: As(III), the reduced form, and As(V), the oxidized form. With an ionic potential of ~52 nm^{-1}, As(III) readily hydrolyzes at circumneutral pH and is most often found as $As(OH)_3$ (arsenous acid, or arsenite), due to its high pK_a values of 9.2, 12.1, and 13.4. Arsenite is relatively mobile in the soil column and has a high affinity for thiol sulfur groups, including those in proteins and enzymes, contributing to its toxicity. Particularly, arsenite is known to complex with glutathione, an important antioxidant in

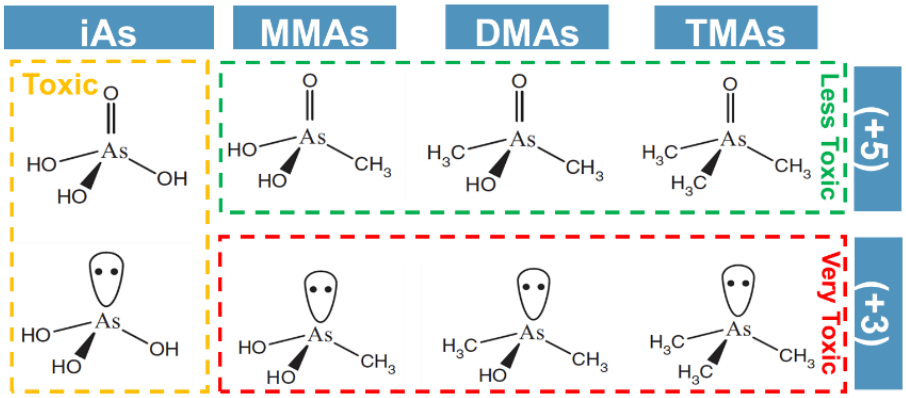

Figure 1. An overview of As species in the environment. The inorganic forms, arsenate and arsenite, are boxed in yellow. Organic arsenic exists as mono-, di-, and tri- methyl As, in either the +5 or +3 oxidation state.

cells, contributing to oxidative stress and the formation of reactive oxygen species which can cause human disease. As(V), with an ionic potential > 140 nm^{-1}, also forms oxyanions in the environment. As(V) is found most commonly as arsenate, $HAsO_4^{2-}$, or hydrogen arsenate $H2AsO_4^-$, with a structure similar to its periodic table neighbor phosphorus. The pK_as of arsenate are 2.2, 6.9, and 11.5; the negatively charged anion at circumneutral pH sorbs strongly to iron oxide phases in soil and is almost always associated with iron (Fe) and manganese (Mn) oxides. While many soil minerals, like clays, have negative surface

charges, the Fe and Mn oxides themselves are the strong soil binding sites. Arsenate may also react with reduced nitrogen groups in organic matter such as amines (Kumaresan and Riyazuddin, 2001). Transformations between arsenate and arsenite are mediated by microbial activity, by plants themselves (Xu et al., 2007), or abiotic reduction by sulfide and other reduced sulfur species. Arsenate-reducing bacteria reduce arsenate in anoxic environments. In terms of the redox ladder, arsenate reduction is less thermodynamically favorable than manganese and nitrate reduction, but more favorable than iron reduction (Phan, 2017).

Arsenic also exists in several organic forms, as mono-, di-, or tri-methyl As(III) or As(V). Oxidative microbial methylation of As is mediated by the As methyltransferase enzyme, encoded by the *arsM* gene, and has been observed in natural environments (Lomax et al., 2012). Methylation is a detoxification mechanism that allows cells to excrete As more easily in oxic conditions (Gebel, 2002). The methylated forms of As are also less toxic than the inorganic forms (Zavala et al., 2008). In anaerobic environments, the role of methylation is less clear; some hypothesize that some organisms methylate arsenic as a form of "chemical warfare" against their neighbors (Li et al., 2016a). However, the methylated forms are often not quantified and distinguished from iAs in reports and regulations related to food safety, and so are included in total As numbers (Schoof et al., 1999). Methylated arsenic species, particularly dimethylarsinic acid (DMA), are also suspected to be the cause of straighthead disorder in rice plants, a physiological disorder that causes sterility and substantially reduced yields (Rahman et al., 2008; Tang et al., 2020).

Demethylation, or the removal of one or more methyl groups from organo-arsenic compounds, is a puzzling phenomenon that has been extensively studied in soil and is an important transformation that occurs in paddy soils. Demethylation is a biological process, and several microbial pathways have been hypothesized. One group isolated a microbial community from golf course soils amended with MSMA and proposed a two-step process whereby MMA(V) is first reduced by *Burkholderia* to MMA(III) and subsequently demethylated by *Streptomyces* to the less toxic As(III) (Yoshinaga 2011). The same group later identified and cloned the gene for a As-C lyase, *arsI* (Yoshinaga 2014). ArsI is thought to be a versatile enzyme capable of demethylating MMA(III) in oxic or anoxic conditions and *arsI* genes are commonly associated with dissimilatory nitrate reductase genes (Chen 2021), presuming a coupling to denitrification. The disappearance of DMAs, on the other hand, has been observed to coincide with methane production, suggesting that methanogenic archaea are involved in demethylation (Chen 2019). Because As speciation is of such critical importance in rice products, understanding controls on microbial demethylation is key for paddy soil management.

Wetting-Drying Cycles

Rice agricultural techniques and practices are unique; in our research sites in the southern United States, fields are prepared and seeded, the allowed to stay relatively dry for several weeks as the plants grow, and then flooded with surface or irrigation water at a level several inches above the ground surface until just before harvest. Rice plants have aerenchyma which allow them to transfer oxygen from the shoot to the root area, maintaining an oxic environment around their root zone (Miro and Ismail, 2013; Yamauchi et al., 2013). Historically, flooding the fields allows for effective weed control, as many

pests do not have these unique tissues. For these reasons, continuous- or delayed-flood rice is the most common around the globe, in addition to its suitability for wet, tropical climates and areas that experience seasonal monsoons. Growing rice in drier conditions is associated with reductions in yield and is stigmatized by many traditional farmers (Lampayan et al., 2015; Carrijo et al., 2017).

Arsenic may be present in agricultural or wetland soil for a variety of reasons; it may be part of the parent rock material, a contaminant in ground water, or present as a residual from historical arsenical pesticide use, urban waste, or mining waste in contaminated areas (Smith et al., 1998; Lim et al., 2009). Under flooded conditions, the As(V) that is associated with soil minerals is released to the porewater through the reductive dissolution of Mn and Fe (oxy)hydroxides by microbial activity (Roberts et al., 2009; Reinsch et al., 2010; Rawson et al., 2016; Maguffin et al., 2020). This As(V) is subsequently quickly reduced to its mobile form, As(III), where it is taken up by phosphorus or silicon transporters from the porewater in rice root systems. As(V) is moved through phosphate channels due to its structural similarity to the P compound. The practice of Alternate Wetting and Drying (AWD) is designed to prevent this release and bioavailability of As by drying the field out during the growing season, altering the biogeochemistry of the rice paddy (Yang et al., 2004; LaHue et al., 2016; Yang et al., 2017a; SURIYAGODA et al., 2018). The introduction of oxygen into the soil column causes As(III) to oxidize to As(V), and sorb to re-oxidized Mn and Fe minerals, rendering the As unavailable for plant uptake (Wang et al., 2019).

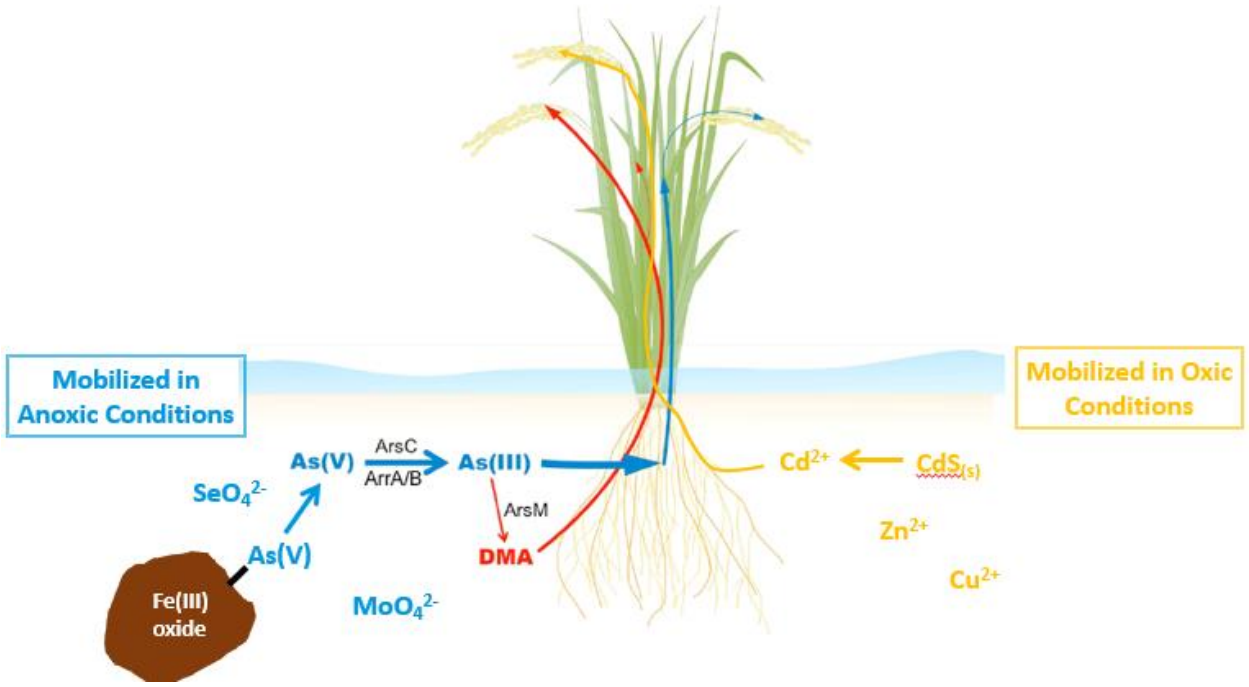

Figure 2. Redox-controlled solubility of toxic and micronutrient elements affects As uptake into grains.

Several factors are influencing alternate irrigation strategies for rice agriculture. Increased attention to As levels in rice products has caused growers to invest in strategies for grain-As reduction, with AWD touted as one solution. Additionally, AWD conserves water, which is becoming increasingly relevant as global climate change contributes to drought and water scarcity (Linquist et al., 2015). AWD also reduces methane emissions from rice paddies, which, as part of the wetlands pool, contribute significantly to the greenhouse gas effect (Yang et al., 2017b; Oo et al., 2018a). However, there are some negatives associated with AWD: while altering the porewater biogeochemistry favors As sequestration by soil minerals, it also favors the mobility and bioavailability of cadmium (Cd), another toxic contaminant that is undesirable in rice (Tsukahara et al., 2003; de Livera et al., 2011; Uraguchi and Fujiwara, 2012). Questions remain as to how AWD affects other redox-sensitive elements that are considered important nutrients such as zinc, selenium,

molybdenum, and copper, especially in regions where nutritional deficiencies are common and rice is a staple food. Decreases in yield may be observed in rice varieties that do not have much drought tolerance. Additionally, the introduction of oxygen perturbs the nitrogen cycle, leading to observed increases in the flux of nitrous oxide, a potent greenhouse gas with over 200 times the global warming potential of carbon dioxide (Johnson-Beebout et al., 2009; Oo et al., 2018b; Verhoeven et al., 2018). Moreover, one challenge with employing AWD is the lack of standard practices and guidelines. Most studies to this point have been pot studies, and more field-scale data is needed (Van Geen and Duxbury, 2009). Questions remain as to which physiological growing stage is the most critical for drydown events, how long drydown events should last, and how many drydown events should occur for optimal results (Li et al., 2019a). There are even questions as to how "dry" the soil should be for effective AWD, and achieving a target soil moisture or water level across an entirely field uniformly can be practically challenging. Lastly, the weather can interfere with AWD and prevent planned drydowns from occurring or lasting for the appropriate duration.

Arsenic-Dissolved Organic Matter Interactions

An overlooked aspect of As speciation in wetland environments is the potential for interactions with dissolved organic matter (DOM). Wetlands and rice paddies have high levels of dissolved organic carbon, often in excess of 100 mg/L DOC in pore water with varying functional groups and ligands available for binding (Kaplan et al., 2016). Much of the focus, however, is on the interactions between As and soil minerals, ignoring the DOM pool. Previous studies have quantified binding of arsenate and/or arsenite to either standard humic or fulvic acid compounds from the International Humic Substances Society (IHSS)

or commercially available humic acid salts using dialysis equilibrium techniques. Shortcomings of these studies include the exclusion of dissolved organic materials isolated from the environment, the oxic handling of DOMs which may alter redox-sensitive functional groups, and the use of environmentally-irrelevant As/DOC ratios(Hsu-Kim, 2007), all of which are important for extending laboratory findings to real-world situations. In particular, while the use of IHSS materials allows for more direct comparison between studies, the isolation methods used for these materials capture only the moderately hydrophobic fractions of DOM and the fractions that precipitate and extreme pH (Kleber and Lehmann, 2019). Observed binding has been as high as 60-80% for one particular DOM and has been modeled with conditional distribution coefficients similar to K_D and stability constants, without identification of binding mechanisms or quantification of the binding sites/ligands (Lenoble et al., 2015).

Possible binding mechanisms for As-DOM complexation differ between As species; As(V) is likely to undergo cation bridging with divalent or trivalent metals associated with DOM (Ritter et al., 2006; Lenoble et al., 2015). As(III), on the other hand, may form ethers in the presence of alcohols, undergo ligand exchange with carboxylates, or complex with thiol functional groups (Buschmann et al., 2006). As(III) is of primary concern in reducing wetland environments as it is the dominant species. Based on knowledge of how $As(OH)_3$ interacts with other chemical constituents in a biological context, some have hypothesized that thiol groups may be important for As(III)-DOM binding. For example, in biological cells, arsenic tri-glutathione forms from the nucleophilic substitution of SH^- for the OH^- groups of arsenite. Indeed, previous studies in peat environments, which are enriched in organic sulfur, have shown evidence for As(III)

sequestration (Langner et al., 2012; Stuckey et al., 2015). One study corroborated this hypothesis with As K-edge X-ray Absorption Spectroscopy data, with samples from peat mimicking an As(III)-glutathione reference material (Langner et al., 2012). Others have related peak formation within the Mekong Delta to the concentration of arsenic within sediment deposits, and found that arsenic an sulfur are co-enriched on the exteriors of peat grains (Stuckey et al., 2015). While laboratory-scale studies with isolated dissolved organic matter and As have failed to show evidence for As-S coordination, preliminary data from our lab shows exciting evidence for As-S complexation within DOM.

Dissertation Objectives

Arsenic remains a priority contaminant in wetlands, especially rice paddy environments, with a variety of strategies from soil amendments to AWD proposed as ways to reduce As bioavailability. The goal of this research is to evaluate controls on As bioavailability, from underexplored As-DOM interactions to mineralogical changes induced by alternate wetting and drying. The specific objectives of the following research chapters are:

1. *Effects of organic sulfur and arsenite/dissolved organic matter ratios on arsenite complexation with dissolved organic matter* :: The goal of this study was to quantify As(III) complexation to standard and environmentally-sourced dissolved organic matters. The key hypothesis wass that organosulfur groups, particularly thiols, control As(III) binding to DOM at low As/DOC ratios. The results of this study demonstrated that organic sulfur content was highly correlated with increased complexation of As(III) to DOM. Scatchard analyses of two selected DOMs were performed using estimated thiol concentrations as “strong” binding sites, and a

whole-cell biosensor assay revealed that DOM-bound As(III) had reduced availability to microorganisms.

2. *Both genotype and irrigation treatment affect speciation and concentration of contaminants and nutrients in rice grains* :: The objective of this study was to combine a rich porewater dataset with rice grain analysis from a field-scale experiment to determine significant effects on rice grain composition. Quantification of contaminants such as As and Cd alongside nutrients such as Mn, Zn, Se, Cu,and Mo was performed and integrated with mixed-effects linear models and ANOVA to identify trends and controls on rice grain elemental content. Results show that both genotype (rice variety) and phenotype (alternate wetting and drying strategies) significantly affect rice grain quality. For some but not all elements, porewater concentrations were significant predictors of final rice grain content.
3. *Alternate wetting and drying changes As speciation in the rhizosphere when compared to conventional delayed flood treatment* :: This study builds on observations made in the previous chapter. The goal of this study was to quantify changes in As porewater speciation across variable redox conditions, which is thought to influence final As speciation in rice grains. Batch reactors with a soil mixture as well as soil microcosms were constructed to monitor As speciation along the AWD redox gradient.

Together, the chapters of this dissertation seek to provide valuable insights into controls on As speciation and bioavailability in wetland environments. These hypothesis-driven research projects at the laboratory, meso, and field scale will advance our knowledge of As

mass balances and speciation in wetland systems, informing agricultural practices to protect human health.

REFERENCES FOR CHAPTER 1

(1) Rawson, J.; Prommer, H.; Siade, A.; Carr, J.; Berg, M.; Davis, J. A.; Fendorf, S. *Environ. Sci. Technol.* 2016, 50 (5), 2459–2467.

(2) Lim, M.; Han, G. C.; Ahn, J. W.; You, K. S.; Kim, H. S. *Int. J. Environ. Res. Public Health* 2009, 6 (11), 2865–2879.

(3) Schoof, R. A.; Yost, L. J.; Eickhoff, J.; Crecelius, E. A.; Cragin, D. W.; Meacher, D. M.; Menzel, D. B. *Food Chem. Toxicol.* 1999, 37 (8), 839–846.

(4) Smith, A.; Lingas, E.; Rahman, M. *Bull. World Health Organ*. 2000, 78 (9), 1093–1103.

(5) Li, G.; Sun, G. X.; Williams, P. N.; Nunes, L.; Zhu, Y. G. *Environ. Int.* 2011, 37 (7), 1219–1225.

(6) Davis, M. A.; Signes-Pastor, A. J.; Argos, M.; Slaughter, F.; Pendergrast, C.; Punshon, T.; Gossai, A.; Ahsan, H.; Karagas, M. R. *Sci. Total Environ.* 2017, 586, 1237–1244.

(7) Balaine, N.; Carrijo, D. R.; Adviento-Borbe, M. A.; Linquist, B. *Soil Sci. Soc. Am. J*. 2019, 83 (5), 1533–1541.

(8) Kumaresan, M.; Riyazuddin, P. Curr. *Sci.* 2001, 80 (7).

(9) Xu, X. Y.; McGrath, S. P.; Zhao, F. *J. New Phytol.* 2007, 176 (3), 590–599.

(10) Phan, T. H. Van. 2017.

(11) Lomax, C.; Liu, W. J.; Wu, L.; Xue, K.; Xiong, J.; Zhou, J.; McGrath, S. P.; Meharg, A. A.; Miller, A. J.; Zhao, F. *J. New Phytol.* 2012, 193 (3), 665–672.

(12) Gebel, T. W. Int. J. Hyg. *Environ. Health* 2002, 205 (6), 505–508.

(13) Zavala, Y. J.; Gerads, R.; Gürleyük, H.; Duxbury, J. M. *Environ. Sci. Technol.* 2008, 42 (10), 3861–3866.

(14) Li, J.; Pawitwar, S. S.; Rosen, B. P. *Metallomics* 2016, 8 (10), 1047–1055.

(15) Rahman, M. A.; Hasegawa, H.; Rahman, M. M.; Miah, M. A. M.; Tasmin, A. *Environ. Exp. Bot.* 2008, 62 (1), 54–59.

(16) Tang, Z.; Wang, Y.; Gao, A.; Ji, Y.; Yang, B.; Wang, P.; Tang, Z.; Zhao, F. J. J. *Exp. Bot.* 2020, 71 (18), 5631–5644.

(17) Miro, B.; Ismail, A. M. *Front. Plant Sci*. 2013, 4 (JUL), 1–18.

(18) Yamauchi, T.; Shimamura, S.; Nakazono, M.; Mochizuki, T. F. *Crop. Res.* 2013, 152, 8–16.

(19) Lampayan, R. M.; Rejesus, R. M.; Singleton, G. R.; Bouman, B. A. M. F. *Crop. Res.* 2015, 170, 95–108.

(20) Carrijo, D. R.; Lundy, M. E.; Linquist, B. A. F. *Crop. Res.* 2017, 203, 173–180.

(21) Smith, E.; Naidu, R.; Alston, A. M. *Adv. in Agron.* 1998, *64*.

(22) Maguffin, S. C.; Abu-Ali, L.; Tappero, R. V.; Pena, J.; Rohila, J. S.; McClung, A. M.; Reid, M. C. *Geochim. Cosmochim. Acta* 2020, 276, 50–69.

(23) Reinsch, B. C.; Lowry, G. V; Erbs, J. J.; Berquo, T. S.; Banerjee, S. K.; Penn, R. L. *Geochim. Cosmochim. Acta* 2010, 74, 3382–3395.

(24) Roberts, L. C.; Hug, S. J.; Dittmar, J.; Voegelin, A.; Kretzschmar, R.; Wehrli, B.; Cirpka, O. A.; Saha, G. C.; Ali, M. A.; Badruzzaman, A. B. M. *Nat. Geosci.* 2009, 3 (1), 53–59.

(25) Suriyagoda, L. D. B.; Dittert, K.; Lambers, H. *Pedosphere* 2018, 28 (3), 363–382.

(26) Yang, J.; Zhou, Q.; Zhang, J. *Crop J*. 2017, 5 (2), 151–158.

(27) Yang, C.; Yang, L.; Yang, Y.; Ouyang, Z. *Agric. Water Manag.* 2004, 70 (1), 67–81.

(28) LaHue, G. T.; Chaney, R. L.; Adviento-Borbe, M. A.; Linquist, B. A. *Agric. Ecosyst. Environ.* 2016, 229, 30–39.

(29) Wang, X.; Yu, H. Y.; Li, F.; Liu, T.; Wu, W.; Liu, C.; Liu, C.; Zhang, X. *Sci. Total Environ.* 2019, 649, 535–543.

(30) Linquist, B. A.; Anders, M. M.; Adviento-Borbe, M. A. A.; Chaney, R. L.; Nalley, L. L.; da Rosa, E. F. F.; van Kessel, C. *Glob. Chang. Biol.* 2015, 21 (1), 407–417.

(31) Oo, A. Z.; Sudo, S.; Inubushi, K.; Mano, M.; Yamamoto, A.; Ono, K.; Osawa, T.; Hayashida, S.; Patra, P. K.; Terao, Y.; Elayakumar, P.; Vanitha, K.; Umamageswari, C.; Jothimani, P.; Ravi, V. *Agric. Ecosyst. Environ.* 2018, 252 (October 2017), 148–158.

(32) Yang, J.; Zhou, Q.; Zhang, J. Crop J. 2017, 5 (2), 151–158.

(33) Tsukahara, T.; Ezaki, T.; Moriguchi, J.; Furuki, K.; Shimbo, S.; Matsuda-Inoguchi, N.; Ikeda, M. *Sci. Total Environ.* 2003, 305 (1–3), 41–51.

(34) Uraguchi, S.; Fujiwara, T. *Rice* 2012, 5 (1), 1–8.

(35) de Livera, J.; McLaughlin, M. J.; Hettiarachchi, G. M.; Kirby, J. K.; Beak, D. G. *Sci. Total Environ*. 2011, 409 (8), 1489–1497.

(36) Johnson-Beebout, S. E.; Angeles, O. R.; Alberto, M. C. R.; Buresh, R. J. *Geoderma* 2009, 149 (1–2), 45–53.

(37) Oo, A. Z.; Sudo, S.; Inubushi, K.; Mano, M.; Yamamoto, A.; Ono, K.; Osawa, T.; Hayashida, S.; Patra, P. K.; Terao, Y.; Elayakumar, P.; Vanitha, K.; Umamageswari, C.; Jothimani, P.; Ravi, V. *Agric. Ecosyst. Environ.* 2018, 252 (October 2017), 148–158.

(38) Verhoeven, E.; Decock, C.; Barthel, M.; Bertora, C.; Sacco, D.; Romani, M.; Sleutel, S.; Six, J. *Soil Biol. Biochem.* 2018, 120 (September 2017), 58–69.

(39) Van Geen, A.; Duxbury, J. M. *Environ. Sci. Technol.* 2009, 43 (10), 3971.

(40) Li, C.; Carrijo, D. R.; Nakayama, Y.; Linquist, B. A.; Green, P. G.; Parikh, S. J. *Agric. Ecosyst. Environ. 2019*, 272 (November 2018), 188–198.

(41) Kaplan, D. I.; Xu, C.; Huang, S.; Lin, Y.; Tolić, N.; Roscioli-Johnson, K. M.; Santschi, P. H.; Jaffé, P. R. *Environ. Sci. Technol.* 2016, 50 (8), 4169–4177.

(42) Hsu-Kim, H. *Environ. Sci. Technol*. 2007, 41 (7), 2338–2342.

(43) Kleber, M.; Lehmann, J. *J. Environ. Qual*. 2019, 48 (2), 207–216.

(44) Lenoble, V.; Dang, D. H.; Loustau Cazalet, M.; Mounier, S.; Pfeifer, H. R.; Garnier, C. *Talanta* 2015.

(45) Ritter, K.; Aiken, G. R.; Ranville, J. F.; Bauer, M.; Macalady, D. L. *Environ. Sci. Technol.* 2006, 40 (17), 5380–5387.

(46) Buschmann, J.; Kappeler, A.; Lindauer, U.; Kistler, D.; Berg, M.; Sigg, L. *Environ. Sci. Technol.* 2006, 40 (19), 6015–6020.

(47) Stuckey, J. W.; Schaefer, M. V.; Kocar, B. D.; Dittmar, J.; Pacheco, J. L.; Benner, S. G.; Fendorf, S. *Geochim. Cosmochim. Acta* 2015, 149, 190–205.

(48) Langner, P.; Mikutta, C.; Kretzschmar, R. *Nat. Geosci.* 2012, 5 (November 2011).

CHAPTER 2: Arsenite binding to dissolved organic matter (DOM) impacts arsenic bioavailability: The role of organosulfur groups

Adapted from: Lena Abu-Ali, Hyun Yoon, and Matthew C. Reid, Published in *Chemosphere*, April 2022.

The speciation and fate of arsenic (As) in soil-water systems is a topic of great interest, in part due to growing awareness of As uptake into rice as an important human exposure pathway to As. Rice paddy and other wetland soils are rich in dissolved organic matter (DOM), leading to As/DOM ratios that are typically lower than those in groundwater aquifers or that have been used in many laboratory studies of As-DOM interactions. In this contribution, we evaluate arsenite (As(III)) binding to seven different DOM samples at As/DOM ratios relevant for wetland pore waters, and explore the chemical properties of the DOM samples associated with high levels of As(III)-DOM complexation. We integrate data from wet chemical analysis of DOM chemical properties, dialysis equilibrium experiments, and two-site ligand binding models to show that in some DOM samples, 15-60% of As(III) can be bound to DOM at environmentally-relevant As/DOM ratios of 0.0032 to 0.016 μmol As/mmol C. Binding decreases as the As(III)/DOM ratio increases. The organic sulfur (S_{org}) content of the DOM samples was strongly correlated with levels of As(III)-DOM complexation and "strong" binding site densities, consistent with theories that thiols are strong binding ligands for As(III) in natural organic matter. Finally, a whole-cell *E. coli* biosensor assay was used to show that DOM samples most effective at complexing As(III) also led to decreased microbial As(III) uptake at low As/DOC ratios. This work demonstrates that naturally-occurring variations

in the S_{org} content of DOM has a significant impact on As(III) binding to DOM, and has implications for As(III) availability to microorganisms.

Introduction

Arsenic (As) is an environmental contaminant and human carcinogen of global importance (Smedley and Kinniburgh, 2002; Jomova et al., 2011). There is growing interest in the speciation and fate of As in rice paddy soils, since rice consumption is an important pathway for human exposure to As (Zhao et al., 2009; Li et al., 2011). The biogeochemical processes regulating the mobilization of As from mineral surfaces in anaerobic subsurface environments are relatively well-understood (Fendorf et al., 2010), but many of the biogeochemical controls on As speciation in reducing pore waters are less well understood. There are notable knowledge gaps around methylation-demethylation reactions (Reid et al., 2017; Chen et al., 2019; Viacava et al., 2022), formation of thioarsenic species (Wang et al., 2020), and As complexation with dissolved organic matter (DOM) (Buschmann et al., 2006; Hoffmann et al., 2012; Ren et al., 2017). The role of DOM may be particularly important in rice paddies and other wetland environments because, in contrast to many surface and groundwaters, these systems are rich in DOM, with dissolved organic carbon (DOC) concentrations frequently exceeding 100 mg C/L (Maguffin et al., 2020; Aftabtalab et al., 2021).

There is a lack of consensus around binding mechanisms between As and DOM, particularly for trivalent arsenite (As(III)) that is considered the predominant inorganic As species in reducing systems. Arsenate (As(V)) is anionic at environmentally relevant pH, and is known to form ternary complexes with DOM through cation bridging reactions with Ca or Fe(III) species (Bauer and Blodau, 2009; Sharma et al., 2011; Langner et al., 2012;

Lenoble et al., 2015; Yao et al., 2020; Aftabtalab et al., 2021). Cation bridging mechanisms have also been shown to influence DOM complexation of As(III) (Liu et al., 2011), which is neutral in most wetland pore waters, but cation bridging is thought to be less significant for As(III) than with As(V) (Warwick et al., 2005). Modeling of As(III)-DOM complexation data indicates the presence of both "strong" and "weak" binding sites for As(III) in humic acids (Liu and Cai, 2013; Fakour and Lin, 2014), though the identity of the "strong" binding sites has been disputed. Buschmann et al. (2006) and Lenoble et al. (2015) postulate a role for ligand exchange reactions between As(III) and oxygen-containing functionalities (e.g., carboxylate and phenolic moieties), and there is spectroscopic evidence for these ligand exchange reactions with a peat natural organic matter (Hoffmann et al., 2013; Eberle et al., 2020). Thiol functional groups (R-SH) have also recently been shown to act as important binding sites controlling As(III) complexation with natural organic matter (Hoffmann et al., 2012; Langner et al., 2012, 2013; Catrouillet et al., 2015a; Eberle et al., 2020). As(III), like other "soft" metal(loid)s, has a high affinity for reduced organic sulfur (S_{org}) moieties (Reid et al., 2017) and is known to bind to thiol groups in proteins, to model thiol compounds like glutathione (Spuches et al., 2005), and thiol functionalities in phytochelatins, which is how plants sequester As(III) in roots and stems (Buschmann et al., 2006; Chen et al., 2019; Wang et al., 2020; Viacava et al., 2022). Many questions remain regarding the role of DOM-associated thiols in mediating aqueous complexation reactions between As(III) and DOM, including conditional stability constants and implications for As bioavailability. Arsenic uptake into bacterial cells is a prerequisite for many microbe-mediated transformations of As like methylation-demethylation reactions and production of volatile arsines (Slyemi and Bonnefoy, 2012;

Zhang and Reid, 2021), so effects of extracellular water chemistry on As(III) bioavailability may be an important control on As biotransformation in the environment (Zhu et al., 2014).

The significance of As(III) binding to DOM in environmental waters is also unclear. Early work on this topic has shown that the fraction of As(III) bound to DOM will depend on both the As/DOC ratio and the composition of the DOM, both of which vary widely in the environment. A number of studies have used laboratory experiments with purified humic acids (HAs) to conclude that As(III) binding to DOM is of minor importance at the As/DOC ratios examined in their studies. However, other studies employing freshly-collected environmental DOM samples have concluded that a significant fraction of As(III) can be bound to DOM. For example, in a groundwater sample with an As/DOC ratio of 1.2 μmol As/mmol C more than 50% of the As was determined to be complexed with DOM. A recent review of As-DOM interactions in soils shows that an As/DOC ratio of 1.2 μmol As/mmol C is relatively high for soil-water systems, with roughly half of the surveyed samples characterized by As/DOC ratios < 0.1 μmol As/mmol C, presumably leading to greater levels of complexation (Table S1). As/DOC ratios observed in a recent study of Arkansas rice paddy pore waters were also lower than values used in many prior laboratory studies, with a median and mean As/DOC ratio of 0.017 and 0.041 μmol As/mmol C, respectively (Figure S1).

The objectives of this study are: (1) Quantify As(III) binding to DOM with different compositions, using As/DOC ratios that are relevant for rice paddies and other DOM-rich soil-water environments; (2) Evaluate the role of the S_{org} content of DOM in As(III) binding to DOM; and (3) Determine the impacts of DOM-As(III) complexation on As

bioavailability, using a whole-cell biosensor fluorescence method. We focused on As(III) because it is thought to be the dominant inorganic As species in reducing environments, and because mechanisms for As(III)-DOM binding are not clear. We hypothesized that the S_{org} content of the DOM will be associated with higher As(III)-DOM binding, particularly at low As/DOC ratios, due to the role of thiol ligands as binding sites for As(III). Greater As(III)-DOM complexation was also expected to decrease microbial uptake, since As bound to DOM molecules is thought to be less bioavailable for uptake through membrane transport channels.

Materials and Methods

DOM Preparation

Suwannee River Humic Acid III (SRHA), Upper Mississippi River Natural Organic Matter (MNOM), and Suwannee River Natural Organic Matter (SRNOM) were purchased from the International Humic Substances Society (IHSS). MNOM and SRNOM were isolated using reverse osmosis, while SRHA was isolated using solid-phase extraction with an XAD-8 resin that adsorbs hydrophobic fractions of the aqueous sample. IHSS materials were dissolved in anoxic Milli-Q water to achieve a final concentration of at least 200 mg C/L. The solution was then vacuum-filtered using a sterile 0.22 µm membrane filter (Corning), wrapped in aluminum foil, and stored in a gas-tight container at 4 °C.

DOM was also extracted from soils and other environmental media. Arkansas soil was collected from the upper 20 cm of rice paddy soil from the Dale Bumpers National Rice Research Center in Stuttgart, AR. This soil was air-dried prior to DOM extraction. Beebe Lake sediment was collected from the upper 20 cm of the shallow shores of Beebe Lake in Ithaca, NY, and immediately transferred to heat-sealed N_2-filled mylar bags.

Sapsucker Woods (SW-1) soil was collected from a *Typha latifolia* dominated wetland in Ithaca, NY, and immediately transferred to a heat-sealed N_2-filled mylar bag. Pine needles and woodchips (PW) were collected from pine trees in Central NY. Solid material was mixed with a 0.05 M KCl solution at a solid:liquid mass ratio of 1:2 and agitated in a gas-tight container on an orbital shaker for 48 h with periodic sonication. The slurry was vacuum filtered using a sterile 0.22 µm membrane filter (Corning) inside an anaerobic chamber. Filtered solutions were stored in gas-tight containers at 4 °C until use. All DOM preparation was performed inside a Coy anaerobic chamber with < 10 ppm O_2 to protect the speciation of the functional groups within the DOM as well as the As(III).

Chemical Characterization of DOM Samples

Dissolved organic carbon was measured via the NPOC method with a Shimadzu TOC-L analyzer. Total sulfur (S_{Tot}) was measured via an Agilent 8900 Triple Quadrupole ICP-MS. The anionic inorganic sulfur (S) species sulfate, sulfite, and thiosulfate were analyzed via anion exchange chromatography, while Ca^{2+} was measured using cation exchange chromatography (Dionex ICS-2100). Sulfide was determined using the Cline method. 4 mL of filtered anoxic sample was preserved by addition of 1 mL of 0.05 M zinc acetate. A 1 mL aliquot of this preserved sample was added to 80 µL of Cline reagent (N,N-dimethyl-p-phenylenediamine sulfate, $FeCl_3 \cdot 6H_2O$, in 50% HCl), shaken, and incubated for 30 minutes in the dark. The absorbance at 664 nm was measured and compared to an Na_2S calibration curve for sulfide determination. To quantify the potential presence of elemental sulfur or polysulfides, the Cline method was performed before and after reducing samples with dithiothreitol (DTT). The ferrozine method was used for determination of

Fe(II). Samples for minor and trace element analysis (As, Al, Fe, Zn) were preserved in 2% trace metal grade nitric acid and measured via ICP-MS (Agilent 7800) with a helium reaction cell and rhodium as an in-line internal standard. Potential polyatomic interference from ArCl at *m/z* = 75 was assessed by testing samples diluted in 2% trace metal grade HCl, and none was detected. Calibration standards were prepared using a traceable multi-element standard.

X-ray Absorption Spectroscopy

To investigate mechanisms of As-DOM binding, synchrotron techniques were used. A solution of 3000 mg/L Aldrich Humic Acid was reacted with a 25 µg/L As(III) solution in a centrifuge tube for 48 h. The resulting solution was freeze-dried and analyzed for As XANES and EXAFS at NSLS-II. Reference standards of As(III), As(III)-glutathione, MMA, DMA, and As(V) were scanned as solutions dried on filter paper or kimwipes wrapped in Kapton tape and used to determine the composition of unknown samples. XANES spectra were imported into Athena and linear combination fitting was used to fit reference spectra and examine transformed data in k-space and R-space.

Dialysis Equilibrium Experiments

Dialysis equilibrium experiments were to quantify the binding of As(III) to DOM. All steps of the dialysis experiments were performed inside an anaerobic chamber. A 7 mL solution of As(III) and DOM at three different As/DOC ratios (0.0032, 0.016, 0.16 µmol As/mmol C; fixed DOC with varying As) were pre-equilibrated inside aluminum foil-wrapped centrifuge tubes for 24 h by mixing on a tube rotator. A subset of these

samples were collected for HPLC analysis, and in these samples there was no evidence of oxidation of As(III) to As(V). After this pre-equilibration period, a 2 mL aliquot of the solution was collected for initial characterization of the As(III)-DOM solution. The remaining 5 mL of the As(III)-DOM solution were then transferred to a Float-A-Lyzer dialysis device (Spectra-Por) with a pore size of 0.1-0.5 kDa. The smallest available pore size range was selected to ensure that As bound to low molecular weight organic molecules would be retained inside the tubing, while unbound As(III) could diffuse through the membrane. The dialysis tubing was placed in 500 mL of As-free bulk solution (0.05 M KCl, 0.15 mM sodium azide, 1 mM bicarbonate buffer, pH 7) in 500 mL opaque HDPE containers at a room temperature of 22°C. Preliminary experiments showed no sorption of As or DOC to HDPE containers, stir bars, or dialysis devices. Dialysis devices were found to leach significant amounts of DOC; this was remedied by soaking devices in 20% ethanol for at least 24 hours before experiments and rinsing thoroughly with DI water. The bulk solution and dialysis devices were stirred on a magnetic plate for 48 h to allow for diffusion of unbound As across the membrane. At the end of the equilibration time, solutions inside and outside the dialysis tubing device were sampled, filtered through 0.22 µm syringe membrane filters, and analyzed for As via ICP-MS.

Concentrations of bound and free As were determined by performing a mass balance on As in the dialysis tubing at t=0 and t=48 h, since free As concentrations in the bulk solution were sometimes below the limit of quantification. Free As concentrations in the bulk solution at t=48 h, $C_{bulk,t=48}$, were estimated using the equation:

$$C_{bulk,t=48} = \frac{C_{tubing,t=0}V_{tubing} - C_{tubing,t=48}V_{tubing}}{V_{bulk}} \qquad \text{(Eqn. 1)}$$

Where $C_{tubing,t=0}$ and $C_{tubing,t=48}$ are the As concentration measured in the dialysis tubing at t=0 and t=48, respectively [mol L^{-1}], V_{tubing} is the volume of solution inside the dialysis tubing (5 ml), and V_{bulk} is the bulk solution volume (500 ml). The percentage of As bound to DOM was then determined using the equation:

$$\%bound = \frac{(C_{tubing,t=48} - C_{bulk,t=48})V_{tubing}}{(C_{tubing,t=0}V_{tubing,t=0})} \times 100 \qquad \text{(Eqn. 2)}$$

Note that in this calculation the system boundaries are defined as the dialysis tubing and bulk solution, so As bound to DOM is expressed as a percentage of the total As in the system, inclusive of the dialysis tubing and the bulk solution.

Scatchard Plot Analysis

Concentrations of free and bound As determined from dialysis equilibrium experiments were used in a graphical Scatchard plot analysis to estimate binding site densities and conditional stability constants for a subset of DOM samples (Liu and Cai, 2010, 2013). The general equation for the Scatchard equation with *i* binding sites is (Brezonik and Arnold, 2011; Attie and Raines, 2017):

$$[As]_{bound} = \sum_{i=1}^{n} \frac{B_{max,i}[As]_{free}}{\frac{1}{K_{s,i}} + [As]_{free}} \qquad \text{(Eqn. 3)}$$

$[As]_{bound}$ and $[As]_{free}$ are the bound and free As concentrations [mol L^{-1}], respectively, $B_{max,i}$ is the total concentration of binding site *i* [mol L^{-1}], and $K_{s,i}$ is the conditional stability constant for binding site *i* [L mol^{-1}]. Previous modeling of As(III) binding to heterogeneous DOM using Scatchard analysis has shown that DOM can be simplified as having n = 2 independent binding sites, a "strong" and "weak" binding site (Liu and Cai, 2013). For the case of n = 2, eqn. 4 has four parameters: $B_{max,ss}$, $B_{max,ws}$, $K_{s,ss}$, and $K_{s,ws}$, where the ss and ws subscripts refer to strong and weak sites, respectively. To estimate these parameters,

$[As]_{bound}/[As]_{free}$ is plotted against $[As]_{bound}$. Methods for estimating the parameters from this graphical approach are described in Brezonik and Arnold (2011) and are illustrated in Figure S2.

E. coli Biosensor Assay

A whole cell fluorescent biosensor method (Stocker et al., 2003; Pothier et al., 2018) was used to determine the microbial uptake of As(III) in the presence of select DOM samples. The principle for the biosensor is that binding of intracellular As(III) to the ArsR As(III)-responsive transcriptional repressor allows for the expression of the fluorescent *mCherry* gene (Stocker et al., 2003), leading to greater fluorescence when intracellular As concentrations are greater. The construction and implementation of this biosensor has been described previously (Pothier et al., 2018, 2020). The biosensor was thawed and plated onto an LB plate containing 120 μg/mL ampicillin, which was incubated overnight at 37 °C. Experiments were performed with biological quadruplicates, with four independent colonies inoculated into different autoclaved narrow mouthed Pyrex® 125-mL flasks containing 100 mL of growth media at pH 7. A complete description of the growth media is available in supporting information (SI). Culture flasks were incubated on an orbital shaker at 37 °C at 200 rpm until OD600 reached ~1.0.

For the As(III) exposure experiments, As(III) was pre-incubated with MNOM and SRHA for 2-3 h inside an anaerobic chamber at the same As(III)/DOC ratios tested in the dialysis equilibrium experiment: 0.0032, 0.016, 0.16 μmol As/mmol C. Unlike the dialysis experiments, it was necessary to fix the As(III) concentration since the biosensor response is highly sensitive to As(III) concentrations, so in order to evaluate differences across different As/DOC ratios it was necessary to maintain a constant As concentration. The

biosensor was then exposed to the As(III)-DOM solution and fluorescence intensities (RFU) and optical density at 600 nm (OD600) were measured with an Infinite 200 fluorescence plate reader (Tecan, Research Triangle Park, NC) for 20 h. The excitation wavelength was 560 nm and fluorescence was measured at 620 nm. Endpoint fluorescence normalized by OD600 at 20 h was used to evaluate differences between microbial uptake of As across different DOM samples and As/DOC ratios. A one-way ANOVA with a Tukey's post hoc test using R were used to assess data, and differences between assays of different conditions were considered significant when $p<0.05$.

Results

DOM Characterization

A summary of the composition of the DOM samples examined in this study is in Table 1. The molar S_{org} to DOC ratios in the IHSS samples and environmental extracts were determined as the difference between S_{Tot} and the sum of the inorganic S species, normalized by the DOC concentration:

$$\frac{[S_{org}]}{[DOC]} = \frac{[S_{Tot}]-([SO_4^{2-}]+[SO_3^{-}]+2[S_2O_3^{2-}]+[S^{2-}])}{[DOC]} \qquad \text{(Eqn. 4)}$$

Quantities in brackets represent molar concentrations. Because SO_4^{2-} was detected in the IHSS samples, the S_{org}/DOC reported for these samples differs somewhat from the elemental ratios reported for these samples by IHSS. Molar S_{org}/DOC ratios ranged from $9.6\text{x}10^{-4}$ for SRHA to $6.38\text{x}10^{-3}$ for MNOM. Fe and Al, which may play a role in ternary complexation reactions, ranged from $1.5\text{x}10^{-4}$ to $1.6\text{x}10^{-2}$ mmol Fe/mmol C and $1.3\text{x}10^{-5}$ to $1.14\text{x}10^{-3}$ mmol Al/mmol C, respectively. SW-1, which was extracted from a reducing wetland soil, had a particularly high Fe

Table 1: Summary of DOM Chemical Properties

NA = Not Applicable; †Based on Elemental Concentrations reported by IHSS; ◊Determined using Eqn. 4

DOM	Source	DOC (mM)	S_{Tot}/C nmol S/mmol C)	S_{Tot}/C from IHSS† (mmol S/mmol C)	S_{org}/C◊ (mmol S/mmol C)	Fe/C (mmol Fe/mmol C)	Al/C (mmol Al/mmol C)	$SUVA_{254}$ (L/mg C * cm)
SRHA	IHSS	31.3	$1.44x10^{-3}$	$3.78x10^{-3}$	$9.60x10^{-4}$	$7.84x10^{-4}$	$1.14x10^{-3}$	0.021
MNOM	IHSS	20.8	$2.17x10^{-2}$	$1.97x10^{-2}$	$6.38x10^{-3}$	$3.42x10^{-4}$	$1.44x10^{-4}$	0.077
SRNOM	IHSS	18.3	$1.46x10^{-2}$	$1.32x10^{-2}$	$2.56x10^{-3}$	$6.90x10^{-4}$	$8.27x10^{-4}$	NA
Arkansas	Environmental extract	5.0	$2.70x10^{-2}$	NA	$4.00x10^{-4}$	$1.72x10^{-4}$	$1.28x10^{-4}$	NA
Beebe	Environmental extract	17.9	$3.35x10^{-4}$	NA	$3.35x10^{-4}$	$1.03x10^{-3}$	$1.32x10^{-5}$	NA
PW	Environmental extract	58.3	$8.13x10^{-3}$	NA	$3.72x10^{-3}$	$1.51x10^{-4}$	$2.71x10^{-4}$	0.0036
SW-1	Environmental extract	15.0	$1.07x10^{-3}$	NA	$1.07x10^{-3}$	$1.59x10^{-2}$	$7.92x10^{-5}$	0.003

concentration. 12% of the total Fe was determined to be Fe(II) using the ferrozine assay, indicating that most of the Fe was Fe(III) complexed with DOM or in colloidal Fe(III) oxyhydroxide phases. None of the samples contained sulfide above the lower limit of quantification (1 µM) and the DTT reduction method showed no evidence of elemental sulfur or polysulfides in any sample. All DOMs had negligible As concentrations.

As(III)-DOM Binding in Dialysis Equilibrium Experiments

The percentage of As bound to DOM was determined using Equation 2. The percentage of bound As ranged from close to 0 to more than 60 percent, with mostly good agreement between duplicates. With the exception of SW-1, all DOMs showed decreasing

binding with increasing As/DOC ratio (Figure 1), in agreement with previous studies (Buschmann et al., 2006; Liu and Cai, 2010) and a conceptual model in which binding is controlled by a finite number of binding sites. Among the IHSS samples, MNOM had the highest binding, with roughly 62% of the As bound at the 0.0032 µmol As/mmol C ratio, followed by SRNOM and SRHA. Roughly 18% of the As was bound to SRHA at the 0.0032 µmol As/mmol C ratio. The percentage of As bound by the Arkansas, Beebe Lake, and PW DOMs was between 25% and 35% at the 0.0032 µmol As/mmol C ratio. At the highest As/DOC ratio of 0.16 µmol As/mmol C, the percentage binding had decreased to < 10% for all DOMs except SW-1. MNOM also had the highest percentage of bound As at this ratio, with 6% of the As bound. The SW-1 DOM stands out as the only DOM to show only a slight decrease in binding from the 0.0032 to 0.16 µmol As/mmol C ratio, and a relatively high percentage of As bound (55%) at the highest As/DOC ratio.

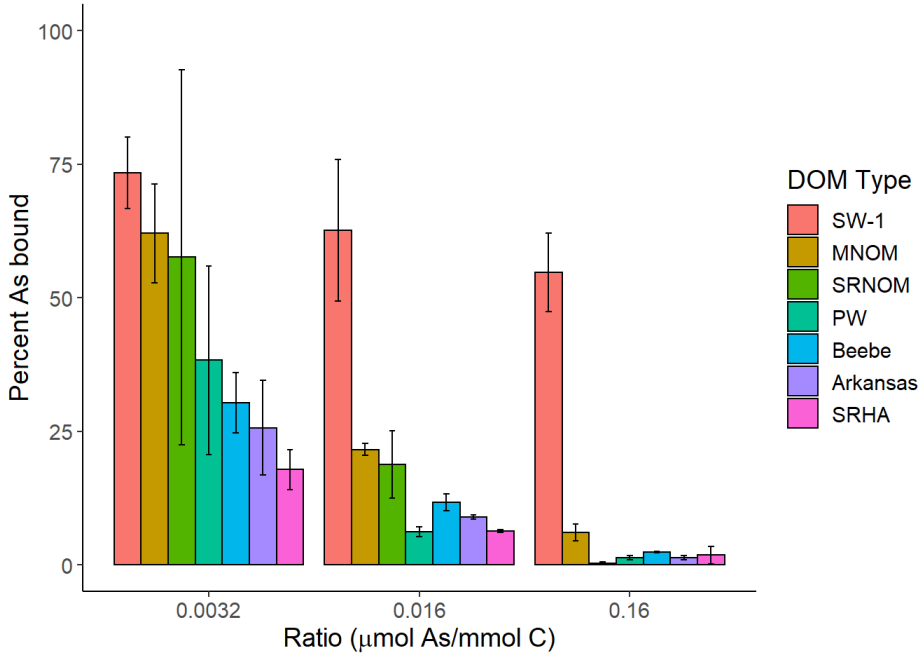

Figure 3: The percentage of As(III) bound to different DOM samples at three different As/DOC ratios. Bars show the mean of duplicate experiments and error bars show the range of the duplicates.

Relationships between As(III)-DOM Binding and DOM Characteristics

A correlation matrix of the DOM chemical properties with the percentage of bound As showed that the S_{org}/DOC ratio was significantly correlated with As-DOM binding ($p<0.001$) (Figure 4). MNOM has the highest S_{org}/DOC ratio and the second highest level of As binding across all As/DOC ratios, behind the Fe(III)-rich SW-1. SRHA, Beebe Lake, and Arkansas DOMs have the lowest S_{org}/DOC ratios and consistently show the lowest levels of bound As. While SW-1 had a high Fe/DOC ratio and a high level of binding across all three As/DOC ratios, there was no relationship between As-DOM binding and the Fe/DOC ratio with the other DOMs.

Further exploration of the data with a principal component analysis (PCA) biplot reveals similar relationships between DOM chemical characteristics and As binding percentages (Figure S3). SW-1 was excluded from the PCA analysis. The percentage of As bound is strongly correlated with the S_{org}/DOC ratio. MNOM, SRNOM, and PW, the three DOM samples with the greatest level of As binding besides SW-1, cluster together in the southeast quadrant. Concentrations of cationic elements (i.e., molar ratios of Fe, Al, Ca, Mg, and Zn to DOC) were not correlated with As binding levels. This is notable since cationic species of Ca and Fe have been linked to DOM complexation with As(V) (Lenoble et al., 2015) and, to a somewhat lesser extent, As(III) (Hoffmann et al., 2013), but here there was no evidence for these cationic species having a large impact on As(III)-DOM binding.

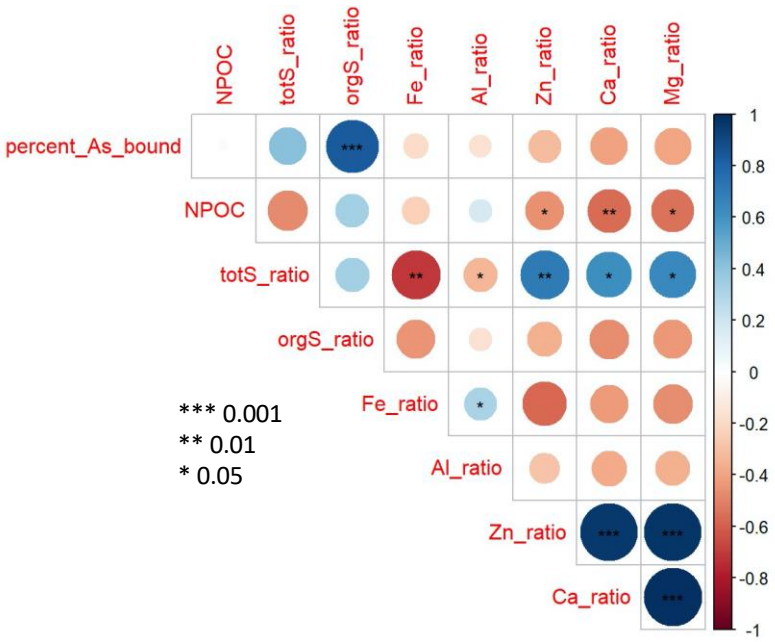

Figure 4: Correlation matrix of macroscopic chemical properties of DOM samples with the percentage of As(III) bound to DOM samples. Ratios refer to the ratio of the analyte concentration to the DOC concentration (e.g., "orgS_ratio" is S_{org}/DOC). The color bar shows the Pearson correlation coefficient, the area of the circle represents the absolute value of the corresponding correlation coefficient, and the significance level is indicated by the number of asterisks.

X-ray Absorption Spectroscopy

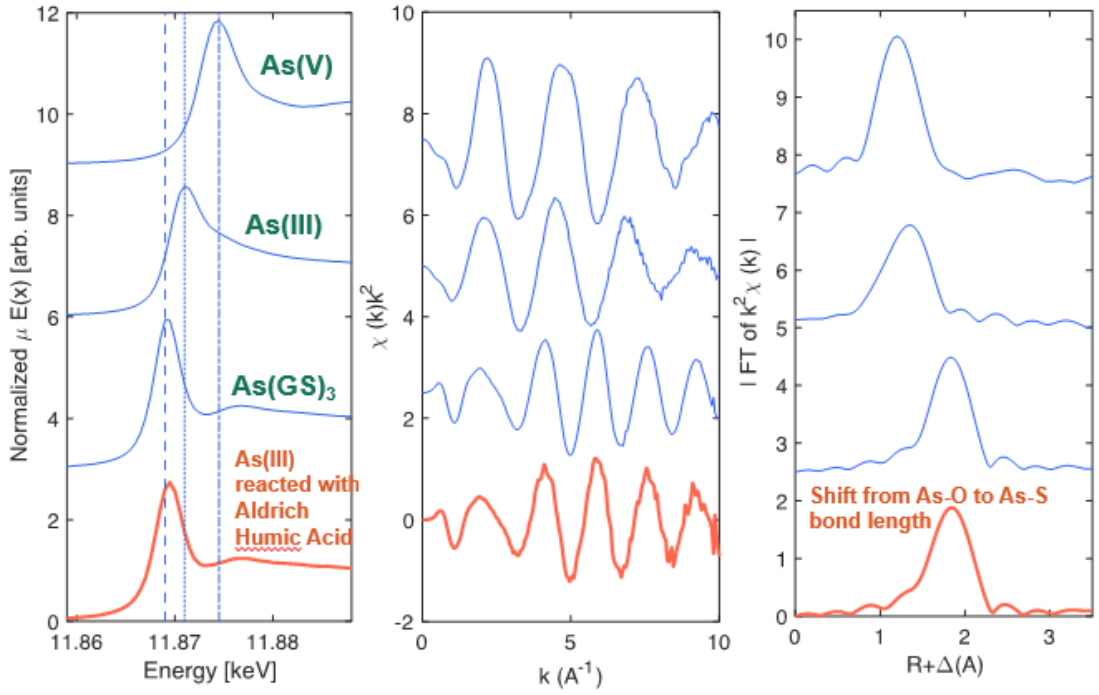

Figure 5. Results of complexation experiment between As(III) and Aldrich Humic Acid (AHA).XANES spectra of the unknown sample closely match spectra from a reference As-triglutathione standard XAFS spectra show a shift from As-O to As-S bond length. Coordination number was calculated as 2.55.

When compared to reference compounds, linear combination fitting revealed that 84% of the As was present in a sulfur-coordinated oxidation state, with a clear shift from an As-O (1.7 Å) to As-S (~2.2 Å) bond length. The coordination number was determined to be 2.55 by fitting the EXAFS equation, which is somewhat similar to the expected 3:1 S:As stoichiometry expected. These results provide more evidence for As-S binding within DOM in the environment. Confirmation of this mechanism, along with modeling techniques, would contribute to our understanding of As distribution, speciation, and fate in wetlands and rice paddies.

Scatchard Analysis

Based on the finding of a relationship between S_{org}/DOC ratios and As(III)-DOM binding, we performed further chemical and biological analysis on MNOM and SRHA to further explore the binding sites responsible for As(III) complexation. These two DOM samples were selected because they exhibited significantly different binding of As(III) (Fig. 3) and represent a high and low S_{org}/DOC ratio (Table 1). Additional dialysis equilibrium experiments were performed with these two DOM samples to gather more data. Scatchard plots and estimated model parameters for these two DOM samples are shown in Figure 3. Nonlinearity in Scatchard plots indicated the presence of both "strong" and "weak" binding sites, as has been shown previously with DOM from other sources (Liu et al., 2011; Fakour and Lin, 2014). The "strong" binding site densities of the MNOM and SRHA were estimated to be 0.018 ± 0.007 and 0.0048 ± 0.0024 μmol/mmol C, respectively. The strong site density in MNOM was 3.8 times higher than the strong site density in SRHA. The conditional stability constants estimated for the two DOM samples were similar, with log K_{ss} = 2.42 for MNOM and log K_{ss} = 2.33 for SRHA, suggesting that the binding mechanism for both DOM samples may be similar.

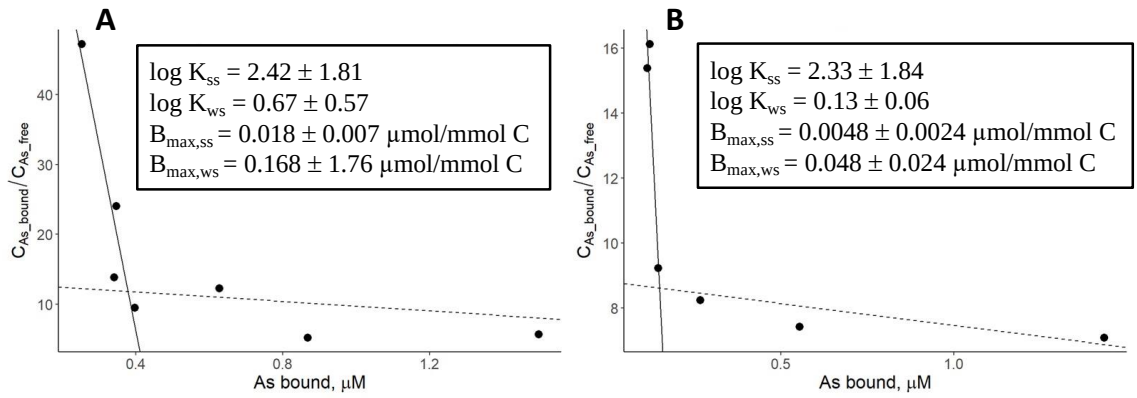

Figure 6: Scatchard plot analysis of As(III) binding with (A) MNOM and (B) SRHA, indicating the existence of "strong" and "weak" binding sites. The x-axis represents the concentration of As bound to DOM in µM. The y-axis represents the ratio of DOM-bound As to free, uncomplexed As. K_{ss} and K_{ws} are the conditional stability constants for the strong and weak sites, respectively, and $B_{max,ss}$ and $B_{max,ws}$ are the maximum binding site densities for the strong and weak sites, respectively. Data come from dialysis equilibrium experiments with an MNOM concentration of 250 mg C/L and SRHA concentration of 375 mg C/L. Model fits are based on linear least-squares regression. See Figure S2 for details on data interpretation.

Biosensor Assay of As Bioavailability

The biosensor assay was used to evaluate the effects of MNOM and SRHA on As(III) bioavailability across the range of As/DOC ratios tested in the dialysis equilibrium experiments. Biosensor fluorescence normalized by microbial biomass at the endpoint of the 20 h growth assay, a measure of As uptake (Pothier et al., 2018), is shown in Figure 7. For both MNOM and SRHA, there was a significant decrease in microbial uptake as the As/DOC ratio decreased, consistent with the expectation that greater As-DOM binding at low As/DOC ratios would lead to a decrease in bioavailability. For MNOM, fluorescence decreased by 54% from the 0.16 to the 0.0032 µmol As/mmol C ratio, while for SRHA the decrease was just 26%. At the 0.0032 µmol As/mmol C, fluorescence was 37% lower in the presence of MNOM compared to measurements in the presence of SRHA. These significant differences in biosensor fluorescence between MNOM and SRHA are consistent with the patterns seen in As(III)-DOM binding from dialysis equilibrium experiments, where As(III) bound to MNOM to a much greater extent than it did SRHA.

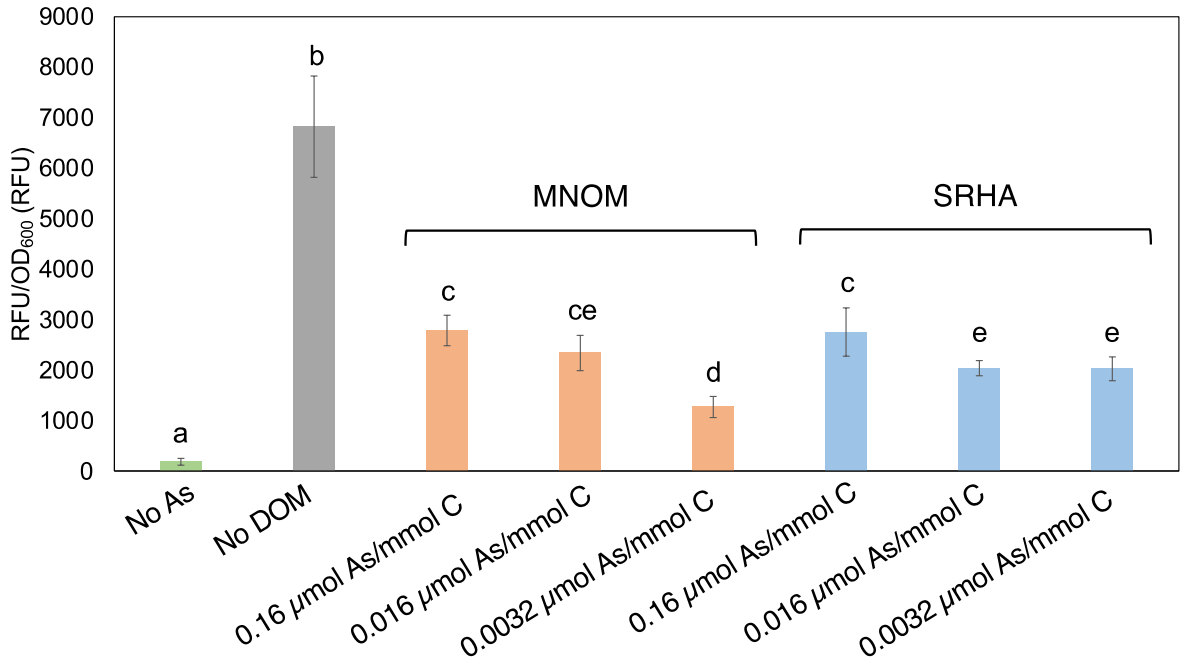

Figure 7: Biosensor fluorescence (RFU) at t = 20 h normalized by OD_{600} as a measure of microbial As uptake. Bars show mean values and error bars show standard deviations of n=4 replicates. Letters refer to statistically significant differences in means between groups.

Notably, all of the experiments with DOM, including those at the highest As/DOC ratio, exhibited significantly lower fluorescence than the No DOM control. This may be due in part to inhibited As uptake even at these high ratios, but it may also be caused by a catabolite repression mechanism in which the presence of labile carbon in the DOM pools leads to a decrease in uptake sites (Pothier et al., 2018).

Discussion

As(III) Binding to DOM: Effects of As/DOC Ratios

The fraction of As(III) bound to DOM depended on both the As/DOC ratio and DOM chemical properties. Our results indicate that a significant fraction of As(III) can be bound to DOM at the environmentally-relevant ratios examined here, with roughly 20-60%

of the As(III) bound to DOM at the 0.0032 µmol As/mmol C ratio and > 15% bound for some DOM samples at the intermediate 0.016 µmol As/mmol C ratio (Fig. 3). While < 5% of the As(III) was bound for most DOM samples at the 0.16 µmol As/mmol C ratio, it is common for environmental soil-water systems to be characterized by As/DOC ratios below this level (Table S1).

Arsenic/DOC ratios in a rice paddy soil with a moderately high As concentration of 19.7 mg/kg were recently shown to have a median As/DOC ratio of 0.017 µmol As/mmol C (Figure S1), similar to the intermediate value tested in dialysis equilibrium experiments. Roughly 20% of the As(III) was DOM-bound for the MNOM and SRNOM DOM samples at this ratio. A recent review of 16 studies on As-DOM interactions in the soil solution found that five studies reported As/DOC ratios < 0.007 µmol As/mmol C (Table S1) (Aftabtalab et al., 2021), a range where our data showed that bound As was an important component of the total As pool (Fig. 3). Half of the studies in the review had As/DOC ratios > 0.16 µmol As/mmol C, where our results suggest that As(III) binding to DOM would be of minor importance. This analysis of environmentally-relevant As/DOC ratios shows that wetland environments with low As/DOC ratios, and consequently the potential for high levels of As(III)-DOM binding, are not uncommon. DOM-bound As(III) is largely unrecognized in geochemical As speciation models, and our results suggest that it could represent an important portion of the total As pool, particularly in systems where As/DOC ratios are less than roughly 0.02 µmol As/mmol C. This is most likely to occur in systems with high levels of DOM and low-to-moderate levels of soil As. We acknowledge that in soils with very high levels of As (e.g., paddy soils in Bangladesh

irrigated with groundwater with high As levels) (Roberts et al., 2011), this condition is unlikely to be met.

As(III) Binding to DOM: Effects of Organic Sulfur

The S_{org} density of DOM samples was strongly correlated with As binding (Fig. 4). This supports the hypothesis that S-containing ligands, like thiols, in DOM serve as key binding sites for As(III). The result is consistent with findings reported in Hoffmann et al. (2012) that As(III) "sorption" to a bisulfide-reacted HA was correlated with the S content of the HA. In our study, the S_{org}/DOC ratio was 6.7 times higher in MNOM than in SRHA, while the "strong" binding site density estimated from Scatchard-plot analysis was only 3.8 times higher. This discrepancy between the S_{org} and "strong" site ratios may be due in part to experimental error, given the relatively large uncertainties in the Scatchard-derived parameters (Fig. 6). The discrepancy may also be due to thiols representing a different fraction of the S_{org} in MNOM compared to SRHA, an observation that has been shown in prior surveys of thiol/S_{org} ratios in aquatic organic matter (Skyllberg et al., 2005).

There has been no clear consensus regarding the mechanisms for As(III) binding by DOM, and until recently many studies of As(III)-DOM interactions did not report the S_{org} content of the DOM samples studied (Redman et al., 2002; Buschmann et al., 2006; Liu and Cai, 2010; Lin et al., 2017). Buschmann et al. (2006) described a range of potential mechanisms involving oxygen-containing functional groups in DOM, while modeling in Lenoble et al. (2015) assumed that the active binding sites in SRHA were carboxylic and phenolic sites. More recent studies have directed more focus on the role of S_{org} ligands. Reacting HAs with bisulfide has been shown to increase both the S content of the HA and

As(III)-HA complexation (Hoffmann et al., 2012; Catrouillet et al., 2015b). This finding is thought to be due to the incorporation of thiol functionalities in HA by the bisulfide reaction. More recent studies have shown that thiol-modified HAs increase the leaching of As from mining-impacted soils, presumably due to complexation between thiol functionalities and As (Xu et al., 2020; Qian et al., 2022). The results of the present study extend these prior findings to show that naturally-occurring variations in the S_{org} content of DOM are also associated with differences in the extent of DOM complexation with As(III). We caution that our data do not provide definitive evidence of thiols as the binding site for As(III), but rather show that DOM samples with higher S_{org} content were associated with higher levels of As(III) complexation.

The Fe-rich SW-1 DOM sample exhibited only a small change in As binding percentages across the As/DOC ratios (Fig. 3). This observation suggests a different binding mechanism controlling As speciation, possibly driven by the relatively high Fe(III) content of this sample (Table 1). In their study of As distributions in the presence of both DOM and Fe(III), Bauer and Blodau (2009) showed that when molar Fe/C ratios > 0.02, As(V) was primarily associated with colloidal or complexed Fe(III). The molar Fe/C ratio in SW-1 of 0.016 was near the ratio observed in Bauer and Blodau (2009) where As-Fe(III) associations became dominant, while all of the other DOM samples in our study had much lower molar Fe/C ratios < 10^{-3}. Only a small fraction of the Fe was Fe(II), so it appears that the Fe was primarily colloidal or DOM-complexed Fe(III) that passed through the 0.2 µm membrane used to filter extracts. This Fe(III) could have been present in the in situ soil samples, or it could have been formed during sample collection and/or DOM extraction. This association of As(III) with DOM-complexed and/or colloidal Fe(III) was

also shown in Liu and Cai (Liu et al., 2011), where size exclusion chromatography hyphenated to ICP-MS was used to show that As(III) was associated with Fe in a sample with a molar Fe/C ratio of 0.037. Our results therefore suggest a balance between colloidal/DOM-complexed Fe(III) phases and S_{org} functionalities in controlling As(III) distributions in waters containing both DOM and Fe(III), with molar Fe/DOC ratios ~0.015 and greater associated with strong As(III)-Fe association.

Environmental Significance of As(III)-DOM Complexation

Binding of As(III) to DOM has traditionally been thought to be of relatively minor environmental importance, especially compared to higher levels of As(V) complexation with DOM (Fakour and Lin, 2014), which is often attributed to cation bridging mechanisms. In this contribution, we show that DOM-bound As(III) can be a significant part of the total As pool in reducing environments. The discrepancy between earlier studies and the current study is due to both the consideration of As/DOC ratios and the chemical properties of DOM samples. Observations in earlier work of high levels of As(III)-DOM binding at As/DOC ratios as low as 0.003 μmol As/mmol C were not thought to be environmentally-relevant (Buschmann et al., 2006), while recent attention to DOM-rich wetland pore waters suggest that these ratios are common. Another key difference is the choice of DOM sample and its isolation method. Many prior studies on As(III)-DOM interactions used SRHA or Aldrich HA to conclude that As(III)-DOM complexation was minor (Buschmann et al., 2006; Liu and Cai, 2010). We show here that SRHA exhibits the lowest levels of As(III) binding of the seven DOM samples examined, potentially due to its low S_{org} content. In contrast, prior work utilizing environmental DOM isolated without

solid-phase extraction showed that >50% of the As(III) was bound to DOM (Redman et al., 2002; Lin et al., 2017). The S content in the hydrophilic fraction of DOM (i.e., the fraction not retained on the moderate hydrophobic XAD-8 resin) is higher than in the humic and fulvic acid fractions (Ma et al., 2001), possibly explaining why the RO-isolated MNOM and SRNOM, which combine HA, FA, and hydrophilic DOM fractions, displayed higher levels of binding to As(III) than SRHA, which is purified using solid-phase extraction. Relatively high dissolved thiol concentrations of 29 µM have been measured in natural waters (Joe-Wong et al., 2012), further suggesting that environmental abundances of thiols may have been traditionally underestimated due to a focus on humic and fulvic acid fractions of DOM.

Geochemical modeling of As(III) complexation with DOM require knowledge of binding site densities and conditional stability constants. The "strong" binding site densities for MNOM and SRHA determined with the Scatchard analysis were small, estimated to be 0.018 and 0.0048 µmol/mmol C, respectively. These binding site densities are similar to values reported in Liu and Cai (2010) for Aldrich HA of 0.0086 µmol/mmol C, but are an order of magnitude lower than values determined for Aldrich HA in Fakour et al. (2014) of 0.14 – 0.24 µmol/mmol C. Under the conservative assumption that thiols represent 10% of the S_{org} concentration (Skyllberg et al., 2005) presented in Table 1, the thiol binding site concentrations in these two DOMs is 0.64 and 0.096 µmol/mmol C, respectively. If thiols are indeed the binding site for As(III), this indicates that only ~2-5% of the total thiols were reactive with As(III). This is similar to the observation made in Hoffman et al. (2012) that reduced S_{org} functional groups in Elliot Soil HA were present in very large excess over complexed As(III), and is also consistent with studies of Hg^{2+}

binding to NOM that have shown that a very small fraction of reduced S_{org} is available as reactive thiols. A comparison of the Scatchard-determined site densities and experimental As/DOC ratios shows that at the lowest tested ratio in the dialysis equilibrium experiments (0.0032 μmol As/mmol C), "strong" sites in MNOM were in significant excess of As, while the "strong" sites in SRHA were close to a 1:1 ratio. At the highest ratio (0.16 μmol As/mmol C), strong sites in both MNOM and SRHA were fully saturated, explaining the low level of complexation at this ratio.

Conditional stability constants for binding of As(III) to "strong sites" in DOM reported in the literature are inconsistent. The values reported here for MNOM and SRHA, log K_{ss} = 2.33 – 2.44, are similar to values reported for As(III) binding to Aldrich humic and fulvic acid in Fakour et al. of log K_{ss} = 1.53 to 2.61. In contrast, Liu and Cai found log K_{ss} to range from 5.9 to 7.0, depending on pH. Neither of these prior studies identified which functional groups the strong sites could be. Catrouillet et al. estimated log K = 2.9 for 1:1 for monodentate binding between As(III) and thiol functionalities in humic acid. Their explanation for the 1:1 binding stoichiometry is that the large, inflexible structure of humic acid molecules combined with their low thiol density makes it difficult for more than one thiol to bind an As(III) molecule. Spectroscopic studies have found S coordination numbers for As(III) of 1.2 and 1.5 in sulfur-reacted humic acid. Our results do not provide direct information on the binding stoichiometry between As(III) and thiol functionalities.

Implications for As Bioavailability to Microorganisms

The results of the biosensor assay suggest that MNOM is more effective than SRHA at inhibiting the microbial uptake of As(III). This finding is in agreement with the dialysis equilibrium results and Scatchard-plot analysis which showed that the S_{org}-rich MNOM had a "strong" binding site density more than three times greater than the site density in S_{org}-poor SRHA, leading to a roughly three-fold difference in binding (Fig. 3). Earlier biosensor-based work has demonstrated the effect of lower As/DOC ratios in decreasing microbial uptake of As(III) (Pothier et al., 2020), but our findings are novel in linking decreased bioavailability to the S_{org} content of the DOM sample. Our findings do not provide information on the mechanism for inhibited As uptake, but it is possible that the larger molecular size of DOM-complexed As(III) restricts its uptake through the aquaglyceroporin channels that mediate transport of As(III) and other small, neutral molecules across cellular membranes (Meng et al., 2004; Rosen and Liu, 2009). Inhibition of As(III) uptake driven by formation of As-DOM complexes may impact As biotransformation reactions that depend on the activity of intracellular As metabolism enzymes (e.g., arsenic methylation catalyzed by ArsM enzymes) (Reid et al., 2017), and follow-up research is underway to explore this further.

Conclusions

The significance and mechanisms of As(III) binding to DOM is not fully understood, and growing concern about As speciation and fate in rice paddies merits new attention to As-DOM interactions in organic-rich environments. Here we show that a significant fraction of As is bound to DOM at As/DOC ratios characteristic of DOM-rich soil-water environments. The S_{org} content of DOM samples with low Fe(III) content was

strongly correlated with the fraction of bound As, suggesting that S_{org} moieties like thiols are important binding sites. The Fe(III)-rich environmental extract SW-1 displayed patterns that were distinct from the other DOM samples, suggesting that As(III) association with colloidal or DOM-complexed Fe(III) phases may be more significant than binding to S_{org} functionalities when molar Fe/C ratios are greater than 0.015. While cannot rule out that the As(III) in SW-1 may have been oxidized to As(V) during the duration of the dialysis equilibrium experiment, such transformations would be consistent with what would happen in an anaerobic soil environment. Results indicate that DOM-bound As(III) should be considered in As speciation modeling if As/DOC ratios are less than roughly 0.02 μmol As/mmol C, and that complexation modeling based on S_{org} concentrations may be effective as long as the colloidal or DOM-complexed Fe(III) content is relatively low.

REFERENCES FOR CHAPTER 2

(1) Jomova, K.; Jenisova, Z.; Feszterova, M.; Baros, S.; Liska, J.; Hudecova, D.; Rhodes, C.; Valko, M., Arsenic: toxicity, oxidative stress and human disease. *Journal of Applied Toxicology* 2011, 31 (2), 95-107.

(2) Smedley, P. L.; Kinniburgh, D. G., A review of the source, behaviour and distribution of arsenic in natural waters. *Applied geochemistry* 2002, 17 (5), 517-568.

(3) Li, G.; Sun, G.-X.; Williams, P. N.; Nunes, L.; Zhu, Y.-G., Inorganic arsenic in Chinese food and its cancer risk. *Environment International* 2011, 37 (7), 1219-1225.

(4) Zhao, F.; Ma, J.; Meharg, A.; McGrath, S., Arsenic uptake and metabolism in plants. *New Phytologist* 2009, 181 (4), 777-794.

(5) Fendorf, S.; Michael, H. A.; van Geen, A., Spatial and temporal variations of groundwater arsenic in South and Southeast Asia. *Science* 2010, 328 (5982), 1123-1127.

(6) Reid, M. C.; Maillard, J.; Bagnoud, A.; Falquet, L.; Le Vo, P.; Bernier-Latmani, R., Arsenic Methylation Dynamics in a Rice Paddy Soil Anaerobic Enrichment Culture. *Environmental Science & Technology* 2017, 51 (18), 10546–10554.

(7) Chen, C.; Li, L.; Huang, K.; Zhang, J.; Xie, W.-Y.; Lu, Y.; Dong, X.; Zhao, F.-J., Sulfate-reducing bacteria and methanogens are involved in arsenic methylation and demethylation in paddy soils. *The ISME Journal* 2019, 13 (10), 2523-2535.

(8) Wang, J.; Kerl, C. F.; Hu, P.; Martin, M.; Mu, T.; Brüggenwirth, L.; Wu, G.; Said-Pullicino, D.; Romani, M.; Wu, L., Thiolated arsenic species observed in rice paddy pore waters. *Nature Geoscience* 2020, 13 (4), 282-287.

(9) Buschmann, J.; Kappeler, A.; Lindauer, U.; Kistler, D.; Berg, M.; Sigg, L., Arsenite and arsenate binding to dissolved humic acids: influence of pH, type of humic acid, and aluminum. *Environmental Science & Technology* 2006, 40 (19), 6015-6020.

(10) Ren, J.; Fan, W.; Wang, X.; Ma, Q.; Li, X.; Xu, Z.; Wei, C., Influences of size-fractionated humic acids on arsenite and arsenate complexation and toxicity to Daphnia magna. *Water Research* 2017, 108, 68-77.

(11) Hoffmann, M.; Mikutta, C.; Kretzschmar, R., Bisulfide reaction with natural organic matter enhances arsenite sorption: Insights from X-ray absorption spectroscopy. *Environmental Science & Technology* 2012, 46 (21), 11788-11797.

(12) Maguffin, S. C.; Abu-Ali, L.; Tappero, R. V.; Pena, J.; Rohila, J. S.; McClung, A. M.; Reid, M. C., Influence of manganese abundances on iron and arsenic solubility in rice paddy soils. *Geochimica et Cosmochimica Acta* 2020, 276, 50-69.

(13) Aftabtalab, A.; Rinklebe, J.; Shaheen, S. M.; Niazi, N. K.; Moreno-Jiménez, E.; Schaller, J.; Knorr, K.-H., Review on the interactions of arsenic, iron (oxy)(hydr) oxides, and dissolved organic matter in soils, sediments, and groundwater in a ternary system. *Chemosphere* 2022, 286, 131790.

(14) Mikutta, C.; Kretzschmar, R., Spectroscopic evidence for ternary complex formation between arsenate and ferric iron complexes of humic substances. *Environmental Science & Technology* 2011, 45 (22), 9550-9557.

(15) Lenoble, V.; Dang, D.; Cazalet, M. L.; Mounier, S.; Pfeifer, H.-R.; Garnier, C., Evaluation and modelling of dissolved organic matter reactivity toward AsIII and AsV–Implication in environmental arsenic speciation. *Talanta* 2015, 134, 530-537.

(16) Yao, Y.; Mi, N.; He, C.; Yin, L.; Zhou, D.; Zhang, Y.; Sun, H.; Yang, S.; Li, S.; He, H., Transport of arsenic loaded by ferric humate colloid in saturated porous media. *Chemosphere* 2020, 240, 124987.

(17) Sharma, P.; Ofner, J.; Kappler, A., Formation of binary and ternary colloids and dissolved complexes of organic matter, Fe and As. *Environmental Science & Technology* 2010, 44 (12), 4479-4485.

(18) Bauer, M.; Blodau, C., Arsenic distribution in the dissolved, colloidal and particulate size fraction of experimental solutions rich in dissolved organic matter and ferric iron. *Geochimica et Cosmochimica Acta* 2009, 73 (3), 529-542.

(19) Liu, G.; Fernandez, A.; Cai, Y., Complexation of arsenite with humic acid in the presence of ferric iron. *Environmental Science & Technology* 2011, 45 (8), 3210-3216.

(20) Warwick, P.; Inam, E.; Evans, N., Arsenic's interaction with humic acid. *Environmental Chemistry* 2005, 2 (2), 119-124.

(21) Liu, G.; Cai, Y., Studying arsenite–humic acid complexation using size exclusion chromatography–inductively coupled plasma mass spectrometry. *Journal of Hazardous Materials* 2013, 262, 1223-1229.

(22) Fakour, H.; Lin, T.-F., Experimental determination and modeling of arsenic complexation with humic and fulvic acids. *Journal of Hazardous Materials* 2014, 279, 569-578.

(23) Hoffmann, M.; Mikutta, C.; Kretzschmar, R., Arsenite binding to natural organic matter: spectroscopic evidence for ligand exchange and ternary complex formation. *Environmental Science & Technology* 2013, 47 (21), 12165-12173.

(24) Eberle, A.; Besold, J.; Kerl, C. F.; Lezama-Pacheco, J. S.; Fendorf, S.; Planer-Friedrich, B., Arsenic fate in peat controlled by the pH-dependent role of reduced sulfur. *Environmental Science & Technology* 2020, 54 (11), 6682-6692.

(25) Catrouillet, C.; Davranche, M.; Dia, A.; Bouhnik-Le Coz, M.; Pédrot, M.; Marsac, R.; Gruau, G., Thiol groups controls on arsenite binding by organic matter: New experimental and modeling evidence. *Journal of Colloid and Interface Science* 2015, 460, 310-320.

(26) Langner, P.; Mikutta, C.; Kretzschmar, R., Arsenic sequestration by organic sulphur in peat. *Nature Geoscience* 2012, 5 (1), 66-73.

(27) Langner, P.; Mikutta, C.; Suess, E.; Marcus, M. A.; Kretzschmar, R., Spatial distribution and speciation of arsenic in peat studied with microfocused X-ray fluorescence spectrometry and X-ray absorption spectroscopy. *Environmental Science &* Technology 2013, 47 (17), 9706-9714.

(28) Spuches, A. M.; Kruszyna, H. G.; Rich, A. M.; Wilcox, D. E., Thermodynamics of the As (III)− thiol interaction: arsenite and monomethylarsenite complexes with glutathione, dihydrolipoic acid, and other thiol ligands. *Inorganic Chemistry* 2005, 44 (8), 2964-2972.

(29) Slyemi, D.; Bonnefoy, V., How prokaryotes deal with arsenic. *Environmental Microbiology Reports* 2012, 4 (6), 571-586.

(30) Zhu, Y.-G.; Yoshinaga, M.; Zhao, F.-J.; Rosen, B. P., Earth abides arsenic biotransformations. *Annual Review of Earth and Planetary Sciences* 2014, 42, 443.

(31) Redman, A. D.; Macalady, D. L.; Ahmann, D., Natural organic matter affects arsenic speciation and sorption onto hematite. *Environmental Science & Technology* 2002, 36 (13), 2889-2896.

(32) Liu, G.; Cai, Y., Complexation of arsenite with dissolved organic matter: Conditional distribution coefficients and apparent stability constants. *Chemosphere* 2010, 81 (7), 890-896.

(33) Lin, T. Y.; Hafeznezami, S.; Rice, L.; Lee, J.; Maki, A.; Sevilla, T.; Stahl, M.; Neumann, R.; Harvey, C.; Suffet, I. M., Arsenic oxyanion binding to NOM from dung and aquaculture pond sediments in Bangladesh: importance of site-specific binding constants. *Applied Geochemistry* 2017, 78, 234-240.

(34) Pothier, M. P.; Hinz, A. J.; Poulain, A. J., Insights into arsenite and arsenate uptake pathways using a whole cell biosensor. *Frontiers in Microbiology* 2018, 9, 2310.

(35) Pothier, M. P.; Lenoble, V.; Garnier, C.; Misson, B.; Rentmeister, C.; Poulain, A. J., Dissolved organic matter controls of arsenic bioavailability to bacteria. *Science of the Total Environment* 2020, 716, 137118.

(36) Kwasniewski, M. T.; Allison, R. B.; Wilcox, W. F.; Sacks, G. L., Convenient, inexpensive quantification of elemental sulfur by simultaneous in situ reduction and colorimetric detection. *Analytica Chimica Acta* 2011, 703 (1), 52-57.

(37) Stookey, L. L., Ferrozine---a new spectrophotometric reagent for iron. *Analytical Chemistry* 1970, 42 (7), 779-781.

(38) Brezonik, P.; Arnold, W., Water chemistry: an introduction to the chemistry of natural and engineered aquatic systems. OUP USA: 2011.

(39) Attie, A. D.; Raines, R. T., Analysis of receptor-ligand interactions. *Journal of Chemical Education* 1995, 72 (2), 119.

(40) Stocker, J.; Balluch, D.; Gsell, M.; Harms, H.; Feliciano, J.; Daunert, S.; Malik, K. A.; Van der Meer, J. R., Development of a set of simple bacterial biosensors for quantitative and rapid measurements of arsenite and arsenate in potable water. *Environmental Science & Technology* 2003, 37 (20), 4743-4750.

(41) RCore, T., R: A language and environment for statistical computing. R Foundation for Statistical Computing, Vienna, Austria. Online: http://www. R-project. org 2013.

(42) Roberts, L. C.; Hug, S. J.; Voegelin, A.; Dittmar, J.; Kretzschmar, R.; Wehrli, B.; Saha, G. C.; Badruzzaman, A. B. M.; Ali, M. A., Arsenic dynamics in porewater of an intermittently irrigated paddy field in Bangladesh. *Environmental Science & Technology* 2011, 45 (3), 971-976.

(43) Skyllberg, U.; Qian, J.; Frech, W., Combined XANES and EXAFS study on the bonding of methyl mercury to thiol groups in soil and aquatic organic matter. *Physica Scripta* 2005, 2005 (T115), 894.

(44) Qian, G.; Xu, L.; Li, N.; Wang, K.; Qu, Y.; Xu, Y., Enhanced arsenic migration in tailings soil with the addition of humic acid, fulvic acid and thiol-modified humic acid. *Chemosphere* 2022, 286, 131784.

(45) Xu, Y.; Wang, K.; Zhou, Q.; Zhang, L.; Qian, G., Effects of humus on the mobility of arsenic in tailing soil and the thiol-modification of humus. *Chemosphere* 2020, 259, 127403.

(46) Ma, H.; Allen, H. E.; Yin, Y., Characterization of isolated fractions of dissolved organic matter from natural waters and a wastewater effluent. *Water Research* 2001, 35 (4), 985-996.

(47) Joe-Wong, C.; Shoenfelt, E.; Hauser, E. J.; Crompton, N.; Myneni, S. C., Estimation of reactive thiol concentrations in dissolved organic matter and bacterial cell membranes in aquatic systems. *Environmental Science & Technology* 2012, 46 (18), 9854-9861.

(48) Dong, W.; Liang, L.; Brooks, S.; Southworth, G.; Gu, B., Roles of dissolved organic matter in the speciation of mercury and methylmercury in a contaminated ecosystem in Oak Ridge, Tennessee. *Environmental Chemistry* 2010, 7 (1), 94-102.

(49) Meng, Y.-L.; Liu, Z.; Rosen, B. P., As (III) and Sb (III) uptake by GlpF and efflux by ArsB in Escherichia coli. *Journal of Biological Chemistry* 2004, 279 (18), 18334-18341.

(50) Rosen, B. P.; Liu, Z., Transport pathways for arsenic and selenium: a minireview. *Environment International* 2009, 35 (3), 512-515.

CHAPTER 3: Interactions between Alternate Wetting and Drying and Rice Cultivar in Controlling Grain Concentrations of Arsenic and other Redox-Sensitive Elements

Adapted from: Lena Abu-Ali, Hyun Yoon, Scott C. Maguffin, Jai S. Rohila, Anna M. McClung and Matthew Charles Reid. To be submitted to *Agricultural Science & Technology*: August 2022.

Rice is a global dietary staple and its traditional cultivation leads to an accumulation of arsenic (As) in rice grains in areas with contaminated soil. In this contribution, we characterize pore water chemistry and five varieties of rice grown in continuously flooded and alternate wetting and drying (AWD) environments in a two-year field study for As content, As speciation, and other trace micronutrients and toxic elements. Concentrations of As and iron (Fe) were significantly affected by AWD drains. The effects of both variety and AWD drains are significant controls on rice grain content; in most cases, variety was more important than AWD drains. Interannual variability was found to be an important random effect for inorganic As and other micronutrients.

Introduction

Rice could be a major source of arsenic (As) to the diets of millions (Zavala et al., 2008; Davis et al., 2017; Nunes et al., 2021), and there is active research interest in soil management strategies to sustainably decrease grain inorganic As concentrations. Specifically, proposed regulations by organizations such as the US Food and Drug Administration for inorganic As levels in infant food products (US Food and Drug Administration, 2020) are accelerating the need for a comprehensive understanding of As

bioavailability to the rice plant. Concurrently, concerns are being raised about other heavy metal contaminants in places with pollution from mining activities; rice has been identified as the most primary source of cadmium (Cd) intake in the general Japanese population (Tsukahara et al., 2003).

The practice of Alternate Wetting and Drying (AWD) helps reduce the accumulation of As by altering the redox biogeochemistry of the rice paddy (Linquist et al., 2015; LaHue et al., 2016). The introduction of oxygen into the soil column causes reduced, mobile As(III) to oxidize to As(V), and sorb to re-oxidized Mn and Fe minerals, rendering the As unavailable for plant uptake (LaHue et al., 2016; Yang et al., 2017a; Suriyagoda et al., 2018). However, while altering the Pore water biogeochemistry favors As sequestration by soil minerals, it also favors the mobility and bioavailability of cadmium (Cd) (de Livera et al., 2011; Uraguchi and Fujiwara, 2012; Rinklebe et al., 2016; Huang et al., 2022) which is normally sequestered in precipitated sulfide minerals under reducing conditions. Additionally, AWD has variable effects on other important micronutrients such as manganese (Mn), molybdenum (Mo), selenium (Se,) zinc (Zn), and copper (Cu) (Norton et al., 2014). As a favorable electron acceptor, Mn oxides readily undergo reductive dissolution by microbes in flooded paddies (Oremland and Stolz, 2005). Mo is a redox-sensitive essential trace element that forms oxyanions and may sorb to Mn oxides in oxic conditions, but is strongly chalcophile and forms highly insoluble Mo-S minerals in the presence of sulfide (Smedley and Kinniburgh, 2017), similar to Cd and Zn (Kirk, 2004). Conversely, Se primarily forms oxyanions, and much like arsenite, selenite sorbs strongly to Fe oxides and precipitates as $Fe_2(SeO_3)_3$ (Kirk, 2004). Selenium also undergoes complex chemistry in submerged soils between precipitation with other metals

and methylation to volatile compounds (Reamer and Zoller, 1980). The behavior of these micronutrients is less studied than As in the context of rice paddy soils, and a comprehensive understanding of the effect of AWD on both pollutants and nutrients is needed.

Prior research on the effects of AWD on rice grain As speciation suggest while both inorganic As (iAs) and organic As concentrations decrease in AWD treatments, reductions in the methylated forms of As such as DMA are the primary driver for reductions in total As (Xu et al., 2008; Li et al., 2009, 2019b; Carrijo et al., 2019). One study found that DMA reductions were greater in medium and high severity AWD scenarios when soil volumetric water content was maintained below 35 percent (Li et al., 2019b). Additionally, new research suggests that what is typically measured as DMA in standard HPLC-ICP-MS methods may in fact be a toxic thiolated species (Dai et al., 2022; Pischke et al., 2022). Therefore, while they do not address reducing currently regulated iAs species, techniques that decrease DMA and can decrease straighthead are in fact valuable. Another technique used to reduce As uptake into rice plants is choosing and breeding cultivars that accumulate less As due to genotypic factors. One study found that temperate japonica varieties exhibited lower grain As concentrations when compared to tropical japonica, indica and aus subpopulations (Norton et al., 2012), citing a low ratio of grain:shoot As; while the mechanism waws not defined, it was hypothesized that japonicas differ in terms of As translocation or shoot-grain As transporters. Clearly, both environmental factors and genotypic factors influence As uptake and speciation in rice, and more research on the relative impacts of AWD and cultivar selection are needed to inform best practices for rice production. Moreover, considering the important role of rice as a nutritional staple across

the globe, the impact of AWD and cultivar selection on other factors such as yield and micronutrient content must be considered.

The objective of this study is to determine effects of alternate wetting and drying, different rice cultivars, and potential interactions between these factors on As speciation, Cd, and redox-sensitive micronutrient concentrations in rice grains. We explore relationships between irrigation treatment, rice variety, and trace metal concentration and speciation in rice grains through correlation analysis, principal component analysis, and modeling techniques. A previously published pore water dataset will be used as a resource for data interpretation. We hypothesize that AWD has a significant effect on pore water chemistry which translates to differences in grain chemistry for both pollutants and micronutrients. We also hypothesize that AWD decreases total grain As content while increasing Cd content, and that oxyanion-forming elements (e.g., Se and Mo) will be comparable to As, while chalcophile elements (e.g., Zn, Cu) will be comparable to Cd.

Materials and Methods

Field Experimental Setup

Field plots were prepared at the Dale Bumpers National Rice Research Center in 2017 and 2018. Details of field experimental setup and pore water monitoring have been published previously (Maguffin et al., 2020). Briefly, field experiments were conducted in adjacent rice paddy fields (40 m x 6 m) at the United States Department of Agriculture, Agricultural Research Service (USDA-ARS) Dale Bumpers National Rice Research Center (DBNRRC) in Stuttgart, Arkansas, USA. The soil texture is characterized as a Dewitt silt loam (fine, smectitic, thermic, Typic Albaqualfs) (5% sand, 78% silt, 17% clay) and the fields, designated for arsenic related studies, have been under rice-soybean crop

rotation for over 20 years. When under rice cultivation, the fields were amended with monosodium methyl arsenate (MSMA), which is known to induce symptoms of the physiological malady straighthead (Wells and Gilmour, 1977). Approximately 1 month prior to planting, phosphorus (P) was added in the form of triple super phosphate (20 kg P ha-1) and potassium (K) was added in the form of muriate of potash (56 kg K ha-1). On the day of planting, 6.7 kg ha-1 of MSMA (corresponding to 1.58 kg As ha-1) was applied and incorporated into the upper 15 cm of soil prior to sowing the seed.

Table 2. Characteristics of rice cultivars used in this study. iAs = inorganic arsenic.

Variety	**PI**	**Origin**	***Oryza* Sub-species**	**2013 Straighthead Rating Under MSMA Soil, Permanent Flood**		**2013 iAs Content Brown Rice from Native Soil, Permanent Flood**	
Cocodrie	606331	USA	Tropical japonica	7	Very susceptible	163.0	Excluder
Katy	527707	USA	Tropical japonica	2	Moderately Resistant	257.9	Accumulator
WC 4644	312777	Philippines	Indica	7	Very susceptible	226.9	Accumulator
Sierra	633623	USA	Tropical japonica	1	Resistant	157.1	Excluder
Zao 402	615218	China	Indica	1	Resistant	252.7	Accumulator

The study consisted of fice rice (Oryza sativa) varieties, replicated three times and arranged in a randomized complete block design in two separate fields with different irrigation management schemes. The varieties were chosen based upon unpublishes results determined in a 2013 replicated field study which included a season-long flood with one field being treated with MSMA as described above to obtain straighthead ratings and another field with untreated, native soil used to determine inorganic arsenic content in

brown rice according to the method of Chaney, et al. 2018 (Chaney et al., 2018). Surface water collected in a reservoir was used for irrigation throughout the season. After seedling establishment, the experimental fields were maintained as either continuously-flooded (CF) by maintaining ~10 cm of standing water for the entire growing season or were subjected to three (2017) or one or two (2018) pre-harvest soil dry-downs targeted to reach a soil tension of -30 to -40 kPa in the rhizosphere.

Table 3. Details of AWD dry-downs in 2017 and 2018. Dry-down date and duration was determined by a change in the soil moisture level measured in 4-inch depth sensors after pipes were opened for field drainage.

	2017			2018		
	Date	**Days after planting**	**Duration (days)**	**Date**	**Days after planting**	**Duration (days)**
1st dry-down	Jul 16th	67	4	Aug 2nd	79	7
2nd dry-down	Aug 18th	100	3	Sep 4th	112	14
3rd dry-down	Sep 4th	117	2	*NA*	*NA*	*NA*

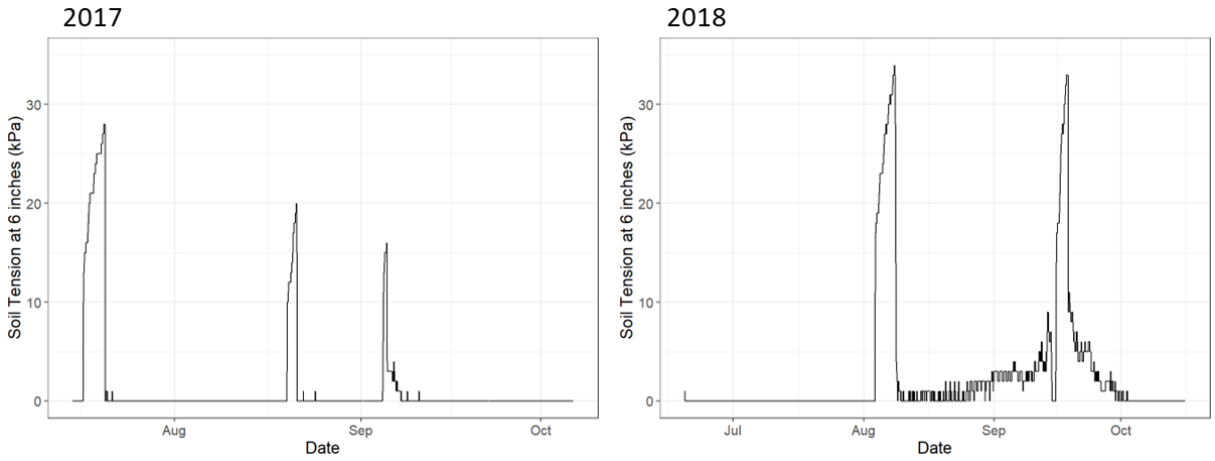

For each dry-down treatment, a 20 cm, gravity-fed outlet pipe was opened to drain the field. Once the target soil moisture was reached in the AWD fields, they were re-flooded to the same level as the CF field. In 2017, the maximum dry-down intensities were 28 (dry-

down 1), 20 (dry-down 2), and 16 (dry-down 3) kPa as measured by in-situ soil tension sensors. In 2018, the maximum dry-down intensities were 34 (dry-down 1) and 33 (dry-down 2) kPa. Paddy rice was harvested manually as each variety reached maturation at about 20% harvest moisture. While most cultivars had roughly the same growing period, Zao 402 matured approximately 2 weeks earlier than the other varieties and was harvested before the last dry-down in both years. Yield harvest was not performed for Sierra in 2017 due to poor plant stands.

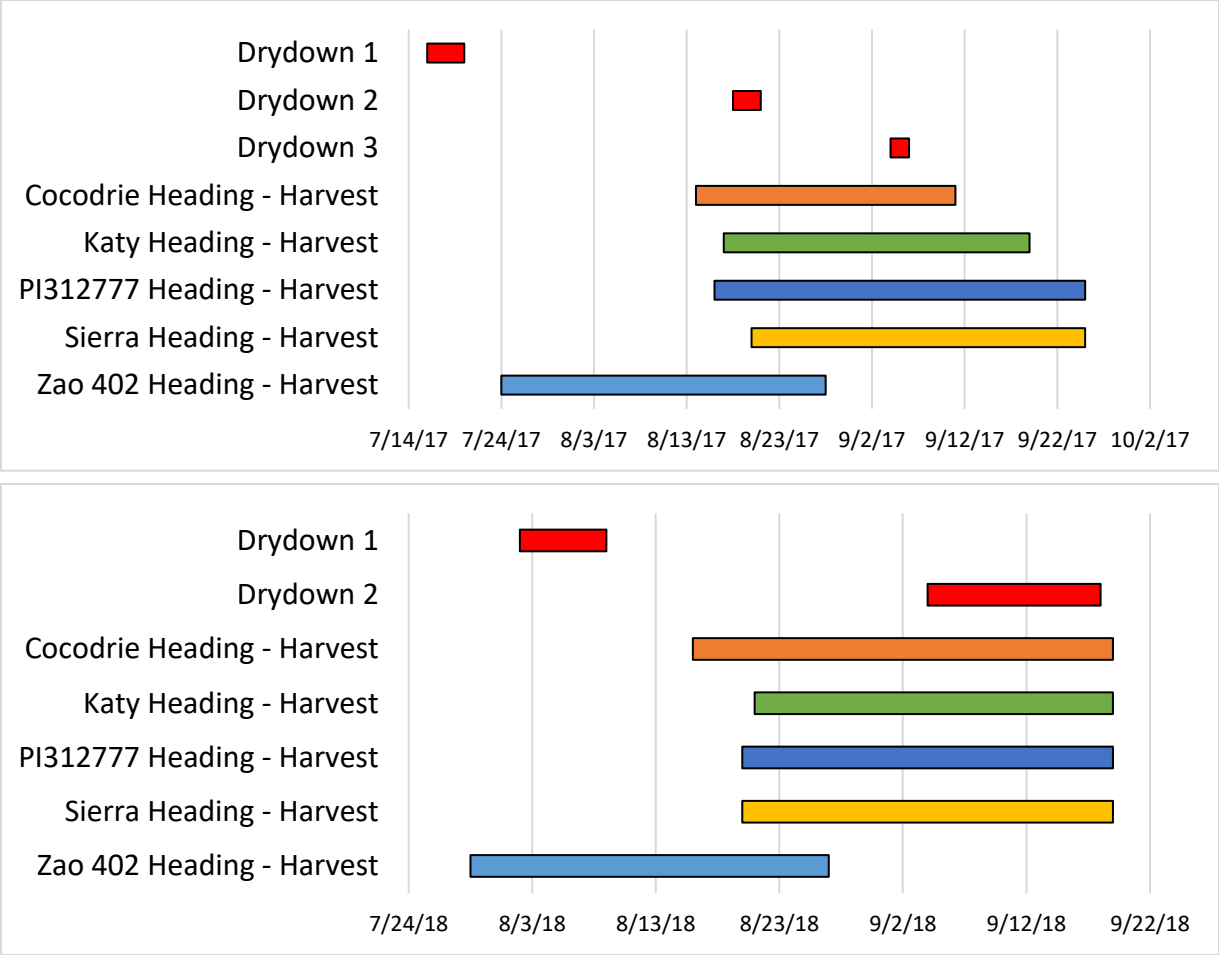

Figure 8. Timeline of AWD dry-downs and rice physiological stages in 2017 (top) and 2018 (bottom).

Table 4. Yields (lb/acre) broken down by year, cultivar, and irrigation treatment. Value in parentheses represents standard deviation of triplicates.

Cultivar	2017 Yields (lb/acre)		2018 Yields (lb/acre)		
	0 Drain	3 Drains	0 Drain	1 Drain	2 Drains
Cocodrie	416 (260)	2560 (562)	2293 (95)	1825 (1981)	1964 (1043)
Katy	540 (424)	2988 (530)	5071 (701)	4138 (557)	4276 (503)
PI312777	1576 (1789)	4913 (1457)	3958 (1605)	3991 (1361)	4780 (766)
Sierra	*NA*	*NA*	5063 (1199)	4172 (604)	4779 (1326)
Zao402	5871 (1006)	7378 (587)	5371 (3363)	6295 (2041)	7080 (406)

In situ Pore water Monitoring

In 2018, Rhizon pore water samplers (Rhizosphere Research Products, Wageningen, Netherlands) were installed in three locations in each rice paddy field by digging a trench and inserting the samplers horizontally into the soil column at 10 cm below the soil surface. Pore water samples were collected using pre-evacuated, crimp-sealed glass serum vials with blue rubber stoppers. All vials were acid washed and triple-rinsed with ultrapure water prior to use and were wrapped in aluminum foil during and after sample collection. Sample collection was performed by attaching a 23-gauge needle to a three-way luer after flushing the tubing of the Rhizon sampler. Sample collection took place over 6-8 hours. After retrieval, serum vials were stored in the dark at 4ºC. Vials were shipped to

Ithaca, NY, in coolers on ice and were stored at 4ºC until analysis. ICP-MS analysis of these pore water samples was performed with an Agilent 8800 operating in oxygen reaction mode.

Pore water data from the reproductive and grain-filling physiological rice stage were used in models to examine effects of AWD management on pore water concentrations of redox-sensitive elements. This time period was chosen because post-heading is considered the most sensitive period for contaminants or micronutrients to be loaded into the grain (Arao et al., 2009). The samples used began with onset of heading, as determined in the field, and included samples through the following 4 weeks. This included triplicates of 10 sampling days in each of the three fields, for 90 samples in total. Averages of the three Pore water replicates from 10 cm depth were calculated across this time series.

Rice Extraction

The method used for rice grain extraction is described elsewhere (Reid et al., 2021). Briefly, brown rice samples were pulverized with a ball mill to a fine flour. Rice flour was dried overnight at 105°C before extraction. For the extraction, 0.5g of rice flour was added to a centrifuge tube with 4 mL of 2% nitric acid and 1 mL of hydrogen peroxide. The liquid-rice flour extraction was homogenized via vortexation and incubated in a 90°C water bath for 3h with periodic vortexing. Controls without rice flour were performed to check for As contamination of reagents, solutions, and glassware. Certified reference materials (NIST 1658b and ERM®-BC211) and controls were extracted alongside rice samples to assess extraction effectiveness. After 3h, the extract was filtered through a sterile 0.22 µm filter into a clean centrifuge tube and centrifuged for 20 minutes at 4800G. The collected supernatant was used for As speciation via HPLC-ICP-MS and total elemental analysis via

standalone ICP-MS. If analyses took place within 48 h of extraction, the supernatant was stored at 4°C. Otherwise, supernatant samples were frozen until analyses took place.

Table 5. CRM quantification. All values in µg/g.

	As		Cd		Mn		Zn		DMA		iAs	
	provided	measured	provided	measured	provided	measured	provided	measured	provided	measured	provided	measured
ERM®-BC211 (1)	0.26	0.311	*N/A*	0.016	*N/A*	13.504	*N/A*	19.928	0.119	0.107	0.124	0.133
ERM®-BC211 (2)	0.26	0.300	*N/A*	0.014	*N/A*	13.204	*N/A*	19.850	0.119	0.115	0.124	0.129
ERM®-BC211 (3)	0.26	0.297	*N/A*	*N/A*	*N/A*	*N/A*	*N/A*	*N/A*	0.119	0.1218	0.124	0.122946
ERM®-BC211 (4)	0.26	0.278	*N/A*	*N/A*	*N/A*	*N/A*	*N/A*	*N/A*	0.119	0.162254	0.124	0.133039
NIST 1568b (1)	0.285	0.340	0.0224	0.019	19.2	18.768	19.42	23.881	0.18	0.186	0.092	0.097
NIST 1568b (2)	0.285	0.388	0.0224	0.023	19.2	18.800	19.42	19.100	0.18	0.162	0.092	0.145
NIST 1568b (3)	0.285	0.335	0.0224	0.021	19.2	18.000	19.42	17.700	0.18	0.156	0.092	0.091

Arsenic Speciation and Elemental Analyses

Trace elements in rice extract samples were preserved in 2% trace metal grade nitric acid and measured via inductively coupled plasma mass spectrometry (ICP-MS) with a helium collision cell (Agilent 7800) with rhodium as an in-line internal standard. Potential polyatomic interference from ArCl at m/z = 75 was assessed by testing samples diluted in 2% trace metal grade HCl, and none was detected. Calibration standards were prepared using a traceable multi-element standard.

Arsenic speciation was measured via high performance liquid chromatography-inductively coupled plasma mass spectrometry (HPLC-ICP-MS) with a Hamilton PRP X100 analytical column. The eluent used was 6.66 mM (NH4)2PO4, 6.66 mM NH4NO3 adjusted to pH 6.2. Calibration standards were prepared by dissolving salts of MMA, DMA, and arsenate in Milli-Q water.

Statistical Methods

Statistical interpretation of data was performed in R (R Core Team, 2013). Because of the hierarchical structure of the data, linear mixed-effects (LME) modeling was chosen. LMEs account for within-group variation that may mask differences between groups of replicates. A sum coding approach was used for the rice variety variable, with concentrations of elements in each variety compared to the mean of all observations from all varieties. LMEs with subsequent ANOVA and Tukey's HSD test were performed using the lme4 package (Bates et al., 2022).

The general form of a linear mixed-effects model is as follows:

$$Y_i \sim N(\mu,\ \sigma^2)$$

$$\mu = (\beta_0 + b_{S,0s}) + \beta_1 X_i + e_{si}$$

Where μ = mean value, σ^2 = variance, β = model coefficients, $b_{S,0s}$ = random group intercept, X_i = model parameter, and e_{si} = error term. An example of the equation generated from the LME of total grain As is as follows:

$$As_i \sim N(\mu, \sigma^2)$$

$$\mu = \alpha_{j[i]} + \beta_1(\text{Variety}_1) + \beta_2(\text{Variety}_2) + \beta_3(\text{Variety}_3) + \beta_4(\text{Variety}_4) +$$
$$\beta_5(\text{Drains}_1) + \beta_6(\text{Drains}_2) + \beta_7(\text{Drains}_1 \times \text{Variety}_1) + \beta_8(\text{Drains}_1 \times \text{Variety}_2) +$$
$$\beta_9(\text{Drains}_1 \times \text{Variety}_3) + \beta_{10}(\text{Drains}_1 \times \text{Variety}_4) + \beta_{11}(\text{Drains}_2 \times \text{Variety}_1) +$$
$$\beta_{12}(\text{Drains}_2 \times \text{Variety}_2) + \beta_{13}(\text{Drains}_2 \times \text{Variety}_3) + \beta_{14}(\text{Drains}_2 \times \text{Variety}_4)$$

$$\alpha_j \sim N\left(\mu_{\alpha j}, \sigma^2_{\alpha j}\right), \text{for Rep j} = 1, \ldots \text{J}$$

Both variety and drains were treated as categorical variables, while the response variable was numeric (continuous). Models were constructed for each year independently since AWD was employed differently between the two years. In addition, continuously-

flooded results for both years were modeled together to investigate whether the random effects of different environmental conditions each year were significant. To enhance the model interpretation, estimated marginal means were calculated using the emmeans package.

Results

Rice grain composition and interannual differences

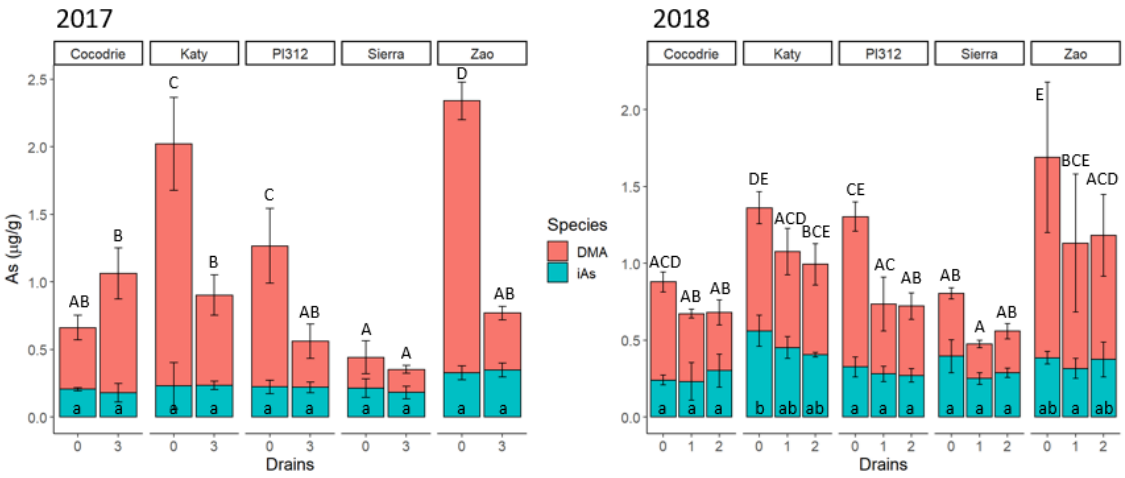

Figure 9. As in brown rice samples. Different letters represent significant ($p<0.05$) differences between treatments and cultivars. Lowercase letters represent iAs and capital letters represent total As.

Figure 9 shows the As concentration and speciation in brown rice samples from both 2017 and 2018, separated by cultivar and irrigation treatment. iAs is consistent across both years, all cultivars and treatments, with no significant differences in any of the 2017 samples. In 2018, only the Katy 0-drain samples had a statistically different iAs concentration than Cocodrie, PI312777, and Sierra. However, there is considerable variability in the DMA, especially between flood and drain conditions. In all but one case, AWD decreased the total As in rice; this is especially evident in 2017 where DMA concentrations differ greatly and is the expected outcome. Differences in total As are less

obvious in the 2018 samples, however, it is clear that the additional effect of two drains versus one was negligible. Varietal differences are also more evident in 2017. Sierra and Cocodrie, which were chosen for this study due to potentially being excluders, consistently takes up less As than the other varieties; however, the effect of AWD is small. Conversely, the effect of AWD on the Zao 402 variety was great in 2017, with a more than 80% reduction in DMA, leading to a 74% reduction in total As.

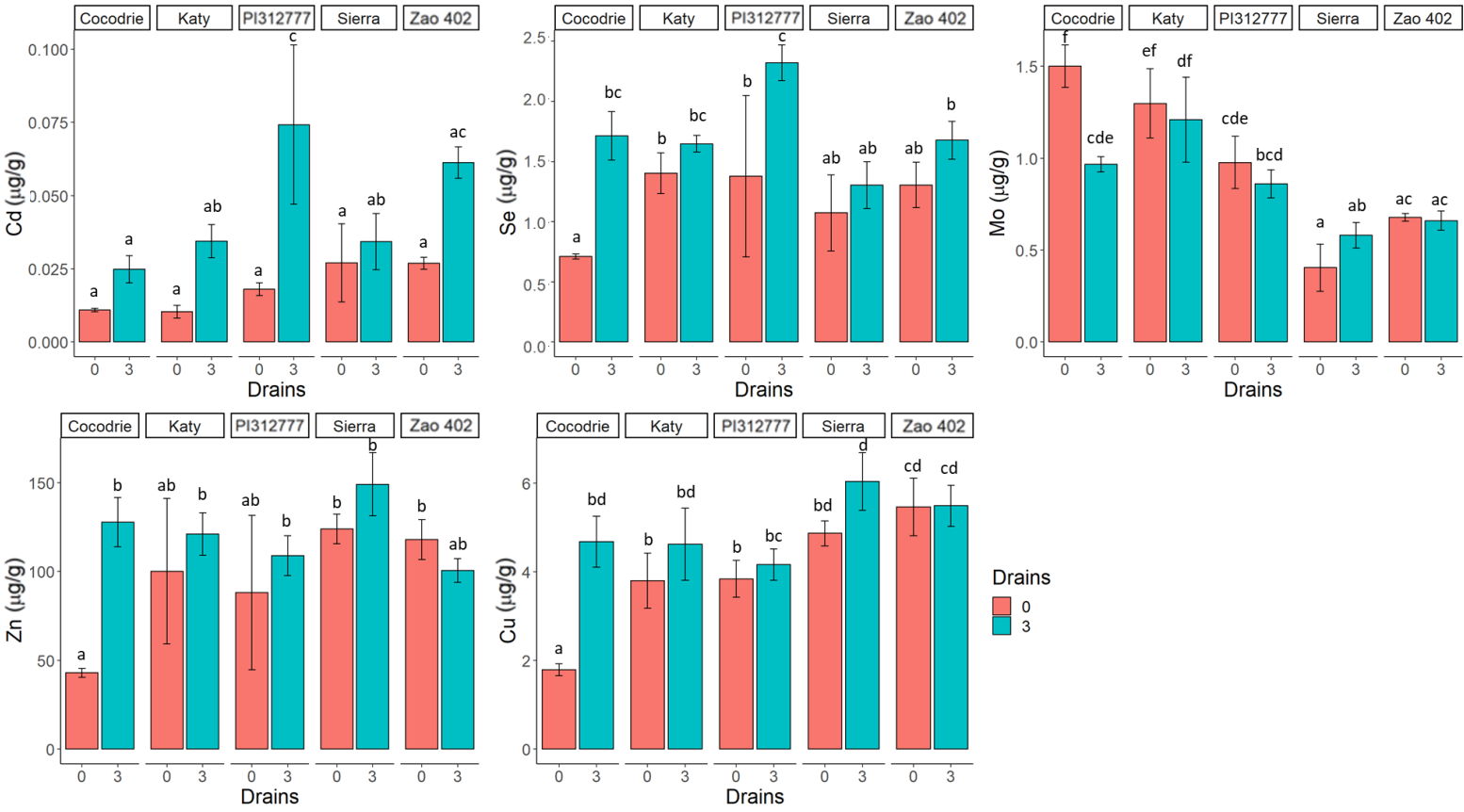

Figure 10. Grain concentrations of selected elements in 2017 brown rice samples. Different letters represent significant ($p<0.05$) differences between treatments and cultivars.

Cadmium concentrations were lowest in the continuously-flooded fields in both 2017 and 2018. AWD increased grain Cd, but in all cases was lower than the EU regulatory limit of 200 µg/kg (Shi et al., 2020). In 2018, the additional effect of 2 drains was not significant

when compared to 1 drain. Interestingly, Se, which is an oxyanion-forming element hypothesized to have similar behavior to As, also increased with AWD for some varieties. Patterns were mixed or unclear for Mo, Cu, and Zn.

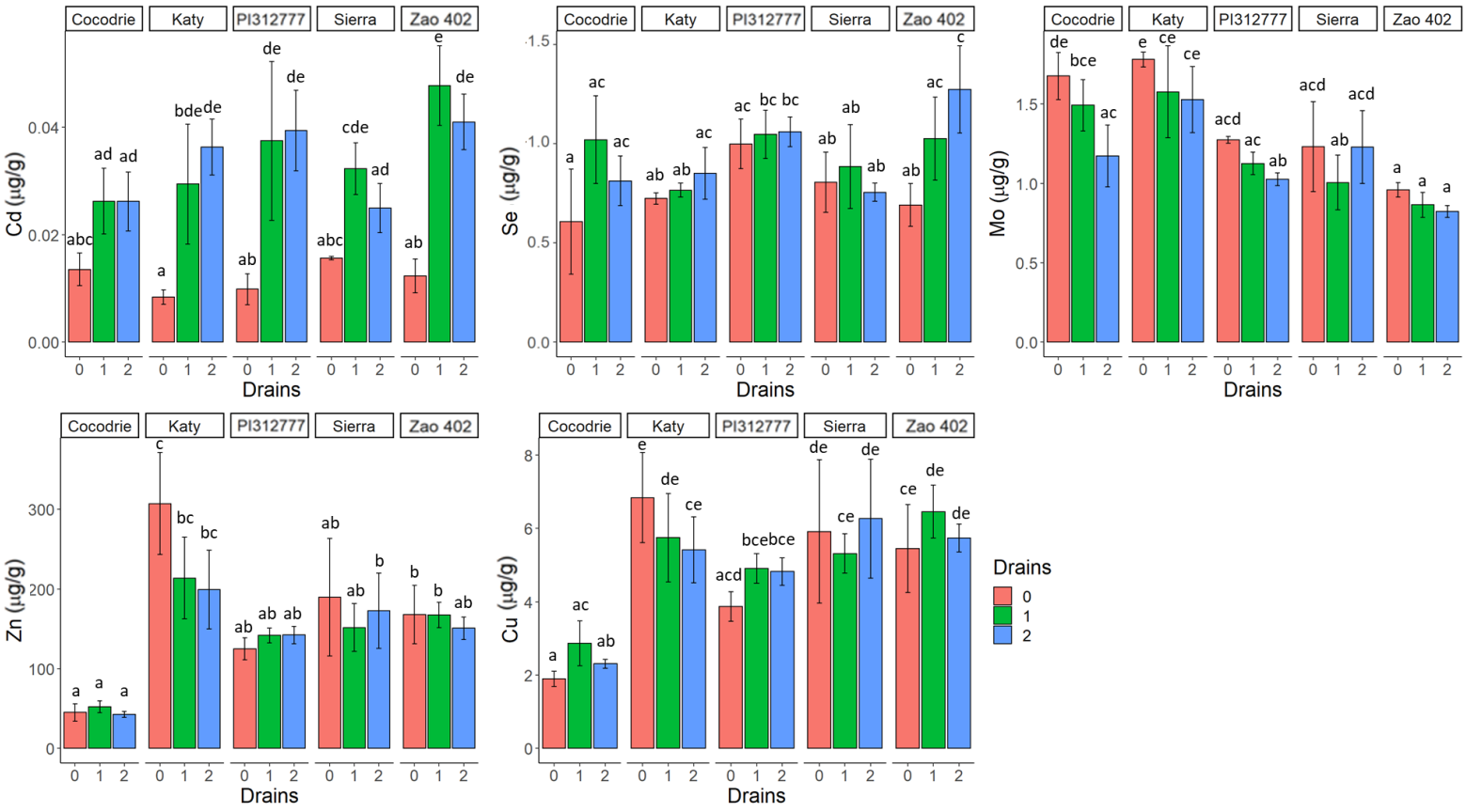

Figure 11. Grain concentrations of selected elements in 2018 brown rice samples. Different letters represent significant ($p<0.05$) differences between treatments and cultivars.

To evaluate the effect of interannual variability between study years, weather data from on-site sensors and the local weather station were compared. Soil and air temperature were of chief interest, as there is some evidence that higher soil temperatures alter

biogeochemical processes in the rhizosphere including mineral precipitation/dissolution, influencing As desorption and subsequent uptake by plants (Neumann et al., 2017; Muehe et al., 2019; Farhat et al., 2021). Soil temperature was measured using a Campbell 107 sensor at 6" depth, and air temperature was measured with a Campbell HPM50-ET Vaisala Temperature/RH probe installed on a weather station.

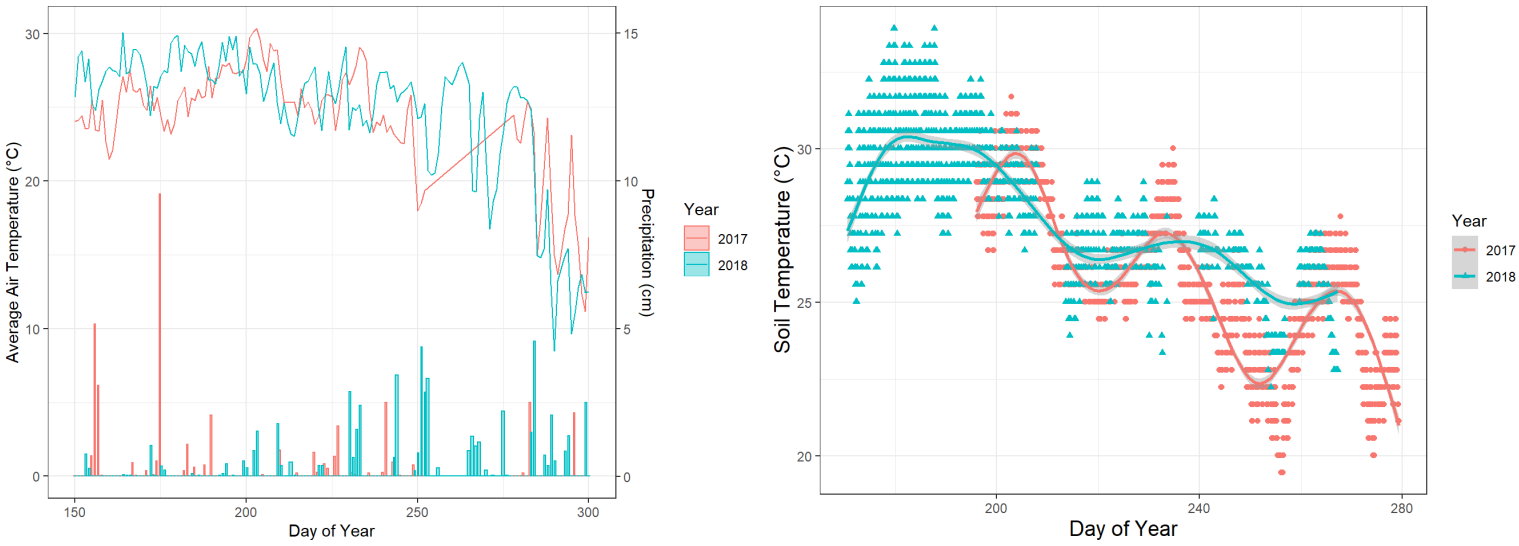

Figure 12. Average air temperature, precipitation, and soil temperature in Dale Bumpers field plots.

Soil temperature is higher on average in 2018 than 2017, while air temperature is similar in both years. Larger rain events occurred in the early growing season of 2017, while 2018 had more frequent rain events of moderate intensity.

Correlation & Principal Component Analysis

Rice Grain Data

Principal component analysis (PCA) was constructed for the rice grain data samples to reduce dimensionality and explore relationships between variables. Samples were grouped according to Variety and the following variables were considered: grain content (As, iAs,

DMA, Se, Fe, Mn, Zn, Cd, Cu, and Mo in µg/g) and mean soil temperature. Two variables were included that describe irrigation practice: "AWD" which refers to the overall irrigation scheme (0 for continuously flooded, 1 for AWD) and "Drains" which refers to the number of drains (0, 1, or 2). The first two components accounted for 51.6% of total variance. Samples did not cluster based on Variety but did cluster according to Year. Analysis of the vector loadings reveals that while total As and DMA have no relationship with mean soil temperature, iAs is positively correlated with mean of soil temperature. iAs has a weakly negative relationship with drains, with the negative correlation is much stronger for DMA and total As. For micronutrients, Se has a weakly positive correlation with drains, Mn, Cu, and Zn appear to have no relationship, and Mo has a weakly negative correlation with drains. Mn and Cu were highly positively correlated.

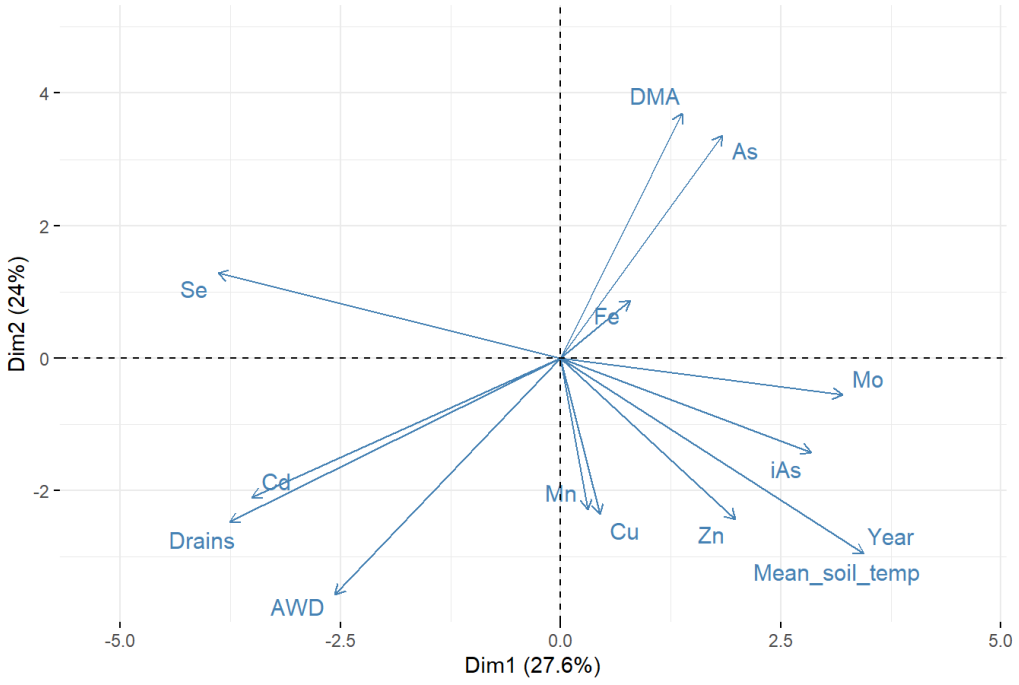

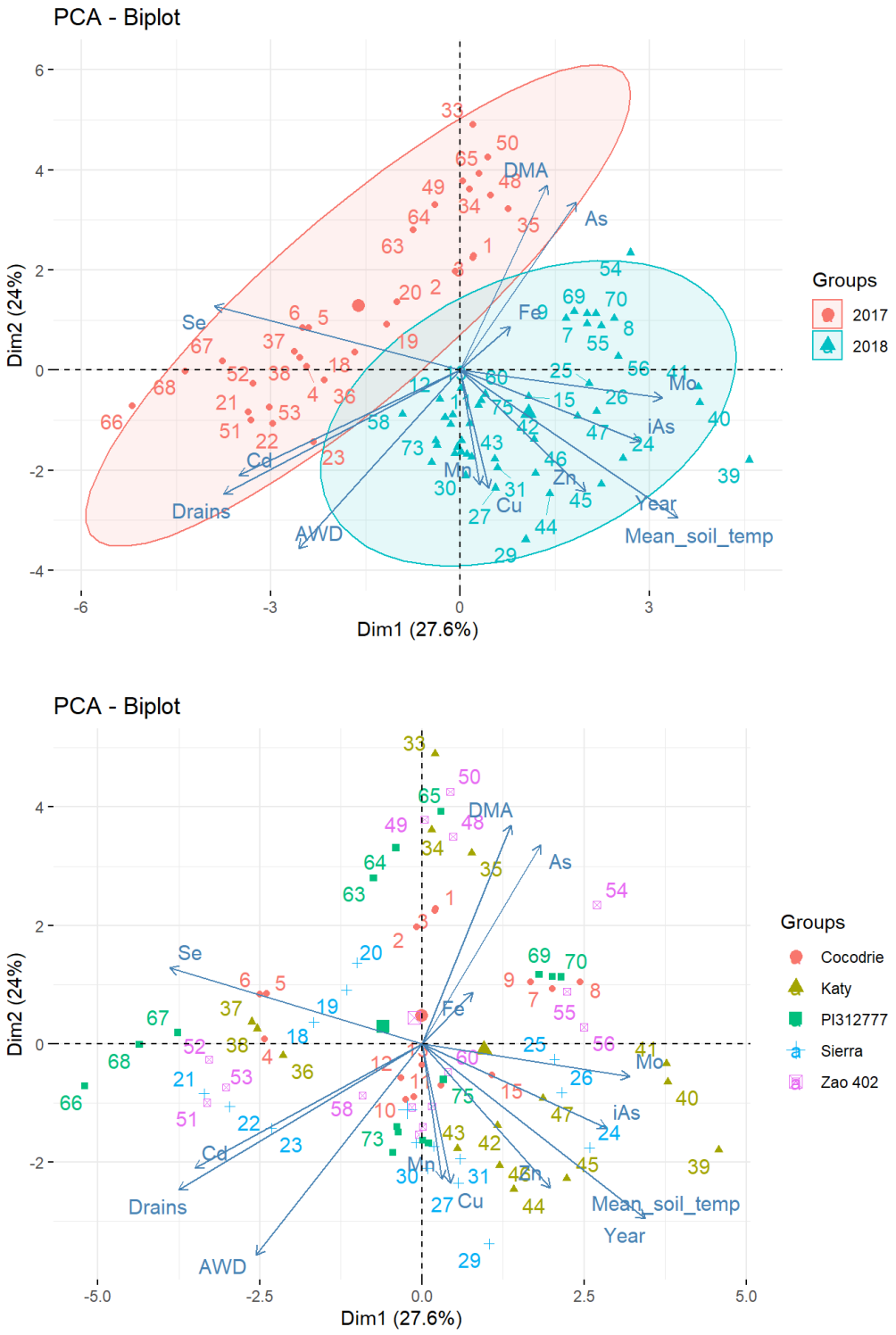

Figure 13. Principal Component Analysis of rice grain data. Top: PCA loading vectors. Middle: PCA biplot clustered by Year. Bottom: PCA biplot categorized by Variety.

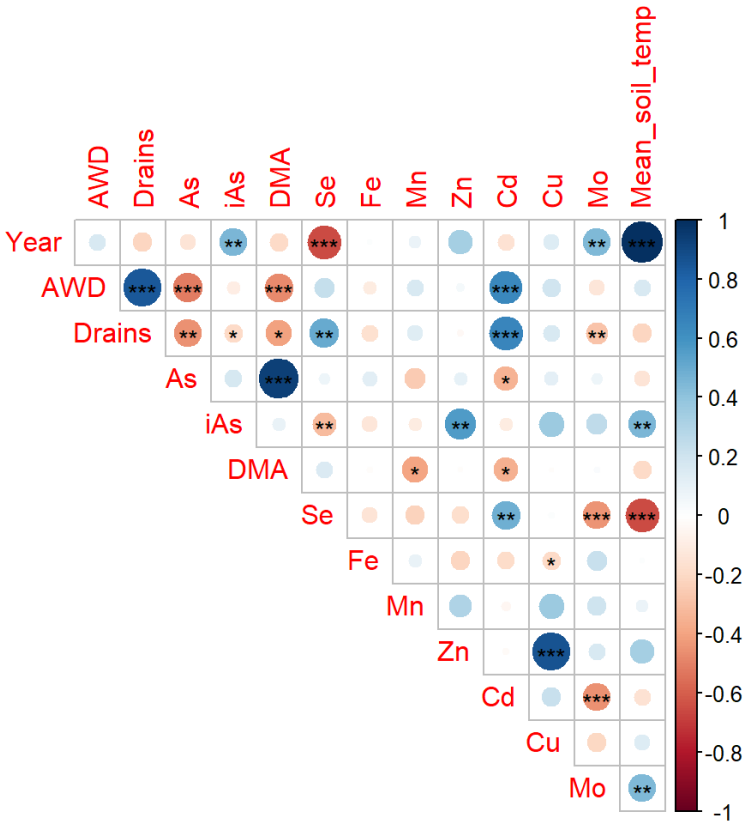

Figure 14. Correlation plot of rice grain data. One, two, and three asterisks denote 0.05, 0.01, and 0.001 levels of significance, respectively.

Pore Water Data

Pore water data from the entirety of the 2018 season from both shallow and deep wells were used to construct a PCA. The following variables were considered: drains (0, 1, 2) and pore water concentration of Mn, Fe, As, Al, P, S, Se, Mo, Cd, Sb, Cs, Ba, Zn, and Cu in µM. The first two components accounted for 63.4% of total variance. Samples clustered weakly according to the number of drains, and the number of drains was found to contribute most to PC2.

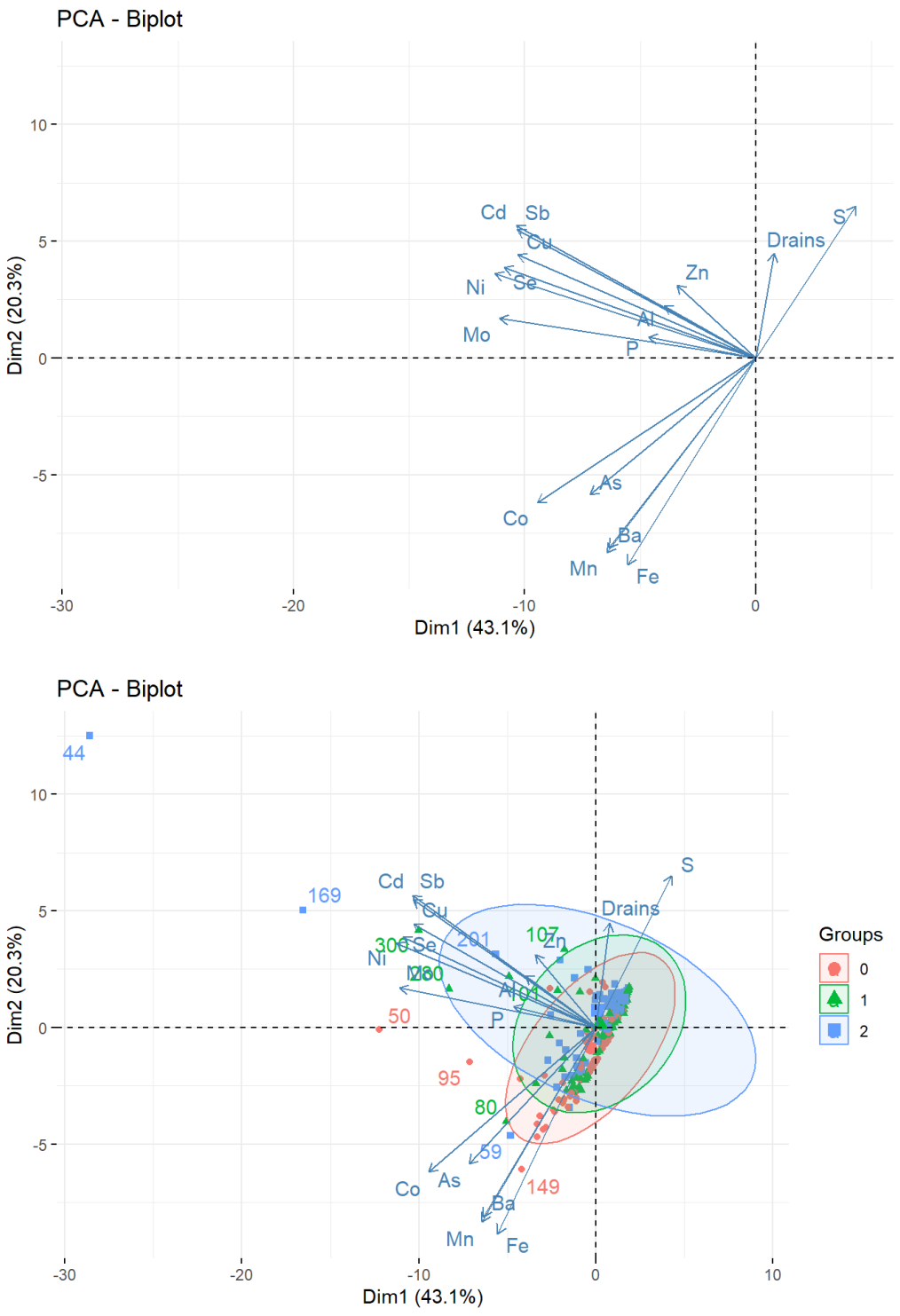

Figure 15. Principal Component Analysis of pore water data. Top: PCA loading vectors. Middle: Bottom: PCA biplot categorized by number of drains.

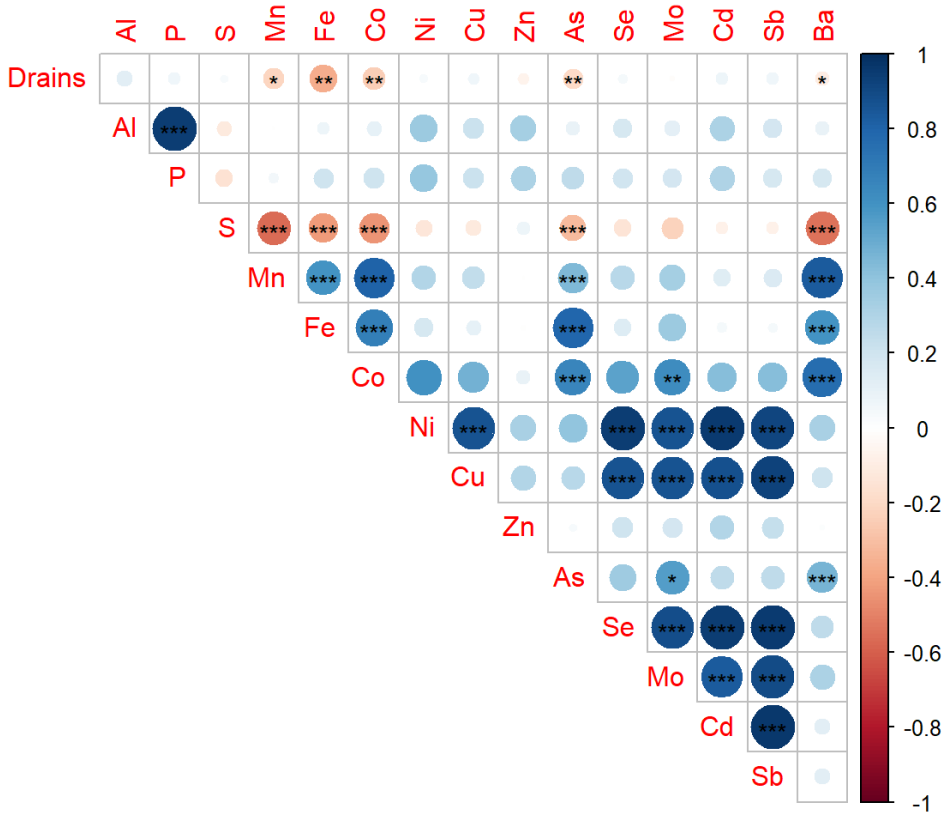

Figure 16. Correlation analysis of pore water data. One, two, and three asterisks denote 0.05, 0.01, and 0.001 levels of significance, respectively.

As, Mn, Fe, Co, and Ba are negatively correlated with drains, implying that oxygenation of the soil decreases solubility and/or release from the soil to the pore water. These same elements were found to be negatively correlated with sulfur (S). The remaining micronutrients have only weak correlation to drains.

The solubility and redox-sensitivity of some elements were also explored by plotting their pore water concentrations with respect to Fe, which is mobilized in reducing conditions (Fig. 17). As expected, Mn and As have a clear positive pattern with Fe. Se, Cu, and Mo also have weakly positive patterns with Fe, while Zn does not have a clear redox sensitivity. However, in the rice grain analysis, Se and Cu decrease with increasing Fe

content. For micronutrients, other factors like biological transporters may be more important than solubility for plant uptake.

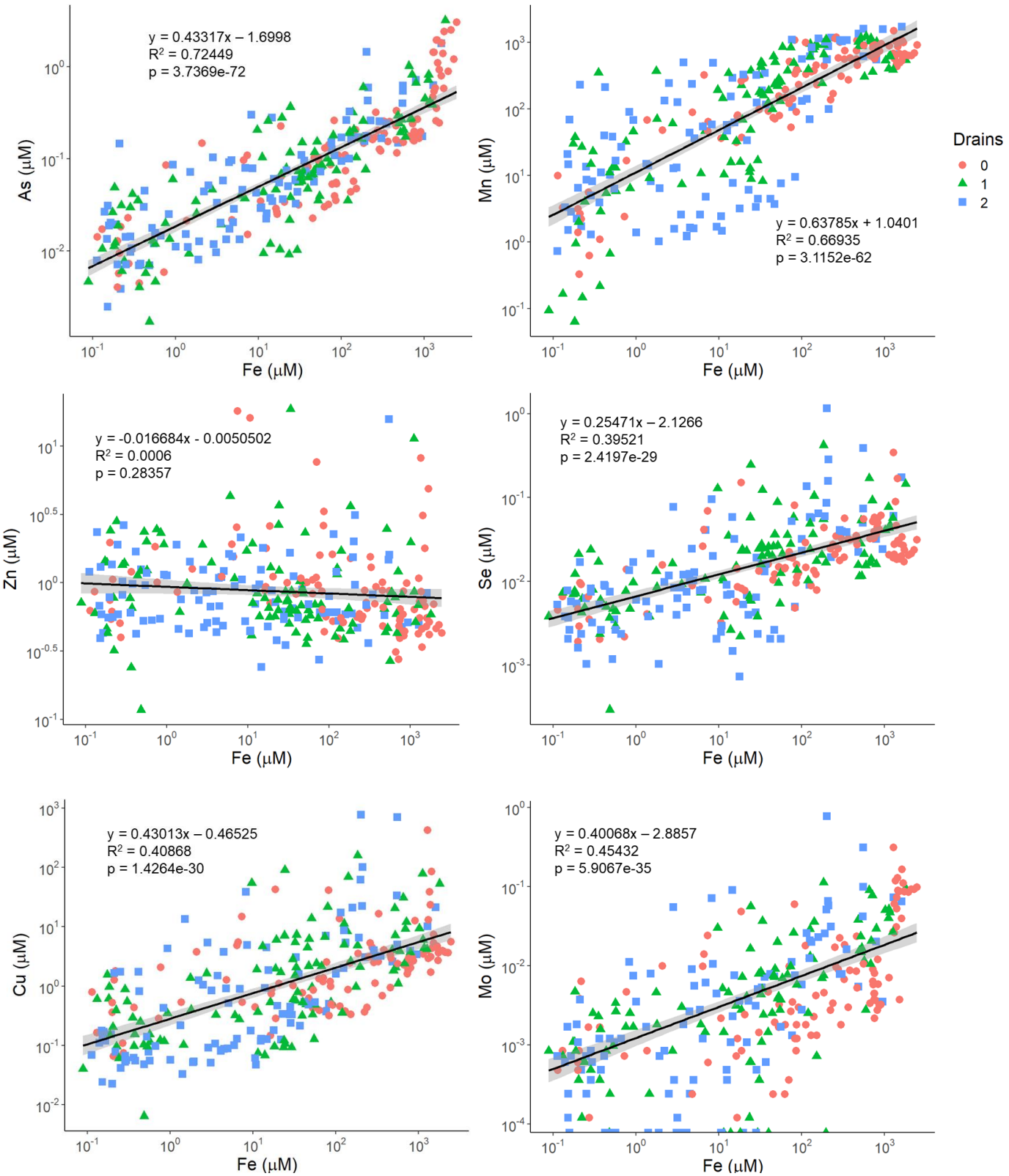

Figure 17. Relationships between dissolved Fe (µM) and As, Mn, Zn, Se, Cu, and Mo (µM) in pore water. Pore water concentrations are plotted on a log scale and fit with a linear model. The grey shading around the regression line represents the 95% confidence interval of the linear model prediction.

Linear Mixed-Effects Models

The pore water model was used to investigate how dry-downs impacted pore water concentrations during the reproductive phase of different cultivars in 2018. The time period chosen is relevant for all cultivars with the exception of Zao 402, which had a much earlier reproductive phase. Of all the elements tested with this model and subsequent ANOVA, only As_{total} and Fe were found to have statistically significant differences between 0 drain, 1 drain, and 2 drains. In both cases, AWD decreased the pore water concentrations as expected. While there are observable patterns that may be practically significant between 1 and 2 drains for other elements such as Mn, Cd, and Zn, they did not meet the $p < 0.05$ threshold. This is most likely attributed to wide variability between replicates in the pore water data.

Table 6. Model coefficients for pore water data collected in 2018 (ug/L). Statistically significant coefficients are highlighted green (positive) or red (negative). P-values < 0.05 are denoted with an asterisk.

	As_{total}	Fe	Mn	Cd	Zn	Cu	Se	Mo
Intercept	69.51	71941.1	38346.3	-0.069	44.00	2.11	2.52	4.27
Drains [1]	-50.29	-47985.8	-274.75	0.36	-5.33	1.33	-0.24	-2.5
Drains [2]	-56.46	-63543.9	-6846.76	3.66	5.98	4.05	1.89	-1.64
ANOVA p-value: Drains	*7.2e-5	*1.6e-11	0.52	0.15	0.48	0.22	0.32	0.22
%Variance explained by sampler:	17%	2%	1%	7%	1%	0%	2%	13%

To further investigate interannual differences, an LME model with the 0-drain condition rice grain data from both 2017 and 2018 was constructed for each element or compound of interest, with variety as the fixed effect and year as a random effect. The baseline is the mean of all observations from all varieties. The response variables used were

total As, iAs, DMA, Zn, Cd, Se, Cu, and Mo. The AWD samples were not compared since AWD was employed differently between years. The intraclass correlation coefficient (ICC), a descriptive statistic used to evaluate if there are systematic similarities among replicates, was significantly high for iAs (0.42), Zn (0.31), Se (0.61), and Mo (0.57). iAs, Zn, and Mo were higher on average in 2018; Se was higher on average in 2017.

Table 7. Model coefficients, ICC, and ANOVA p-values for 0-drain samples in 2017 and 2018 (µg/g). Statistically significant coefficients are highlighted green (positive) or red (negative). P-values < 0.05 are denoted with an asterisk.

	As_{total}	iAs	DMA	Zn	Cd	Se	Cu	Mo
Intercept	1.134	0.288	0.702	129.95	0.029	116.99	4.712	1.083
Variety [Cocodrie]	-0.28	-0.066	-0.129	-71.86	-0.009	-14.13	-2.034	0.245
Variety [Katy]	0.301	0.079	0.206	54.32	-0.005	-3.59	0.542	0.362
Variety [PI312]	-0.039	-0.034	-0.035	-12.79	0.007	24.67	-0.421	-0.063
Variety [Sierra]	-0.515	-0.032	-0.427	23.39	-0.002	-14.98	0.937	-0.226
% Variance explained by year:	3%	42%	8%	31%	3%	61%	6%	57%
ANOVA p-value:								
Variety	*4.31E-06	*1.15E-05	*3.89E-06	*1.46E-09	*1.57E-02	*4.22E-03	*2.78E-12	*6.43E-15

The 2017 and 2018 models were constructed with the same response variables, with variety and drains as the fixed effects and replicate as the random effect. The interaction term was also included in the models. The model coefficients determined to be statistically significant are highlighted in the tables below. The ANOVA p-value is given for the effect of Variety, Drains, and the interaction of Variety X Drains.

Table 8. Model coefficients (µg/g) and ANOVA p-values for 2017 rice grain data. Statistically significant coefficients are highlighted green (positive) or red (negative). P-values < 0.05 are denoted with an asterisk.

	As_{total}	iAs	DMA	Zn	Cd	Se	Cu	Mo
Intercept	1.680	0.241	1.106	94.612	0.019	117.459	3.955	0.9
Variety [Cocodrie]	-1.010	-0.035	-0.650	-51.674	-0.008	-46.335	-2.159	0.5

Variety [Katy]	0.505	-0.008	0.683	5.475	-0.008	22.851	-0.152	0.3
Variety [PI312]	0.202	-0.018	-0.062	-6.445	-0.001	20.485	-0.113	0.0
Variety [Sierra]	-1.239	-0.026	-0.878	29.279	0.008	-10.135	0.915	-0.5
Drains [3]	-0.878	-0.007	-0.609	26.818	0.027	55.795	1.043	-0.1
Variety [Cocodrie] * Drains [3]	1.296	-0.019	1.036	57.929	-0.013	44.435	1.839	-0.4
Variety [Katy] * Drains [3]	-0.266	0.010	-0.512	-5.901	-0.003	-31.295	-0.223	0.0
Variety [PI312] * Drains [3]	-0.394	0.005	-0.093	-6.092	0.029	38.345	-0.721	0.0
Variety [Sierra] * Drains [3]	0.882	-0.025	0.552	-1.699	-0.020	-32.802	0.124	0.2
ANOVA p-values:								
Variety	*1.35E-10	*0.012	*7.71E-09	*0.008	*5.34E-05	*0.0032	*1.25E-06	*3.08
Drains	*1.50E-01	0.772	*8.62E-09	*0.003	*1.16E-07	*2.53E-05	*2.95E-05	*1.73
Variety:Drains	*8.04E-10	0.96	*2.39E-08	*0.01	*0.001	*0.048558	*0.001	*0.001

Table 9. Model coefficients and ANOVA p-values for 2018 rice grain data. Statistically significant coefficients are highlighted green (positive) or red (negative). P-values < 0.05 are denoted with an asterisk.

	totAs	**iAs**	**DMA**	**Zn**	**Cd**	**Se**	**Cu**	**Mo**
Intercept	1.38	0.382	0.826	167.1	0.012	76.56	4.795	1.384
Variety [Cocodrie]	-0.246	-0.141	-0.188	-121.7	0.001	-15.76	-2.894	0.292
Variety [Katy]	0.185	0.179	-0.026	140.3	-0.003	-4.18	2.045	0.396
Variety [PI312]	0.056	-0.056	0.152	-42.1	-0.002	23.35	-0.928	-0.11
Variety [Sierra]	-0.462	0.014	-0.418	22.7	0.004	4.01	1.122	-0.153
Drains [1]	-0.497	-0.076	-0.314	-21.6	0.023	18.61	0.265	-0.171
Drains [2]	-0.503	-0.0539	-0.326	-25.4	0.022	18.48	0.116	-0.228
Variety [Cocodrie] * Drains [1]	0.057	0.066	0.118	28.5	-0.01	22.87	0.7	-0.013
Variety [Katy] * Drains [1]	0.068	-0.034	0.138	-71.9	-0.002	-14.07	-1.357	-0.032
Variety [PI312] * Drains [1]	-0.166	0.031	-0.212	38.5	0.005	-13.54	0.78	0.023
Variety [Sierra] * Drains [1]	0.102	-0.069	0.13	-16.3	-0.006	-10.39	-0.866	-0.055
Variety [Cocodrie] * Drains [2]	0.006	0.115	0.068	22.9	-0.009	2.01	0.292	-0.276
Variety [Katy] * Drains [2]	0.138	-0.101	0.113	-82.4	0.006	-5.75	-1.543	-0.024
Variety [PI312] * Drains [2]	-0.206	-0.002	-0.2	42.8	0.008	-12.46	0.843	-0.019
Variety [Sierra] * Drains [2]	0.3	-0.055	0.19	8.2	-0.012	-23.5	0.233	0.225
ANOVA p-values:								

Variety	*9.35E-08	*1.14E-05	*1.53E-06	*2.15E-10	*2.20E-03	*2.70E-03	*4.54E-09	*5.75E-10
Drains	*1.10E-07	*0.028	*8.65E-05	0.131	*1.39E-11	*3.20E-03	0.732	*1.00E-03
Variety:Drains	0.4473	0.39	0.585	0.123	*0.014	*0.0326	0.246	0.192

Discussion

A key outcome of this work is that variation in rice grain As content across irrigation treatments was controlled primarily by changes in DMA. In all but one case, DMA was lower in AWD fields than 0-drain fields. iAs, on the other hand, varied very little between treatments and was not statistically different in almost all cases. Carrijo et al. noticed a similar trend in white rice subjected to a single drying event but observed some variation in iAs in brown rice samples (Carrijo et al., 2019). A recent study observed little change in iAs between treatments in 2013, but a greater change the following year in 2014 when the soil moisture content was allowed to reach lower values during drains, suggesting that AWD may be effective at reducing grain iAs if a target soil moisture of 25-30% volumetric water content (~15 kPa) can be reached (Fernández-Baca et al., 2021). While both variety and drains were significant in determining total As concentrations, the effect of variety outweighed drains, observed in lower p-values (see Tables 6 & 7). This is in contrast to a previous study that found that As concentrations were more dependent on environment, with factors such as soil and sampling location accounting for 59.9% of variation in grain As concentration (Liu et al., 2021). However, this study did not vary irrigation techniques. The combined effects of Variety X Drains were significant in 2017 for total As and DMA, but were not significant for any As species in 2018. Previous studies have found significant environment X genotype interactions in field studies (Mahmudur et al., 2017; Liu et al., 2021). Norton et al. observed significant interactions between cultivars

grown in sites in India and Bangladesh (Norton et al., 2009) that were subjected to similar irrigation schemes, suggesting that the source of As contamination may be a relevant control on uptake. The varieties that had the greatest decrease in grain DMA across AWD treatments were Katy, PI312777, and Zao 402, the latter two being indica varieties. Conversely, the Sierra variety, selected because of its reputation as an As excluder, accumulated the least amount of As with little variation in species between irrigation treatments. Interestingly, Zao 402, which has a much shorter time to maturity than the other cultivars, has the highest amount of total As. This may be due to the timing of drying events; as a particularly early variety, Zao 402 entered the reproductive and grain-filling stages much earlier than the other varieties in this study, and therefore the dry-downs took place at a much later stage in the plant's development (Fig. 1). It has been suggested that there is a relationship between days to heading and total grain As concentrations, but a previous study of 69 World Rice Core Collection cultivars showed no significant relationship across many genotypes (Kuramata et al., 2018).

A second important outcome is that interannual differences play an important role in evaluating multi-year field studies. Modeling the 0-drain condition between 2017 and 2018 with year as the random effect revealed that grain levels of iAs, Zn, Se, and Mo were significantly impacted by year. We observed higher soil temperatures in 2018, especially in the first part of the growing season, and accelerated biogeochemical processes may have contributed to these differences. While As_{total} and DMA were not affected by year, iAs is of particular interest because of its status as a regulated compound in rice products. In 2018, there was a small, but statistically significant effect of 1 drain on iAs (-0.076 µg/g) which was not observed in 2017. A prior study also suggested there are strong environmental

factors controlling As speciation, and particular iAs content, when the same variety was planted in two different locations (Norton et al., 2009). The 2017 and 2018 plots were planted on opposite sides of a large field, introducing some possible spatial variability. Additionally, the dry-down intensities in 2017 varied from a maximum of 28 to 19 to 16 kPa at 6 inch depth, whereas the dry-downs in 2018 were both ~33 kPa. It is possible that the more intense dry-downs in 2018 led to great impact where the less intense dry-downs in 2017 did not. In our study, it is unclear whether the differences in adjacent field sites, dry-down duration and/or intensity, weather effects, or natural seasonal variability caused this to occur; average soil temperature higher in the beginning of the growing season in 2018 than 2017 and was comparable during the mid- and late- stages of growth.

Another outcome of this study is that both cultivar and environment are significant controls on rice micronutrients (Zn, Se, Cu, Mn) in addition to As. Notably, in 2018 the effect of cultivar was more significant than the effect of water management. Combined effects were significant in 2017, suggesting that different cultivars responded differently to AWD, but the same patterns were not observed in all cases in 2018. For example, in 2017, Cocodrie showed a genotype X environment coefficient of 44.435 for grain Se, while in 2018 the interaction term for 1 drain was 22.87 and for 2 drains was 2.01. More noticeable differences between varieties are evident in 2018; among varieties, Cocodrie accumulated the least Zn and Cu. Our hypothesis than divalent cations would behave similarly to Cd and oxyanion-forming metals would behave similarly to As is not confirmed by this study; the patterns are much less clear for the nutrients when compared to As and Cd. This is promising, as AWD could be employed to achieve reductions in contaminants while having a neutral or beneficial impact on the nutritional quality of the

rice. Biomass dilution may play some role in controlling nutrient concentrations, as yields varied between cultivar and irrigation type. In 2017 yields of all cultivars benefitted from AWD (Table 4), especially in straighthead susceptible varieties such as PI312777; decreased uptake of DMA may improve yields by reducing straighthead occurrence. Specifically, PI312777 yields in 2017 improved from an average of 1576 to 4913 lb/acre concurrent with a decrease in grain DMA from 1 µg/g to 0.34 µg/g. There was more nuance in 2018. Mahmudur et al. observed a 7-38% increase in yields in AWD fields when compared to continuously flooded (Mahmudur et al., 2017), which is consistent with our 2017 results. The 2018 dry-down periods were generally more intense and much longer than in 2017, which may have contributed to a decrease in yields in some varieties.

Pore water modeling revealed that As and Fe pore water concentrations varied significantly between treatments, while differences in redox-sensitive rice micronutrient pore water concentrations were not statistically significant. The dissolution and precipitation of Fe minerals, which act as binding sites for As in paddy soils, is largely dependent on redox poise and is unsurprisingly significantly affected by drains. While the pairwise comparisons between 0 – 1 drain and 0 – 2 drains is significant ($p<0.05$), there was no observable difference between 1 – 2 drains. This may be because the 2nd drain took place late in the growing season just before harvest, or because the residual effects of the 1st drain carried over for the rest of the season. This is corroborated by previously published work; Fe and As concentrations had not rebounded significantly after the 1st drain (Maguffin et al., 2020).

REFERENCES FOR CHAPTER 3

(1) Zavala, Y. J.; Gerads, R.; Gürleyük, H.; Duxbury, J. M. *Environ. Sci. Technol.* 2008, 42 (10), 3861–3866.

(2) Davis, M. A.; Signes-Pastor, A. J.; Argos, M.; Slaughter, F.; Pendergrast, C.; Punshon, T.; Gossai, A.; Ahsan, H.; Karagas, M. R. *Sci. Total Environ*. 2017, 586, 1237–1244.

(3) Nunes, L. M.; Li, G.; Chen, W. Q.; Meharg, A. A.; O'Connor, P.; Zhu, Y. G. *Environ. Sci. Technol.* 2021.

(4) Tsukahara, T.; Ezaki, T.; Moriguchi, J.; Furuki, K.; Shimbo, S.; Matsuda-Inoguchi, N.; Ikeda, M. *Sci. Total Environ.* 2003, 305 (1–3), 41–51.

(5) Linquist, B. A.; Anders, M. M.; Adviento-Borbe, M. A. A.; Chaney, R. L.; Nalley, L. L.; da Rosa, E. F. F.; van Kessel, C. *Glob. Chang. Biol*. 2015, 21 (1), 407–417.

(6) LaHue, G. T.; Chaney, R. L.; Adviento-Borbe, M. A.; Linquist, B. A. *Agric. Ecosyst. Environ.* 2016, 229, 30–39.

(7) Yang, J.; Zhou, Q.; Zhang, J. *Crop J.* 2017, 5 (2), 151–158.

(8) Suriyagoda, L. D. B.; Dittert, K.; Lambers, H. *Pedosphere* 2018, 28 (3), 363–382.

(9) Uraguchi, S.; Fujiwara, T. *Rice* 2012, 5 (1), 1–8.

(10) Rinklebe, J.; Shaheen, S. M.; Yu, K. *Geoderma* 2016, 270, 21–32.

(11) de Livera, J.; McLaughlin, M. J.; Hettiarachchi, G. M.; Kirby, J. K.; Beak, D. G. *Sci. Total Environ*. 2011, 409 (8), 1489–1497.

(12) Huang, B. Y.; Zhao, F. J.; Wang, P. *Environ. Pollut.* 2022, 293 (September 2021), 118497.

(13) Norton, G. J.; Douglas, A.; Lahner, B.; Yakubova, E.; Guerinot, M. Lou; Pinson, S. R. M.; Tarpley, L.; Eizenga, G. C.; McGrath, S. P.; Zhao, F. J.; Islam, M. R.; Islam, S.; Duan, G.; Zhu, Y.; Salt, D. E.; Meharg, A. A.; Price, A. H. *PLoS One* 2014, 9 (2).

(14) Oremland, R. S.; Stolz, J. F. *Trends Microbiol.* 2005, 13 (2), 45–49.

(15) Smedley, P. L.; Kinniburgh, D. G. *Appl. Geochemistry* 2017, 84, 387–432.

(16) Kirk, G. The Biogeochemistry of Submerged Soils; 2004.

(17) Reamer, D. C.; Zoller, W. H. *Science* (80-.). 1980, 208 (4443), 500–502.

(18) Carrijo, D. R.; Li, C.; Parikh, S. J.; Linquist, B. A. *Sci. Total Environ.* 2019, 649, 300–307.

(19) Li, C.; Carrijo, D. R.; Nakayama, Y.; Linquist, B. A.; Green, P. G.; Parikh, S. J. *Agric. Ecosyst. Environ.* 2019, 272 (November 2018), 188–198.

(20) Li, R. Y.; Stroud, J. L.; Ma, J. F.; Mcgrath, S. P.; Zhao, F. J. *Environ. Sci. Technol.* 2009, 43 (10), 3778–3783.

(21) Xu, X. Y.; McGrath, S. P.; Meharg, A. A.; Zhao, F. J. *Environ. Sci. Technol.* 2008, 42 (15), 5574–5579.

(22) Dai, J.; Tang, Z.; Gao, A.-X.; Planer-Friedrich, B.; Kopittke, P. M.; Zhao, F.-J.; Wang, P. *Environ. Sci. Technol.* 2022.

(23) Pischke, E.; Barozzi, F.; Blanco, A. E. C.; Kerl, C. F.; Planer-friedrich, B.; Clemens, S. 2022.

(24) Norton, G. J.; Pinson, S. R. M.; Alexander, J.; McKay, S.; Hansen, H.; Duan, G. L.; Rafiqul Islam, M.; Islam, S.; Stroud, J. L.; Zhao, F. J.; McGrath, S. P.; Zhu, Y. G.; Lahner, B.; Yakubova, E.; Guerinot, M. Lou; Tarpley, L.; Eizenga, G. C.; Salt, D. E.; Meharg, A. A.; Price, A. H. *New Phytol.* 2012, 193 (3), 650–664.

(25) Maguffin, S. C.; Abu-Ali, L.; Tappero, R. V.; Pena, J.; Rohila, J. S.; McClung, A. M.; Reid, M. C. *Geochim. Cosmochim. Acta* 2020, 276, 50–69.

(26) Wells, B. R.; Gilmour, J. T. *Agron. J.* 1977, 69 (3), 451–454.

(27) Chaney, R. L.; Green, C. E.; Lehotay, S. J. *Anal. Bioanal. Chem*. 2018, 410 (22), 5703–5710.

(28) Arao, T.; Kawasaki, A.; Baba, K.; Mori, S.; Matsumoto, S. *Environ. Sci. Technol.* 2009, 43 (24), 9361–9367.

(29) Reid, M. C.; Asta, M. P.; Falk, L.; Maguffin, S. C.; Cong Pham, V. H.; Le, H. A.; Bernier-Latmani, R.; Le Vo, P. *Chemosphere* 2021, 265.

(30) R Core Team. Vienna, Austria 2013.

(31) Bates, D.; Maechler, M.; Bolker, B.; Walker, S.; Haubo, R.; Christensen, B.; Singmann, H.; Dai, B.; Scheipl, F.; Grothendieck, G.; Green, P.; Fox, J.; Bauer, A.; Krivitsky, P. N. *Package 'lme4'*; 2022.

(32) Shi, Z.; Carey, M.; Meharg, C.; Williams, P. N.; Signes, A. *J. Expo. Heal.* 2020, 12 (4), 869–876.

(33) Muehe, E. M.; Wang, T.; Kerl, C. F.; Planer-Friedrich, B.; Fendorf, S. *Nat. Commun.* 2019, 10 (1), 1–10.

(34) Neumann, R. B.; Seyfferth, A. L.; Teshera-Levye, J.; Ellingson, J. *Agric. Environ. Lett*. 2017, 2 (1), 170006.

(35) Farhat, Y. A.; Kim, S. H.; Seyfferth, A. L.; Zhang, L.; Neumann, R. B. *Sci. Total Environ*. 2021, 763, 143049.

(36) Fernández-Baca, C. P.; McClung, A. M.; Edwards, J. D.; Codling, E. E.; Reddy, V. R.; Barnaby, J. Y. *Front. Plant Sci.* 2021, 11 (January), 1–15.

(37) Liu, S.; Ji, X.; Liu, Z. *Water, Air, Soil Pollut.* 2021, 1–11.

(38) Mahmudur, M.; Islam, M. R.; Naidu, R. *Sci. Total Environ.* 2017, 609, 311–318.

(39) Norton, G. J.; Duan, G.; Dasgupta, T.; Islam, M. R.; Lei, M.; Zhu, Y.; Deacon, C. M.; Moran, A. C.; Islam, S.; Zhao, F. J.; Stroud, J. L.; Mcgrath, S. P.; Feldmann, J.; Price, A. H.; Meharg, A. A. *Environ. Sci. Technol*. 2009, 43 (21), 8381–8386.

(40) Kuramata, M.; Abe, T.; Kawasaki, A.; Ebana, K.; Shibaya, T.; Yano, M.; Ishikawa, S. *Rice* 2018, 11 (1), 1.

CHAPTER 4: Transformation of Dimethylarsinic Acid in Rice Paddy Soils Under Alternate Wetting and Drying: Effects of Aerobic and Nitrate-Reducing Conditions

Adapted from: Lena Abu-Ali, Hyun Yoon, Scott Maguffin, Jai Rohila, Anna McClung, and Matthew C. Reid. To be submitted to *Agricultural Science & Technology*: August 2022.

Introduction

Arsenic (As) is a non-threshold human carcinogen and a contaminant of global importance (Miller et al., 2002; Smedley and Kinniburgh, 2002; Jomova et al., 2011). The ingestion of rice (*Oryza sativa*) has been identified as a major human exposure pathway to As (Schoof et al., 1999; Li et al., 2011; Davis et al., 2017; Nunes et al., 2021), since rice plants are grown in flooded conditions that promote As bioavailability and plant uptake (Roberts et al., 2009; Reinsch et al., 2010; Rawson et al., 2016). Concerns about dietary exposure to As have prompted regulatory agencies to introduce policy to limiting concentration of As in rice products. The United States Food and Drug Administration (FDA) has finalized an action level of 100 ug/kg of inorganic As in infant rice cereals (US Food and Drug Administration, 2020), prompting a need for more careful control of As-affected rice cultivation. However, this regulation is limited to inorganic arsenic (iAs), and disregards organic forms of As, which are less toxic but comprise a significant portion of total As in rice products (Marin et al., 1992; Seyfferth et al., 2014). Therefore, understanding the mechanisms that control As speciation in rice paddy environments is of crucial importance.

One strategy for reducing As uptake into rice grains is the practice of alternate wetting and drying (AWD), in which the water level in a typically continuously-flooded

rice paddy is allowed to drop and the soil becomes oxygenated (Linquist et al., 2015; LaHue et al., 2016; Yang et al., 2017a; Li et al., 2019a). The precipitation of previously dissolved Fe in Fe oxide minerals allows for adsorption of As, decreasing the amount available for plant uptake (Maguffin et al., 2020). The effect of AWD on total rice grain As concentrations has been studied extensively, with some attention to As speciation. Inorganic As occurs in either the trivalent form arsenite (As(III)), which is dominant in reducing environments, or the pentavalent form arsenate (As(V)), which dominates in oxidizing conditions (Masscheleyn et al., 1991). iAs can transform to organic As through the addition of one, two, or three methyl groups, which is a microbially-mediated process involving the *arsM* enzyme (Lomax et al., 2012; Li et al., 2016b). The most commonly observed organic forms of As are monomethyl- and dimethyl- arsenic acid (MMA and DMA, respectively). DMA in rice grains is associated with the physiological disorder straighthead in rice, which causes sterility and greatly decreases yields (Wells and Gilmour, 1977; Tang et al., 2020). Methylation of As has been observed in wetland environments, occurring under sulfate-reducing and methanogenic conditions as a microbial detoxification mechanism (Gebel, 2002; Chen et al., 2019). Demethylation, which is the removal of methyl groups from organic As, has been observed as well but is less understood (Chen et al., 2019; Zhang and Reid, 2021), with some claiming that microbes releasing more toxic forms of As may be a form of "chemical warfare" against neighbors (Huang et al., 2007; Yoshinaga et al., 2011; Chen et al., 2021).

Many prior studies of demethylation in soils focus on aerobic conditions, which are not always relevant to the deeply reducing environment of continuously-flooded rice paddies but may be applicable during the dry-down periods of AWD. Several microbial

pathways have been hypothesized for the biological process of demethylation. A previous study isolated a microbial community from golf course soils amended with an organoarsenical pesticide and proposed a two-step process whereby MMA(V) is first reduced by *Burkholderia* to MMA(III) and subsequently demethylated by *Streptomyces* to As(III) (Yoshinaga et al., 2011). The same group later identified and cloned the gene for an enzyme capable of degrading organoarsenical pesticides and other agricultural chemicals, *arsI* (Yoshinaga and Rosen, 2014). ArsI is posited to be a versatile enzyme capable of demethylating MMA(III) in oxic or anoxic conditions and *arsI* genes are commonly associated with dissimilatory nitrate reductase genes (Chen et al., 2021), linking demethylation to denitrification. The disappearance of DMAs, on the other hand, has been observed to coincide with methane production, suggesting that methanogenic archaea are involved in demethylation (Chen et al., 2019). Because As speciation is critically important in rice products, understanding controls on microbial demethylation is key for paddy soil management.

This study is motivated by observations that variable redox conditions in rice paddies primarily decrease the organic pool of rice grain As, rather than the regulated inorganic pool. Prior unpublished research on grain As speciation amongst different rice cultivars and irrigation strategies found that iAs was relatively constant across all conditions of genotype and environment, while DMA varied greatly and was the cause of reductions in As_{total} under AWD. The decrease in DMA concentrations with AWD has been observed in previous studies (Carrijo et al., 2019; Li et al., 2019a). However, no mechanism for this decrease has been confirmed. One hypothesis is that microbial methylation activity dominates in anoxic conditions and is inhibited by the oxic conditions brought on by AWD,

thus a decrease in the amount of methylated As is available for plant uptake. Interestingly, DMA sorbs less well to Fe oxides than iAs (Lafferty and Loeppert, 2005), suggesting that it would be less affected by AWD than iAs, adding another layer of uncertainty to the underlying mechanism. However, questions remain on the role of demethylation in decreasing rice grain DMA during oxic periods induced by AWD.

The objective of this study is to quantify changes in As speciation under variable redox conditions in both the aqueous and solid phases of a rice paddy environment. Soil microcosms created to mimic field conditions were incubated under both continuously-flooded and AWD water management schemes and monitored for approximately 6 weeks. The microcosms were monitored for concentrations of various metals and As speciation. Separately, batch reactors containing paddy soil were inoculated with DMA and maintained under anoxic and oxic conditions; the reactors were carefully monitored over a 12-day period. A subset of reactors was used for subsequent experiments investigating the effect of nitrate addition on demethylation rates. We hypothesize that (1) aerobic conditions promote demethylation in paddy soils and (2) the addition of nitrate increases demethylation by serving as a source of oxygen for demethylating microorganisms.

Materials and Methods

Soil Analysis

The paddy soil used in this study was sourced from Dale Bumpers National Rice Research Center in the mid-south U.S. rice production region, the dominant source of U.S.-grown rice. Previously published work has been done with these soils (Maguffin et al., 2020; Zhang and Reid, 2021). Samples were sent to the Cornell Nutrient Analysis Laboratory for characterization (Table 10). The soil texture was characterized as a Dewitt

silt loam (fine, smectitic, thermic, Typic Albaqualfs) (5% sand, 78% silt, 17% clay). The organic matter content was measured by the loss on ignition. The soil came from field plots designated for arsenic-related studies, and when under rice cultivation, the fields were amended with monosodium methyl arsenate (MSMA). Additional toxic and trace elements were determined by ICP-OES.

Table 10. Soil characteristics.

Organic Matter	As 189.042	Cd 214.438	Cu 324.754	Zn 206.200	Al 308.215	Fe 275.573	Mn 257.611	P 213.618	S 182.034
%	mg/Kg	mg/Kg	mg/Kg	mg/Kg	mg/Kg	mg/Kg	mg/Kg	mg/Kg	mg/Kg
1.65	15.57	0.15	3.39	33.29	4520	16178	900	393	90

Soil Microcosms

250 g of homogenized, air-dried soil mixed with 3 g of ground leaves was placed in clear plastic containers. A rhizon porewater sampler was inserted into the soil column at the halfway point of the column. The soil was first saturated and inundated with synthetic porewater (2 mM KCl, 1 mM $NaHCO_3$, pH 7) to achieve about 2 inches of standing water above the surface of the soil. All microcosms were placed into a plastic bin filled with water to the same height of the standing water in the individual containers to prevent oxygen diffusion through the clear plastic. Microcosms were kept in an environmental growth chamber at 27 °C and 80% relative humidity for 4 weeks to establish reducing conditions and As mobilization via reductive dissolution of Fe oxides. Approximately once per week, deionized water was gently poured into each microcosm to replenish water lost via evaporation. To simulate AWD, the relative humidity was lowered to 50% and half of the reactors were moved to a separate plastic container in front of a fan to encourage evaporation. The water level of the separated reactors was allowed to drop to the surface

of the soil for 7 days. On the 7th day, the soil was sampled from each microcosm for acid ammonium oxalate (AAO) extraction and the AWD reactors were re-flooded with deionized water. The purpose of the AAO extraction was to quantify the abundance and speciation of As associated with poorly-crystalline Fe oxide phases. Three subsamples were taken from different locations in each microcosm and pooled into one homogenized sample for the extraction. A 4th sample was taken from each microcosm, weighed, and dried overnight to determine the water content of the wet soil; the moisture content was used to normalize AAO measurements to dry mass of soil. Porewater samples were taken from the soil periodically by attaching a syringe to a three-way stopcock connected to the rhizon sampler. For all samples, the first few milliliters were discarded to null the void volume of the sampler tubing, and a subsequent aliquot was acidified for downstream ICP-MS and HPLC-ICP-MS analysis and stored in a refrigerator at 4 °C. Unacidified samples post re-flood were taken and stored for anion-IC analysis.

Soil slurry batch reactors

Thirteen soil slurry reactors were used in the batch experiments: 100 mL synthetic porewater (2 mM KCl, 1 mM $NaHCO_3$, pH 7) was added to 10 g (dry weight) of paddy soil and 1 g of crushed ground leaves in 250 mL glass media bottles. DMA solution was added to six of the reactors (3 anaerobic, 3 AWD) to achieve a starting concentration of 20 µM As. Another six reactors (3 anaerobic, 3 AWD) were not spiked with DMA. A sterile control with a final concentration of 1 mM sodium azide was monitored alongside the others. Long needles were used to bubble ultra-high purity N_2 into all reactors at the start of the experiment, with an additional needle inserted into the cap to promote sparging of the headspace. The reactors were sampled with sterile needles approximately daily for 6

days. A portion of the soil slurry was saved for subsequent AAO extraction; the rest of the slurry was filtered through a 0.22 μm filter and aliquots were acidified for ICP-MS and HPLC-ICP-MS. After the 6th day, the AWD reactors were disconnected from the N_2 supply and connected to an air pump to introduce oxygen. All reactors were monitored for an additional 6 days.

Nitrate experiments

After the conclusion of the prior experiment, the 3 anaerobic spiked reactors were split into 6 reactors of approximately equal volume in a Coy anaerobic chamber (O_2 < 10 ppm) to minimize oxygen exposure. All reactors were supplied with an additional 1 g of ground leaves to replenish the organic matter supply and an additional spike of DMA. Half the reactors were spiked with 10 mmol/kg nitrate in the form of $NaNO_3$. These reactors were sampled in the same way as described earlier at times 0, 9 h, 24 h, 48 h, and 72 h. Unacidified aqueous aliquots were used for anion IC to measure the disappearance of NO_3^- and aliquots diluted in 2% trace metal grade nitric acid were used for ICP-MS and HPLC-ICP-MS.

Chemical Analyses

Samples for minor and trace element analysis (As, Mn, Fe) were preserved in 2% trace metal grade nitric acid and measured via ICP-MS (Agilent 7800) with a helium reaction cell and rhodium as an in-line internal standard. Potential polyatomic interference from ArCl at *m/z* = 75 was assessed by testing samples diluted in 2% trace metal grade HCl, and none was detected. Calibration standards were prepared using a traceable multi-element standard. Arsenic speciation was measured via high performance liquid chromatography-inductively coupled plasma mass spectrometry (HPLC-ICP-MS) with a

Hamilton PRP X100 analytical column and an ammonium phosphate eluent method. The eluent used was 6.66 mM $(NH_4)_2PO_4$, 6.66 mM NH_4NO_3 adjusted to pH 6.2. Calibration standards were prepared by dissolving salts of MMA, DMA, and arsenate in Milli-Q water. Nitrate (NO_3^-) was measured using anion chromatography.

To extract As sorbed to poorly crystalline Fe minerals, an acid ammonium oxalate extraction (AAO) method was performed: A known amount of wet soil slurry was weighed into clean centrifuge tubes to which a 4:3 (v/v) mixture of 0.2 M ammonium oxalate and 0.2 M oxalic acid mixture adjusted to pH 3 was added. Tubes were capped, wrapped in aluminum foil, and mixed for 4 hours in a tube rotator or shaking plate. After mixing, tubes were centrifuged briefly to clarify the solution and the supernatant was filtered through a 0.2 µm filter. Extracts were stored at 4 °C until analysis with ICP-MS and HPLC-ICP-MS.

Results and Discussion

Soil microcosms

Dissolution of Mn and Fe minerals occurred rapidly in the soil microcosms, with high levels of dissolved Mn and Fe detected after 7 days. Dissolved As concentrations increased simultaneously and reached 100 µg/L after 7 days of inundation. Initially, Mn, Fe, and As concentrations were similar in the continuously flooded and AWD microcosms. After two weeks, Mn and Fe concentrations began to decrease, which may have been due to the precipitation of carbonate or sulfide minerals (Maguffin et al., 2020), which is likely in a reducing soil enriched with organic matter. Similar trends were seen in an anaerobic soil incubation in a previous study (Maguffin et al., 2020). Dissolved As increased for the first three weeks and leveled out between 200-400 µg/L just before the dry-down began on day 28. During the dry-down, dissolved Fe and As fell sharply in the AWD microcosms

and remained near limit-of-quantification levels for the following 7 days. A gradual decrease in As concentrations was also seen in the continuously flooded microcosms, which could have been caused by lower As solubility associated with precipitating minerals scavenging As (Wolthers et al., 2005; Burton et al., 2014) and is in agreement with the decreases in dissolved Mn and Fe during the same period (Fig. 19).

Arsenic speciation varied with time and experimental treatment. In the first four weeks of the experiment, the AWD and continuously-flooded microcosms had similar amounts of dissolved As, dominated by iAs, with ~20-25% of total As present as DMA. Unknown species of As were also detected, along with minimal amounts of MMA. In the

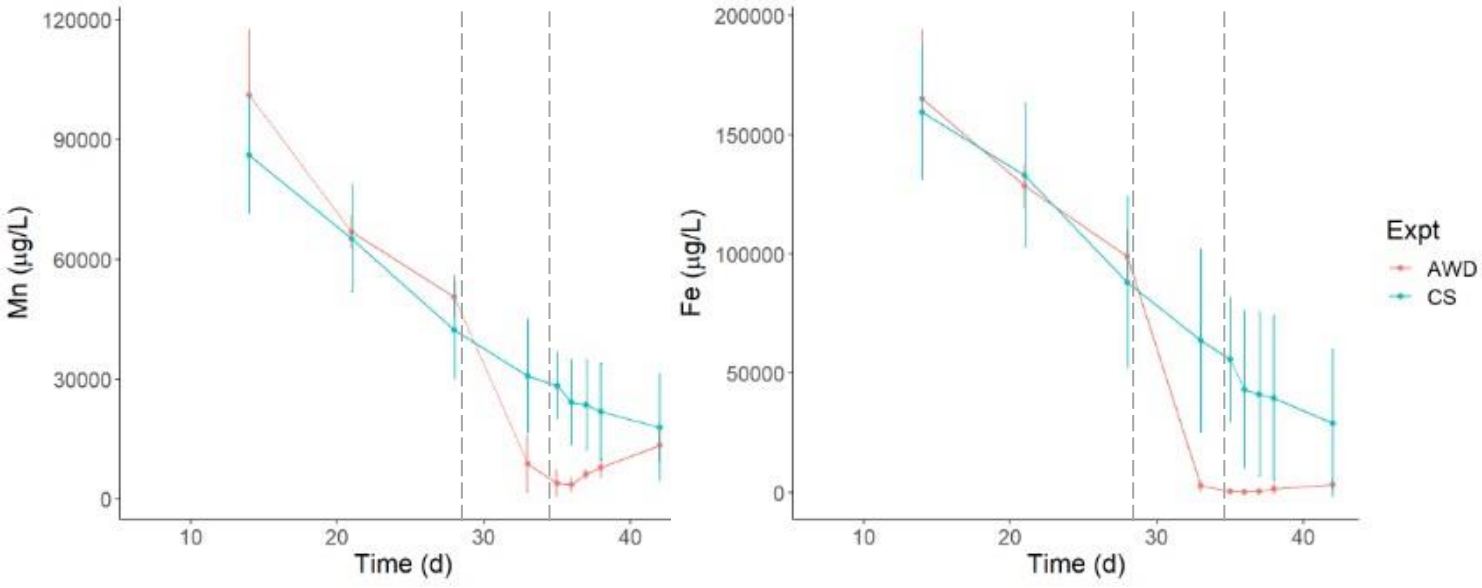

Figure 18. Dissolved Mn (left) and Fe (right) in soil microcosm experiments. Error bars represent range of triplicates. Vertical dashed lines represent the period in which the reactors were drained and reflooded.

continuously-flooded microcosms, the amount of DMA remained stable through the first 5 weeks, while iAs decreased with considerable variation between triplicates. After the dry-down, the only species observable in aqueous samples from the AWD microcosms was iAs. AAO analysis of the AWD soil (data not shown) during the dry-down showed that

only iAs was associated with the solid phase; it is possible that the aqueous DMA was first demethylated to iAs before sorbing to Fe minerals.

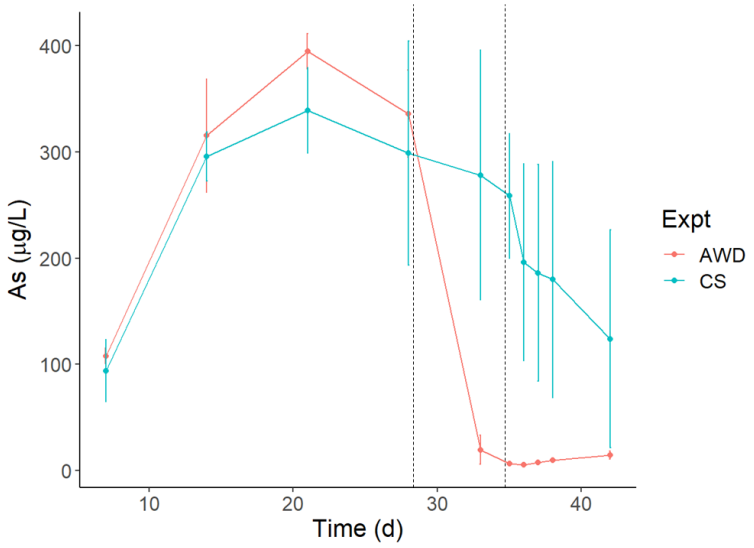

Figure 19. Dissolved As in soil microcosms. Error bars represent range of triplicates.

High levels of nitrate (~60 mg/L as NO_3^-) were detected in aqueous samples from AWD microcosms immediately following the re-flood (Fig. 21), showing that aerobic conditions caused nitrification of reduced N in the AWD soils. This nitrate was rapidly depleted over the course of 48 hours as anaerobic conditions were re-established, allowing denitrification to occur. Conversely, nitrate levels were consistently low but detectable in the continuously flooded microcosms during the reflooding period. Both molecular oxygen and nitrate are posited to be sources of oxygen for demethylating organisms (Yoshinaga and Rosen, 2014; Chen et al., 2021), so it is unclear if changes in As speciation are attributed to the dry-down or the presence of nitrate in the AWD microcosms. The de-coupling of these mechanisms in the batch soil slurry experiments allowed for evaluation of each mechanism separately.

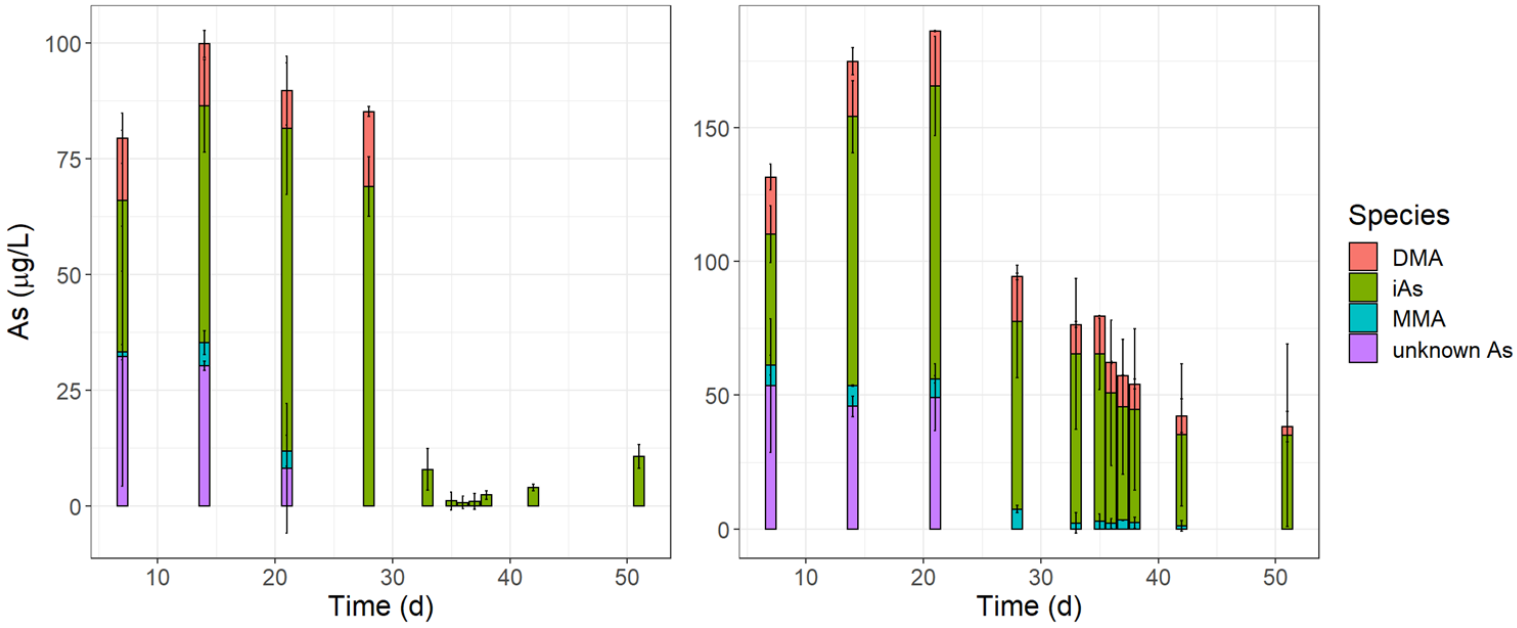

Figure 20. Arsenic speciation in soil microcosms. Error bars represent range of triplicates.

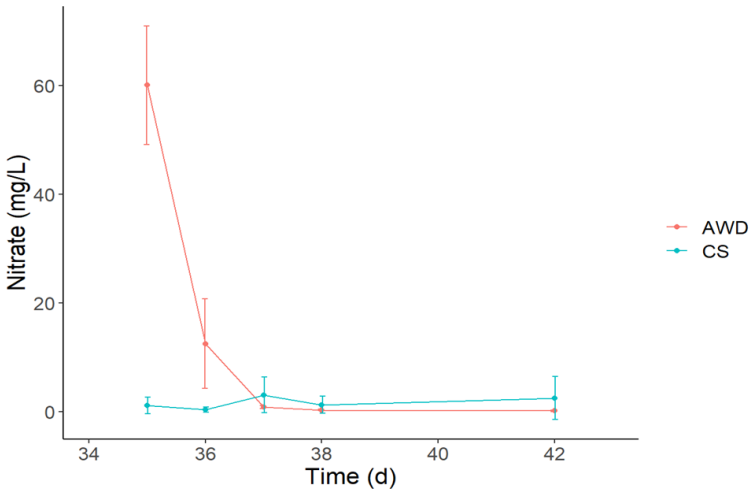

Figure 21. Nitrate (mg/L as NO_3^-) in soil microcosms following re-flood on day 35. Error bars represent range of triplicates.

Batch soil slurries

Dissolved Mn and Fe (Fig. 18) were used as redox indicators in the batch experiments. Concentrations of aqueous species are express as µg/g soil (dry weight) to enable comparisons between aqueous and solid-phase data. Dissolved Mn is observed immediately in all experiments and increases steadily throughout the duration of the experiment in anaerobic reactors. In the AWD reactors, dissolved Mn decreases slightly after the oxic transition but remains elevated in solution. Some Mn release is observed in the sterile control, which is attributed to desorption of Mn^{2+} from soil mineral surfaces and has been observed in a previous study (Maguffin et al., 2020). Dissolved Fe appeared in all aqueous samples after 2 days, except for the sterile control which showed no Fe throughout the course of the experiment. Fe release was steady in the anaerobic reactors, suggesting that anoxic conditions were maintained, and mineral dissolution was constant. In contrast,

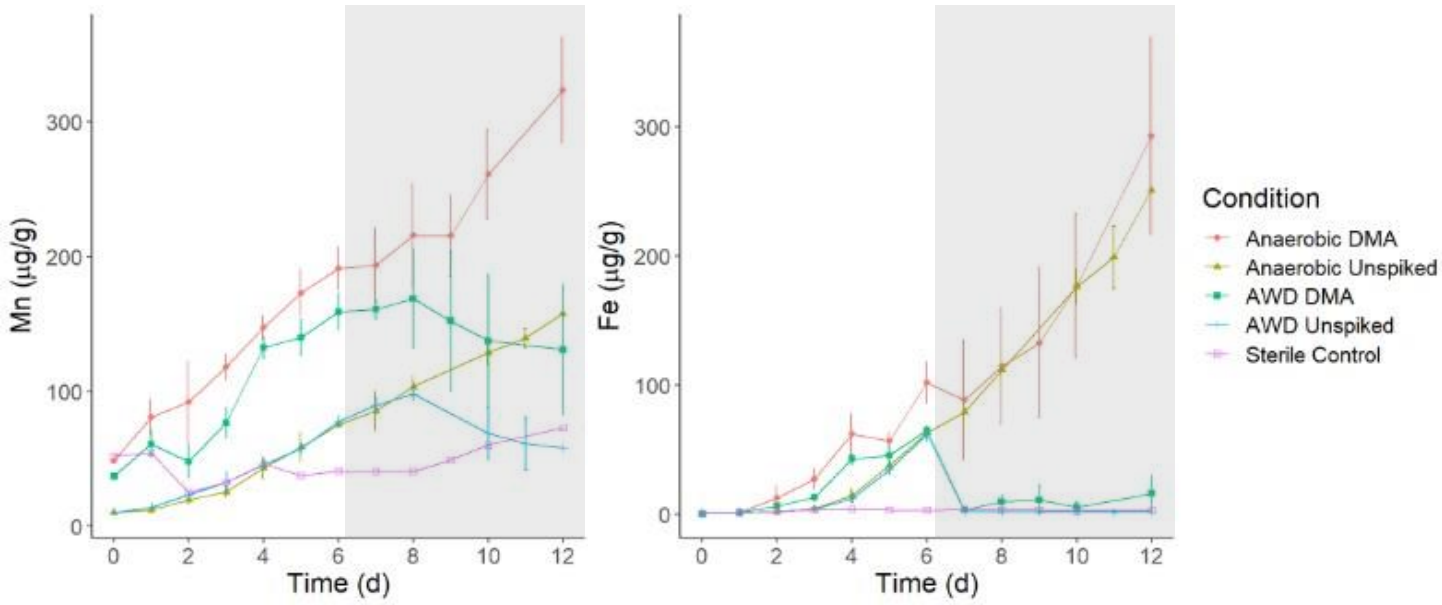

Figure 22. Dissolved Mn and Fe in batch soil slurries. Shaded area represents the time when AWD reactors were bubbled with air to introduce oxic conditions. Error bars represent range of triplicates.

dissolved Fe dropped to near-zero after the oxic transition in the AWD reactors and only recovered minimally over the remaining 6 days.

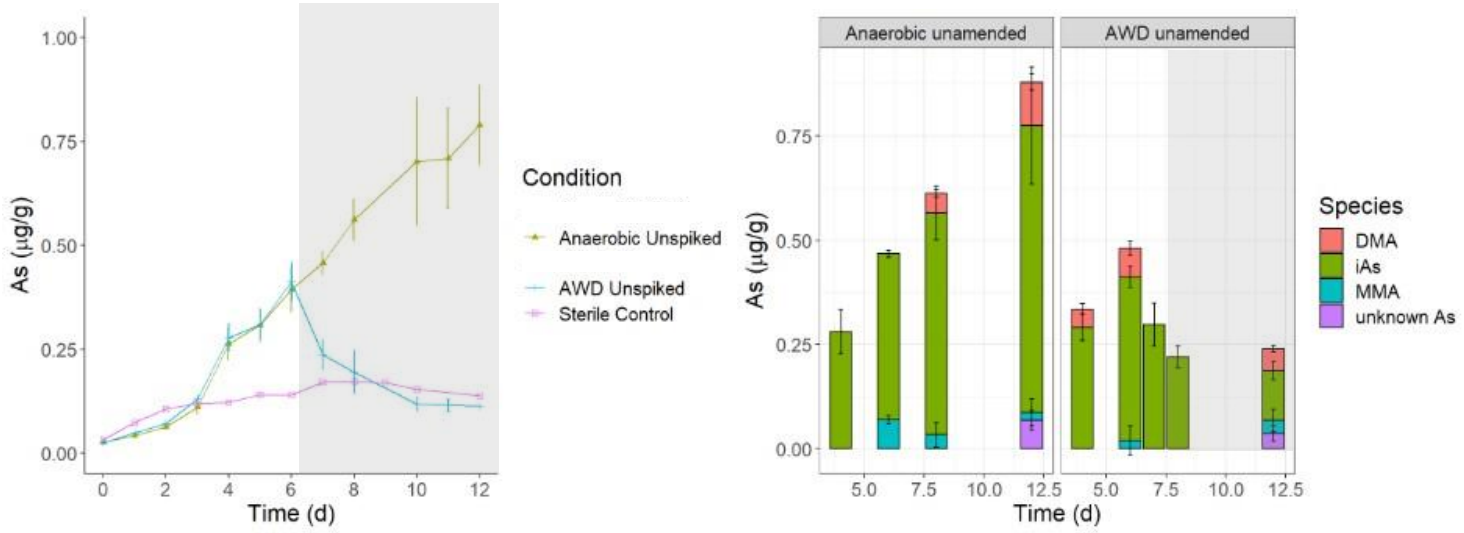

Figure 23. Dissolved As in unspiked reactors and sterile control; error bars represent range of triplicates (left). As speciation in unspiked reactors (right). Error bars represent standard deviation of triplicates.

Dissolved As measurements of the unspiked reactors show a release of ~ .75 µg/g As over 12 days in anaerobic conditions (Fig. 23). This residual As associated with the soil was identified to be predominantly iAs, with DMA detected in samples in day 8 and later. Trace amounts of MMA and an unidentified As species were also present in the unspiked samples. Under AWD, dissolved As decreased by nearly 50% and only iAs was measured in samples on day 7 and 8; on day 12, DMA, MMA, and unknown As were also detected.

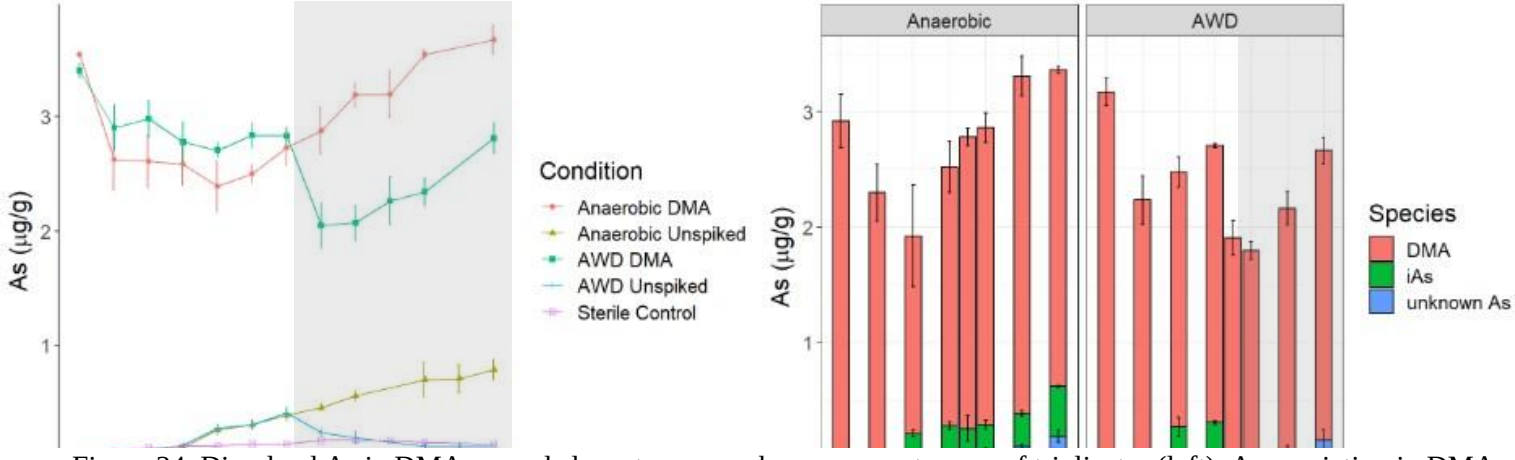

Figure 24. Dissolved As in DMA-amended reactors; error bars represent range of triplicates (left). As speciation in DMA spiked reactors (right). Error bars represent standard deviation of triplicates.

The DMA-amended reactors had a slightly different pattern; there is a decrease in dissolved As measured over the first 4 days of the experiment, probably due to sorption to soil minerals. After 4 days, dissolved As climbs steadily in the anaerobic reactors to an average of 3.5 µg/g on day 12 due to reductive dissolution of Fe oxide phases (Fig. 22). Only DMA is detected before day 4; after day 4 iAs is detected and increases through day 12. Unknown As is detected in samples after day 8 and increases through day 12. In the AWD condition, As begins to increase on day 4 but decreases sharply from an average of 2.8 µg/g to an average of ~2 µg/g after the oxic transition on day 6. Interestingly, the As levels rebound slightly to an average concentration of 2.5 µg/g on day 12. The speciation in the AWD reactors is very similar to the anaerobic reactors until the oxic transition, after which iAs is no longer detected on days 7 and 8. It is likely that the aqueous iAs sorbed to newly formed Fe minerals during this time, as iAs (especially As (V)) has a high affinity for Fe oxides. Notably, there is a decrease in the dissolved DMA as well, and our solid phase extraction results (Fig. 25) show a corresponding increase in sorbed iAs, providing some evidence for denitrification. Similar to the anaerobic condition, a small amount of unknown As appears on day 8 and increases until day 12.

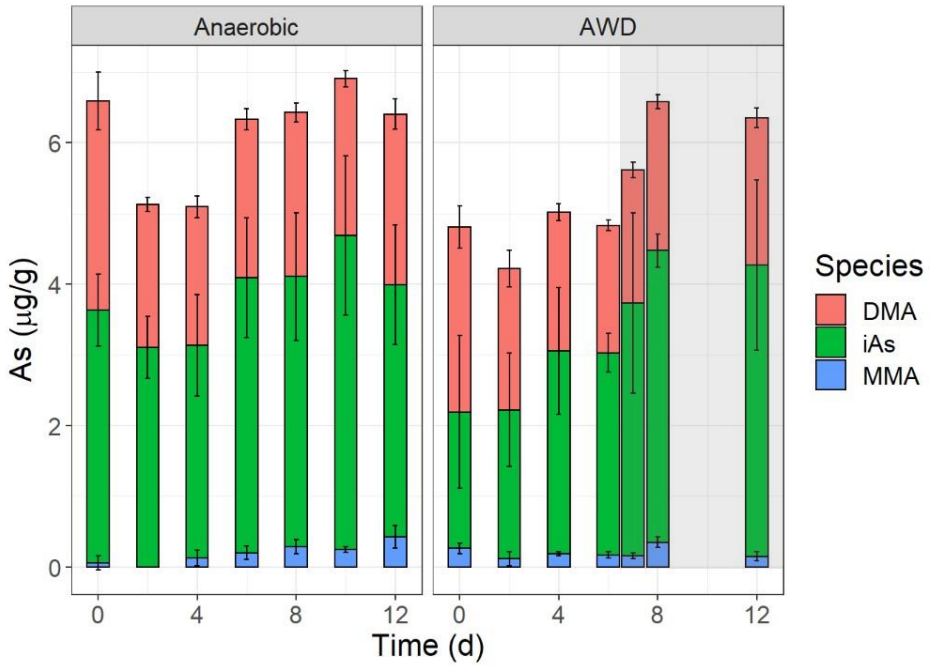

Figure 25. As speciation in AAO extracts in DMA-amended reactors. Error bars represent standard deviation of triplicates.

Extraction of the solid phase of the anaerobic DMA-amended reactors revealed that the relative amount of DMA was high after the first sample but decreased slightly and stayed relatively stable for the duration of the experiment. The amount of iAs was relatively consistent at approximately 4 µg/g but increased slightly over time. There was very little MMA detected in these samples, but the proportion appears to increase slightly over time. In the AWD reactors, DMA is stable while the proportion of iAs increases over time, concurrent with a loss of iAs in the dissolved phase (Figure 26), pointing to likely sorption of iAs. During the dry-down, As(III) which dominates in anaerobic conditions may have oxidized to As(V) which sorbed more strongly the newly precipitated iron oxides in the reactor (Lafferty and Loeppert, 2005). The dissolved DMA also decreases between the anoxic-oxic transition and corresponds with the large increase of iAs to the solid phase;

demethylation of DMA to iAs and subsequent sorption to soil minerals may have also contributed to the additional 1 µg/g iAs sorbed.

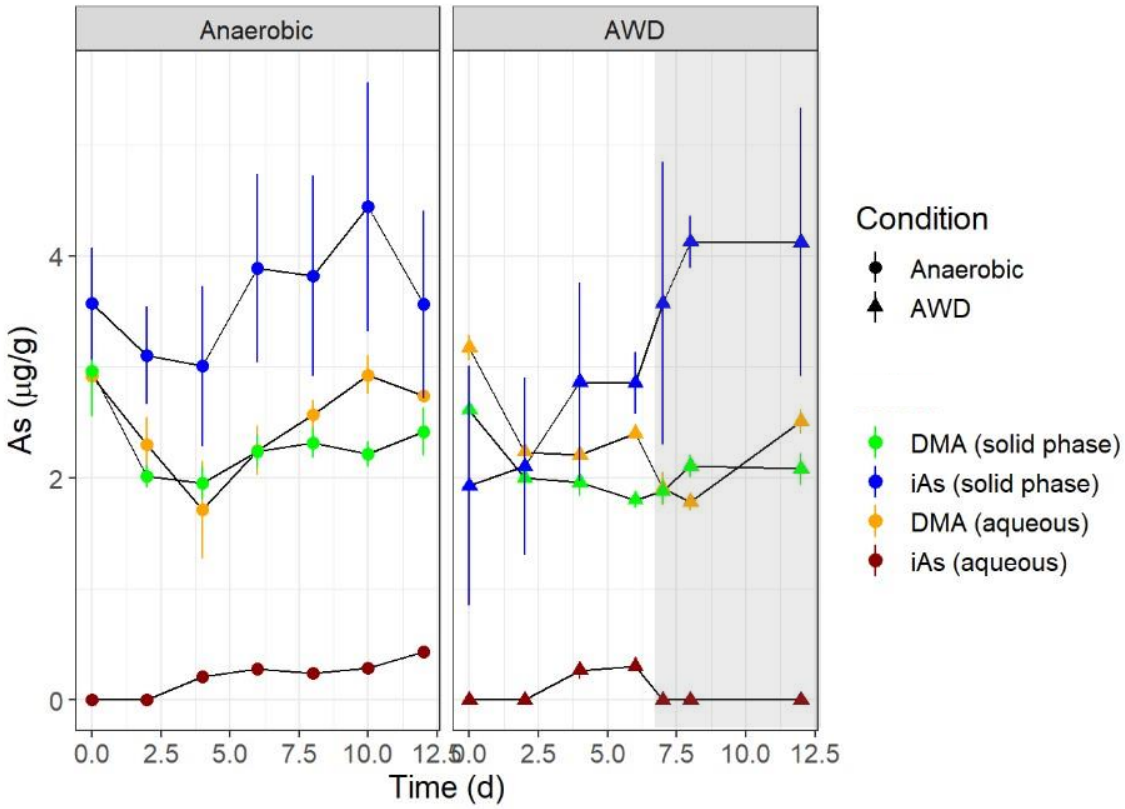

Figure 26. DMA and iAs in the solid and aqueous phases of the DMA-amended reactors. Error bars represent standard deviation of triplicates.

Nitrate experiment

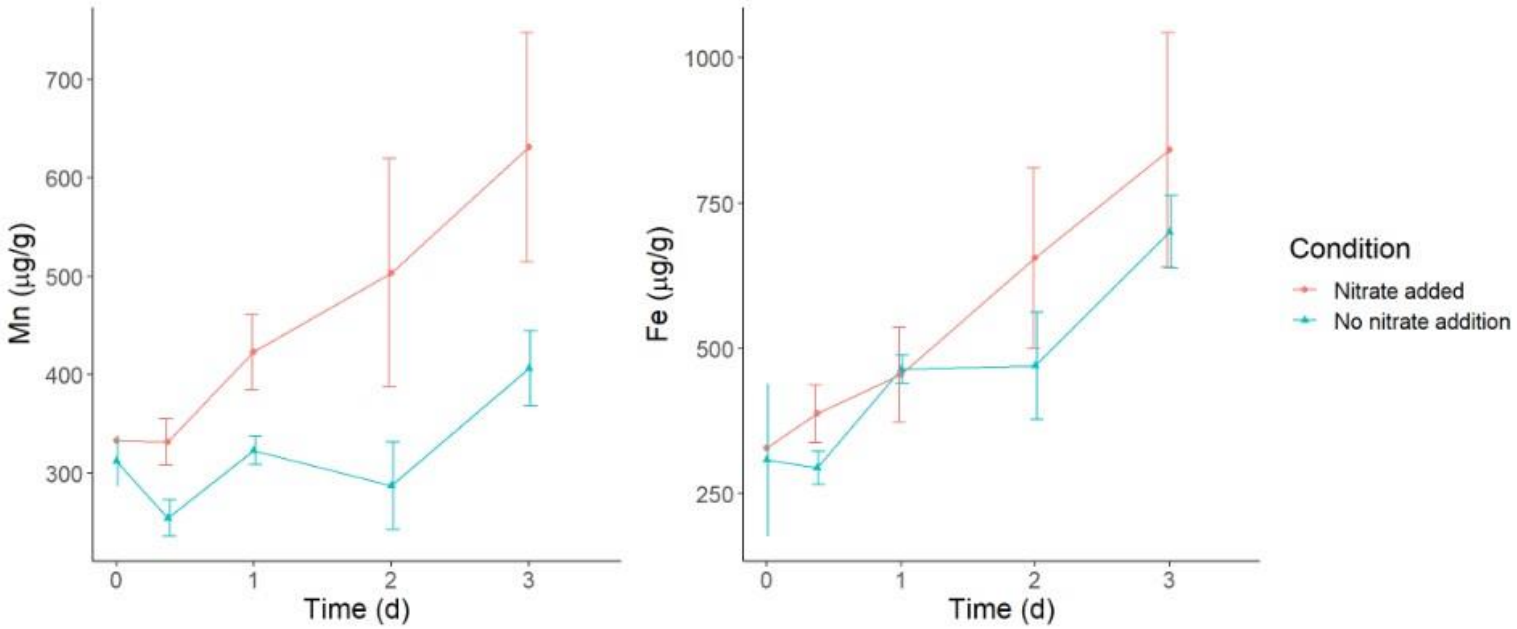

Figure 27. Dissolved Mn (left) and Fe (right) in nitrate experiments. Error bars represent range of triplicates.

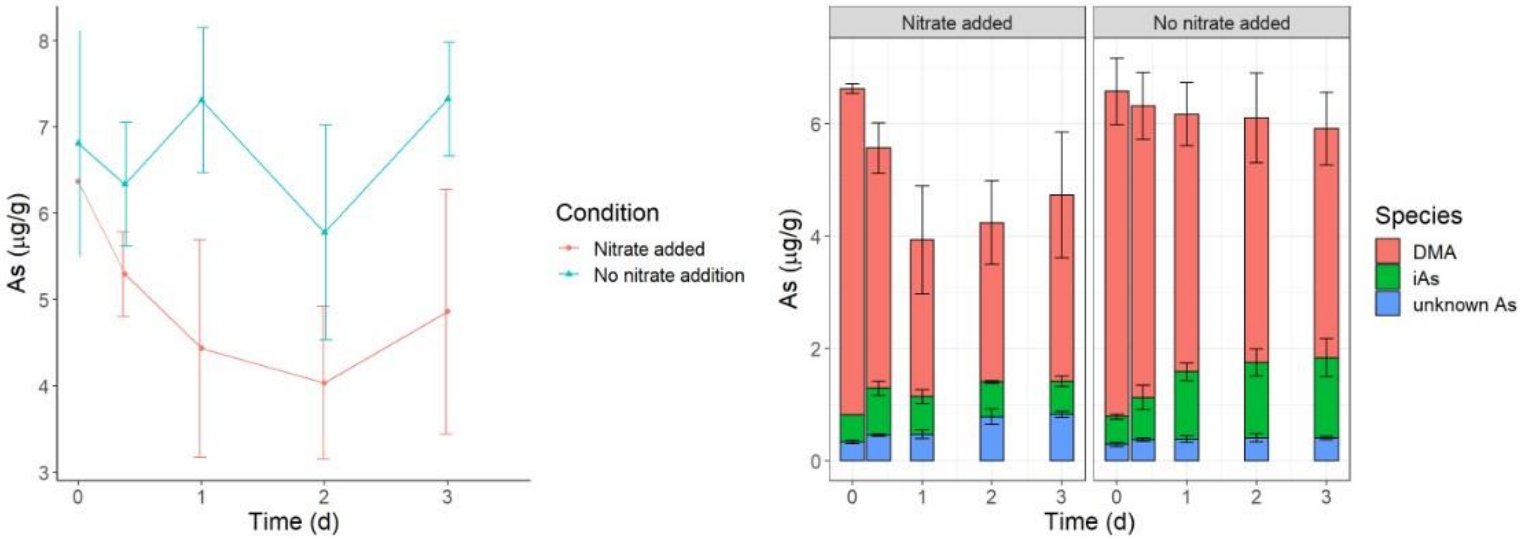

Figure 28. As concentration and speciation in nitrate experiments. Error bars represent range of triplicates (left). Error bars represent standard deviation of triplicates (right).

As stated previously, the three anaerobic DMA-amended batch reactors from the 12-day experiment were split into 6 for the nitrate experiment in an anaerobic chamber. All received additional leaves as an organic matter source and another spike of DMA solution, while half were also spiked with nitrate. During the first 9 hours of the experiment, there

was little change in the dissolved Mn and Fe concentrations in both the nitrate added and no nitrate added reactors. After this brief lag, dissolved Mn and Fe continued their upward trends, suggesting that redox conditions were still reducing. Dissolved Mn was higher in the reactors with nitrate added and dissolved Fe was similar in both conditions. The addition of nitrate had a significant effect on the As in the system when compared to the no nitrate added condition. The reactors with added nitrate had lower As throughout the experiment, with a decrease in average concentration over the first 2 days. Where there was no nitrate added, As concentrations were relatively stable and higher overall. As speciation in the aqueous samples reveals that DMA decreases ~50% in 24 h in the nitrate added reactors, while iAs remains stable. In the no nitrate added reactors, there is a ~30% gradual decrease in DMA and an increase in iAs, while the total As remains relatively stable. In all reactors there was some amount of unknown As that was not identified as

DMA, MMA, or iAs; its low column retention time suggests it may the tri-methylated species trimethylarsine oxide (Huang et al., 2012).

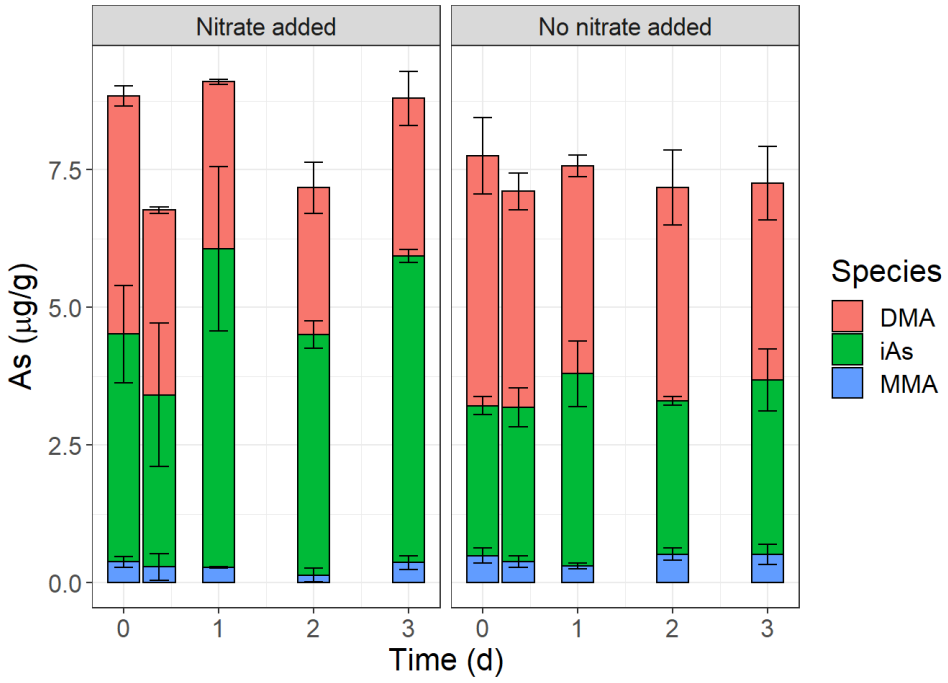

Figure 29. As speciation in AAO extracts in nitrate experiments. Error bars represent standard deviation of triplicates.

The solid-phase AAO data (Fig. 29) shows that there was significantly more sorbed iAs in the nitrate-amended reactors, despite being supplied with an equal amount of DMA. Solid-phase iAs increases concurrently with the disappearance of aqueous DMA (Figure 30), offering strong evidence for denitrification-driven demethylation of DMA to iAs with a subsequent sorption step. This observation is in agreement with previous claims that denitrification is coupled to demethylation, and that the oxygen supplied by nitrate may be compatible with the arsI enzyme(Chen et al., 2021). It is also possible that microbes could have utilized the added nitrate to oxidize Fe(II) to Fe(III) in autotrophic denitrification (Tian et al., 2020), however, dissolved Fe data (Fig. 27) do not show evidence of less dissolved Fe in the presence of nitrate addition.

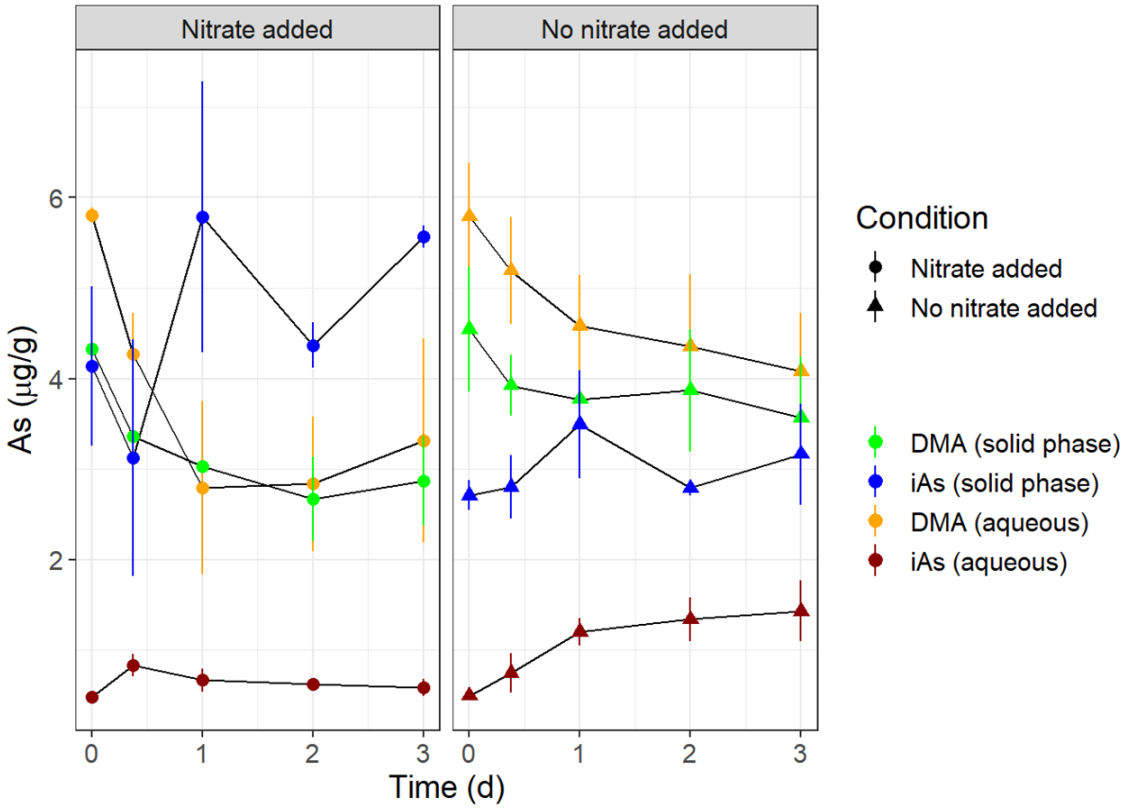

Figure 30. Aqueous and solid-phase DMA and iAs in nitrate experiments. Error bars represent standard deviation of triplicates.

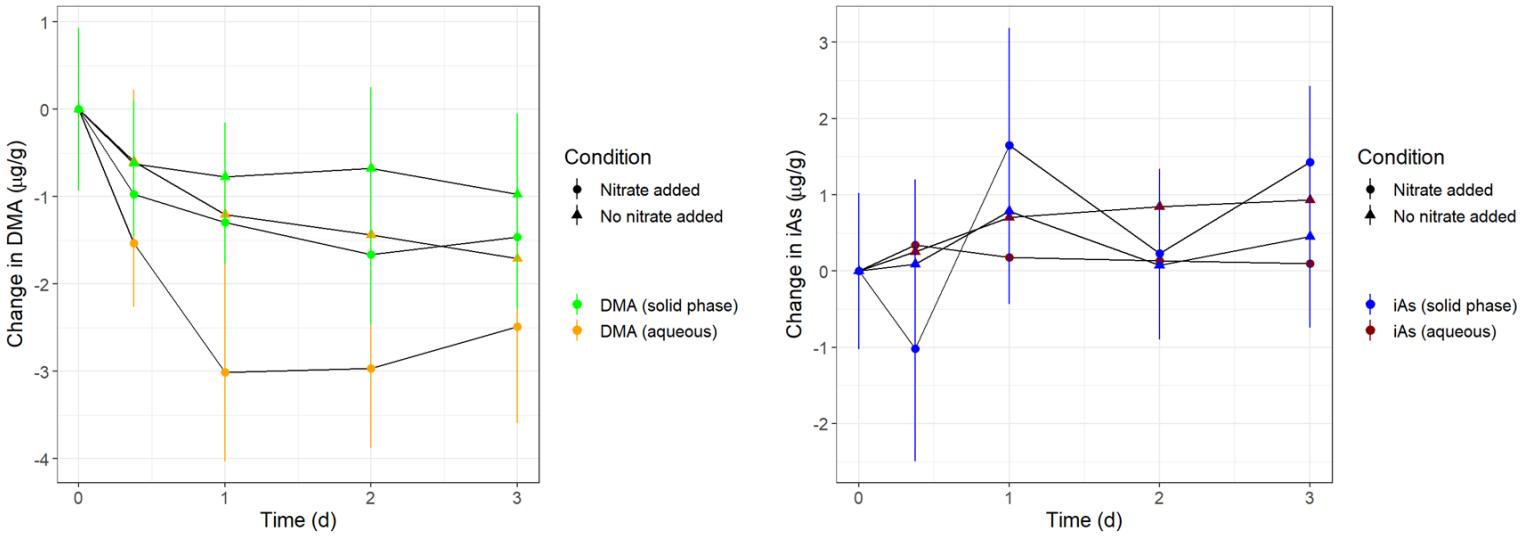

Figure 31. Change in As species over time in nitrate experiments. Error bars represent standard deviation of triplicates.

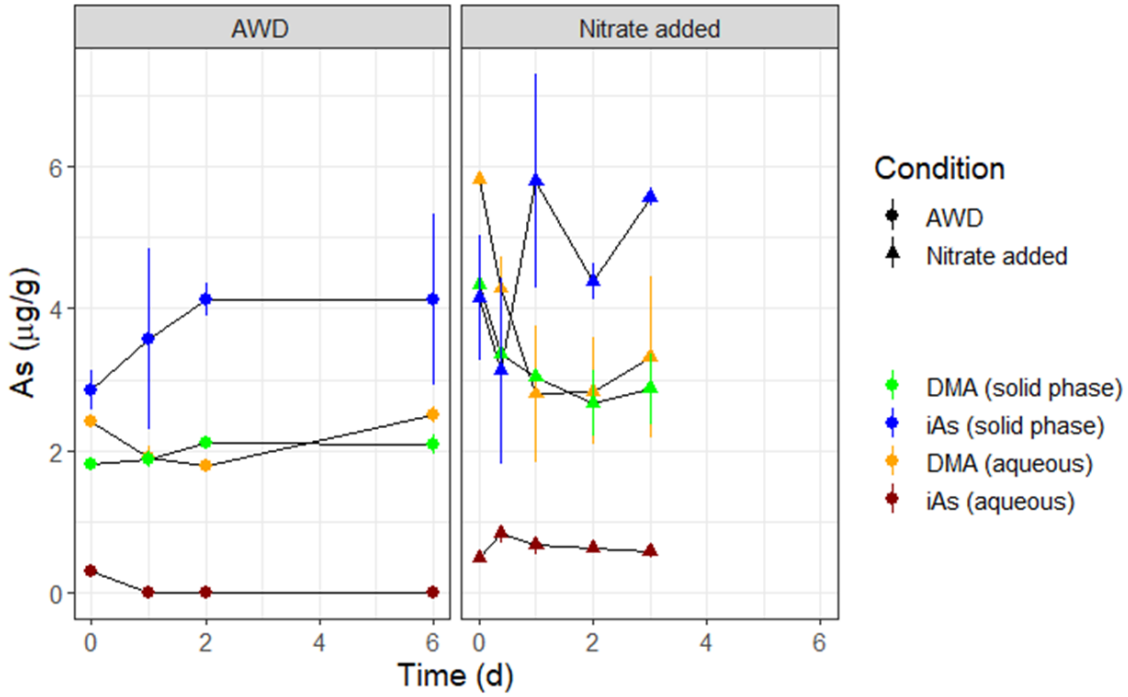

Figure 32. As speciation changes after introduction of oxygen (left) and nitrate (right). Error bars represent standard deviation of triplicates.

Conclusion

Demethylation has been linked to molecular oxygen-dependent and nitrate-dependent processes (Yoshinaga et al., 2011; Chen et al., 2021), but these mechanisms have not studied separately in the same system. In the context of AWD in rice paddies, it is unclear which of these oxygen sources is associated with decreases in pore water DMA concentration and grain DMA content. We expanded on the work of previous studies by examining both the aqueous and solid phases; an AAO extraction and subsequent speciation of As allowed us to quantify all As in our systems. Additionally, while other studies have chosen MMA as the starting species for demethylation (Yoshinaga et al., 2011; Yoshinaga and Rosen, 2014; Chen et al., 2021), we chose DMA which is more

relevant for rice-growing environments (Zavala et al., 2008). In the microcosm experiment, we found that AWD introduces nitrate to the pore water, indicating that both sources of oxygen were present. In our batch study, the oxygen coming from nitrate is having a more clear effect on the reduction of DMA mass in the system. There is a clear decrease in DMA mass concurrent with an increase in iAs mass (Fig. 30). This is incongruent with prior work that characterized the arsI enzyme as a dioxygenase that requires molecular oxygen to cleave the As-C bond between As and a methyl group (Yoshinaga and Rosen, 2014). More research is needed on the versatility of the arsI enzyme. Sierra-Alvarez (2006) identified MMA as the product of DMA demethylation (Sierra-Alvarez et al., 2006), however MMA was not observed in the aqueous phase and very little was produced in our experiments. It is possible that MMA was a transient intermediate species that underwent subsequent demethylation to iAs. Huang et al. 2007 also observed DMA conversion to iAs in the form of As(V) in soil extracts (Huang et al., 2007). Future work including microbial community analysis of similar experiences and genomics techniques for abundances of denitrification genes would support the link between demethylation and denitrification.

REFERENCES FOR CHAPTER 4

(1) Jomova, K.; Jenisova, Z.; Feszterova, M.; Baros, S.; Liska, J.; Hudecova, D.; Rhodes, C. J.; Valko, M. *J. Appl. Toxicol.* **2011**, *31* (2), 95–107.

(2) Smedley, P. L.; Kinniburgh, D. G. **2002**, *17*, 517–568.

(3) Miller, W. H.; Schipper, H. M.; Lee, J. S.; Singer, J.; Waxman, S. *Cancer Res.* **2002**, *62* (14), 3893–3903.

(4) Schoof, R. A.; Yost, L. J.; Eickhoff, J.; Crecelius, E. A.; Cragin, D. W.; Meacher, D. M.; Menzel, D. B. *Food Chem. Toxicol.* **1999**, *37* (8), 839–846.

(5) Li, G.; Sun, G. X.; Williams, P. N.; Nunes, L.; Zhu, Y. G. *Environ. Int.* **2011**, *37* (7), 1219–1225.

(6) Nunes, L. M.; Li, G.; Chen, W. Q.; Meharg, A. A.; O'Connor, P.; Zhu, Y. G. *Environ. Sci. Technol.* **2021**.

(7) Davis, M. A.; Signes-Pastor, A. J.; Argos, M.; Slaughter, F.; Pendergrast, C.; Punshon, T.; Gossai, A.; Ahsan, H.; Karagas, M. R. *Sci. Total Environ.* **2017**, *586*, 1237–1244.

(8) Rawson, J.; Prommer, H.; Siade, A.; Carr, J.; Berg, M.; Davis, J. A.; Fendorf, S. *Environ. Sci. Technol.* **2016**, *50* (5), 2459–2467.

(9) Roberts, L. C.; Hug, S. J.; Dittmar, J.; Voegelin, A.; Kretzschmar, R.; Wehrli, B.; Cirpka, O. A.; Saha, G. C.; Ali, M. A.; Badruzzaman, A. B. M. *Nat. Geosci.* **2009**, *3* (1), 53–59.

(10) Reinsch, B. C.; Lowry, G. V; Erbs, J. J.; Berquo, T. S.; Banerjee, S. K.; Penn, R. L. *Geochim. Cosmochim. Acta* **2010**, *74*, 3382–3395.

(11) US Food and Drug Administration. **2020**, *6* (August), 1–9.

(12) Marin, A. R.; Masscheleyn, P. H.; Jr, W. H. P. **1992**, No. V, 175–183.

(13) Seyfferth, A. L.; McCurdy, S.; Schaefer, M. V.; Fendorf, S. *Environ. Sci. Technol.* **2014**, *48* (9), 4699–4706.

(14) LaHue, G. T.; Chaney, R. L.; Adviento-Borbe, M. A.; Linquist, B. A. *Agric. Ecosyst. Environ.* **2016**, *229*, 30–39.

(15) Linquist, B. A.; Anders, M. M.; Adviento-Borbe, M. A. A.; Chaney, R. L.; Nalley, L. L.; da Rosa, E. F. F.; van Kessel, C. *Glob. Chang. Biol.* **2015**, *21* (1), 407–417.

(16) Li, C.; Carrijo, D. R.; Nakayama, Y.; Linquist, B. A.; Green, P. G.; Parikh, S. J. *Agric. Ecosyst. Environ.* **2019**, *272* (November 2018), 188–198.

(17) Yang, J.; Zhou, Q.; Zhang, J. *Crop J.* **2017**, *5* (2), 151–158.

(18) Maguffin, S. C.; Abu-Ali, L.; Tappero, R. V.; Pena, J.; Rohila, J. S.; McClung, A. M.; Reid, M. C. *Geochim. Cosmochim. Acta* **2020**, *276*, 50–69.

(19) Masscheleyn, P. H.; Delaune, R. D.; Patrick, W. H. *Environ. Sci. Technol.* **1991**, *25* (8), 1414–1419.

(20) Lomax, C.; Liu, W. J.; Wu, L.; Xue, K.; Xiong, J.; Zhou, J.; McGrath, S. P.; Meharg, A. A.; Miller, A. J.; Zhao, F. J. *New Phytol.* **2012**, *193* (3), 665–672.

(21) Li, J.; Pawitwar, S. S.; Rosen, B. P. *Metallomics* **2016**, *8* (10), 1047–1055.

(22) Wells, B. R.; Gilmour, J. T. *Agron. J.* **1977**, *69* (3), 451–454.

(23) Tang, Z.; Wang, Y.; Gao, A.; Ji, Y.; Yang, B.; Wang, P.; Tang, Z.; Zhao, F. J. *J. Exp. Bot.* **2020**, *71* (18), 5631–5644.

(24) Gebel, T. W. *Int. J. Hyg. Environ. Health* **2002**, *205* (6), 505–508.

(25) Chen, C.; Li, L.; Huang, K.; Zhang, J.; Xie, W. Y.; Lu, Y.; Dong, X.; Zhao, F. J. *ISME J.* **2019**, *13* (10), 2523–2535.

(26) Zhang, X.; Reid, M. C. *Sci. Total Environ.* **2021**, No. xxxx, 151696.

(27) Chen, C.; Shen, Y.; Li, Y.; Zhang, W.; Zhao, F. J. *Environ. Sci. Technol.* **2021**, *55* (22), 15484–15494.

(28) Yoshinaga, M.; Cai, Y.; Rosen, B. P. *Environ. Microbiol.* **2011**, *13* (5), 1205–1215.

(29) Huang, J. H.; Scherr, F.; Matzner, E. *Water. Air. Soil Pollut.* **2007**, *182* (1–4), 31–41.

(30) Yoshinaga, M.; Rosen, B. P. *Proc. Natl. Acad. Sci. U. S. A.* **2014**, *111* (21), 7701–7706.

(31) Carrijo, D. R.; Li, C.; Parikh, S. J.; Linquist, B. A. *Sci. Total Environ.* **2019**, *649*, 300–307.

(32) Lafferty, B. J.; Loeppert, R. H. *Environ. Sci. Technol.* **2005**, *39* (7), 2120–2127.

(33) Burton, E. D.; Johnston, S. G.; Kocar, B. D. *Environ. Sci. Technol.* **2014**, *48* (23), 13660–13667.

(34) Wolthers, M.; Charlet, L.; van Der Weijden, C. H.; van der Linde, P. R.; Rickard, D. *Geochim. Cosmochim. Acta* **2005**, *69* (14), 3483–3492.

(35) Huang, H.; Jia, Y.; Sun, G.; Zhu, Y. **2012**.

(36) Tian, T.; Zhou, K.; Xuan, L.; Zhang, J. X.; Li, Y. S.; Liu, D. F.; Yu, H. Q. *Water Res.* **2020**, *170*, 115300.

(37) Sierra-Alvarez, R.; Yenal, U.; Feld, J. A.; Kopplin, M.; Gandolfi, A. J.; Garbarino, J. R. *J. Agric. Food Chem.* **2006**, *54* (11), 3959–3966.

CHAPTER 5: Conclusion

Management of agricultural systems to minimize the amount of Arsenic (As) that enters the food supply via rice remains a priority in the United States and across the globe. Public health concerns have brought the topic of heavy metals in foods to the attention of lawmakers, who notably, have made recent regulation changes to lower the acceptable limit of As in rice infant food cereals. Management practices have also impacted farmers on a national level, who are focused on the optimization of crops production while managing temperature change, water supply, and resources related to climate change. Strategies such as AWD and genetic modification of rice cultivars are currently in development but have not been optimized for universal adoption. Agencies, such as the United States Department of Agriculture (USDA), rely heavily on high impact research that investigates underexplored aspects of As biogeochemistry in rice paddies for novel advancements and critical understanding of impacted agricultural systems.

This work examined controls on As bioavailability from two angles: organic matter interactions and redox fluctuations. DOM can be considerably abundant in the reducing pore waters of flooded rice paddies, and common agricultural practices aimed at managing plant waste and recycling nutrients contribute to this observation. Due to the immense amount of leftover plant material left behind after rice grains are harvested, a common management technique is to burn fields post-harvest to re-incorporate the husks, leaves and stems back into the soil as organic matter. This practice maintains high DOM during the growing season. While As-organic matter interactions have been previously studied, they have been largely dismissed as insignificant, despite theoretical support for As-DOM complexation. The redox-related controls on As bioavailability are centered on AWD,

which has been proven to reduce rice grain As experimentally, but standard guidelines regarding timing, frequency, and severity that are scientifically sound and compatible with rice growers have not yet been developed. While many producers are cautious to adopt newly developed strategies that may reduce their yields, climate change-induced water supply shortages are pushing grows to conserve water, which is an important benefit of AWD. Additionally, the cooperation of biogeochemists and plant biologists is necessary to couple the knowledge of soil chemistry with plant physiology to engineer resilient cropping systems.

This dissertation seeks to accurately characterize both organic matter and redox controls on As fate in wetland environments, by considering the complex chemical, mineralogical, and biological processes that occur in rice paddy soils.

The first research chapter (1) carefully characterizes both commercially-available and environmentally-sourced DOMs, (2) quantifies binding of As(III) to these DOMs, and (3) evaluates the bioavailability of DOM-complexed As(III) to microbes using a whole-cell microbial biosensor. Extraction and characterization of DOMs using practical wet chemical techniques enabled us to make environmentally-relevant interpretations. The continued study of environmental DOM sources is essential to understand the complexation chemistry that occurs in the environment. The results of dialysis equilibrium experiments demonstrated that As(III)-DOM complexation was significant and highly correlated with the organic sulfur content of DOM, especially at low As:DOC ratios commonly observed in wetland soils. The completely anoxic handling of the DOMs throughout the experimental process enabled these observations by preserving the oxygen-sensitive organic sulfur moieties, a novel outcome of this study. Quantifying organic sulfur

can be quite challenging due to limitations in sulfur speciation techniques. Future work could build on the wet chemical techniques used to quantify OrgS by analyzing carefully-prepared DOM samples for sulfur XANES to estimate the proportion of multiple sulfur species. Sulfur XANES can be challenging to perform due to the anoxic preparation required, small hutch size which requires thorough flushing with inert gases, and low total mass of S in DOM samples. However, previous studies have showed S XANES to be feasible. Combing this technique with As XANES and XAFS could provide a complete picture of the speciation and coordination of complexed As and offer mechanistic proof of an As-OrgS association. Our result with freeze-dried Aldrich Humic Acid mixed with an As (III) solution offers preliminary evidence for this important finding.

The second research chapter examines an applied, field-scale study of rice As management through AWD and cultivar selection. Field plots were prepared and maintained in 2017 and 2018, providing a comparison for two years of experimental data in the same location. Importantly, there was some interannual variability detected in the trace metal and micronutrient content of rice grains in the same cultivars planted in the same conditions, emphasizing the importance of climatological impacts on rice agriculture. The results of pore water monitoring revealed that AWD has a significant effect on some redox-sensitive elements such as Fe and As but has an insignificant effect on micronutrient concentrations. Although some small reductions in iAs were observed, AWD was found to reduce total As in rice grains primarily through the reduction of DMA, which introduces new questions with regards to As speciation in rice paddies. Linear Mixed-Effects Modeling identified both cultivar and number of drains as important controls on the trace metal and micronutrient content of rice, and in our study, the effect of variety was often

more influential than the effect of drains. This result underscores the need for an understanding of the genetic and physiological differences between rice cultivars, such as the transporters for translocating elements to the rice grain. This will inform selection of favorable genetic traits for breeding rice that is resistant to As, able to withstand the dry conditions of AWD, and rich in the important nutrients required in the human diet.

The final research chapter builds directly on the second research chapter and the finding that AWD has a more significant effect on reducing DMA than iAs. The roles of both molecular oxygen and nitrate on As demethylation and speciation in rice paddy soils were investigated through experiments at the microcosm and benchtop scale. Soil microcosms constructed to emulate paddy soils were maintained under both continuously-flooded and AWD conditions, and the AWD dry-down was found to decrease As concentration, alter As speciation, and introduce high levels of nitrate to the pore water. Batch reactors maintained to simulate both the introduction of oxygen and nitrate in soil slurries disaggregated the effects of this electron acceptors on observed changes in As speciation. The results of the batch experiments support the idea that demethylation may be nitrate-dependent, with implications for the versatility of the arsI enzyme. Follow-up experiments with analysis of the microbial community and special attention to the presence of denitrification genes and activity will push the ideas in this study forward and strengthen the important link between As biogeochemistry and the nitrogen cycle.

In summary, this work addresses the overarching goal of understanding As bioavailability to grow healthier rice and protect human health. Both traditional and developing techniques were employed at a variety of physical scales. These research

chapters contain strong motivation for a multidisciplinary effort to understand dynamic wetland ecosystems and improve rice agriculture.

APPENDIX A: SUPPLEMENTARY MATERIAL FOR CHAPTER 2

Additional Materials and Methods

Growth Media for Biosensor

The growth media prepared in Milli-Q water was composed of 0.46 g/L glycerol, 4.18 g/L MOPS buffer, 1.17 g/L NaCl, 1.49 g/L KCl, 4.23 g/L $(NH_4)_2SO_4$, 0.31 g/L beta-glycerophosphate, 2.41 mg/L $MgSO_4$, and 0.02 g/L LB broth, Lennox. The 1:100 amino acids valine, L-Leucine, L-isoluecine and 1:1000 trace metals were added before adding 120 μg/mL ampicillin. Sterile solutions of each chemical were added after filtration with 0.22 μm membrane filters, except for the trace metals solution which was autoclaved at 121°C for 20 min. Beta-glycerophosate, MOPS, $MgSO_4$, and all amino acids were purchased from Alfa Aesar (Ward Hill, MA), VWR international (Radnor, PA), MilliporeSigma (Burlington, MA), and Acros Organics (Morris Plains, NJ), respectively. All other chemicals were purchased from Fisher Scientific Co. (Pittsburgh, PA).

Additional Figures and Tables

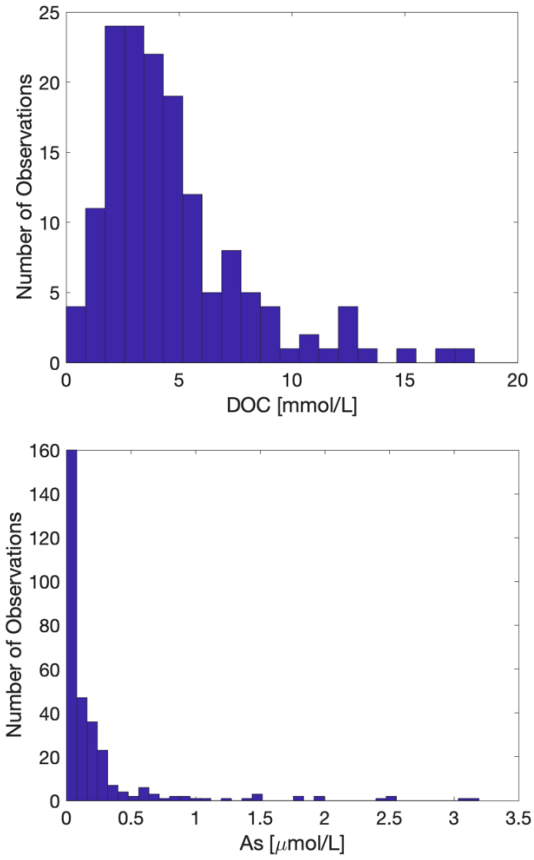

Figure S1: Distributions of DOC and As concentrations observed in rice paddy pore water in Maguffin et al (2020)[1]. The median and mean As/DOC ratios were 0.017 and 0.041 µmol As/mmol C, respectively

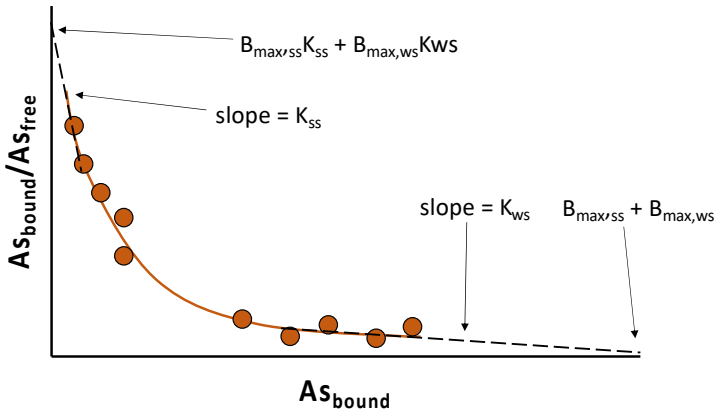

Figure S2: : Illustration of parameter estimation from Scatchard plot analysis. Modified from Figure 18.15 in Brezonik and Arnold (2011)[2]. Parameters are defined in the main manuscript text.[3]

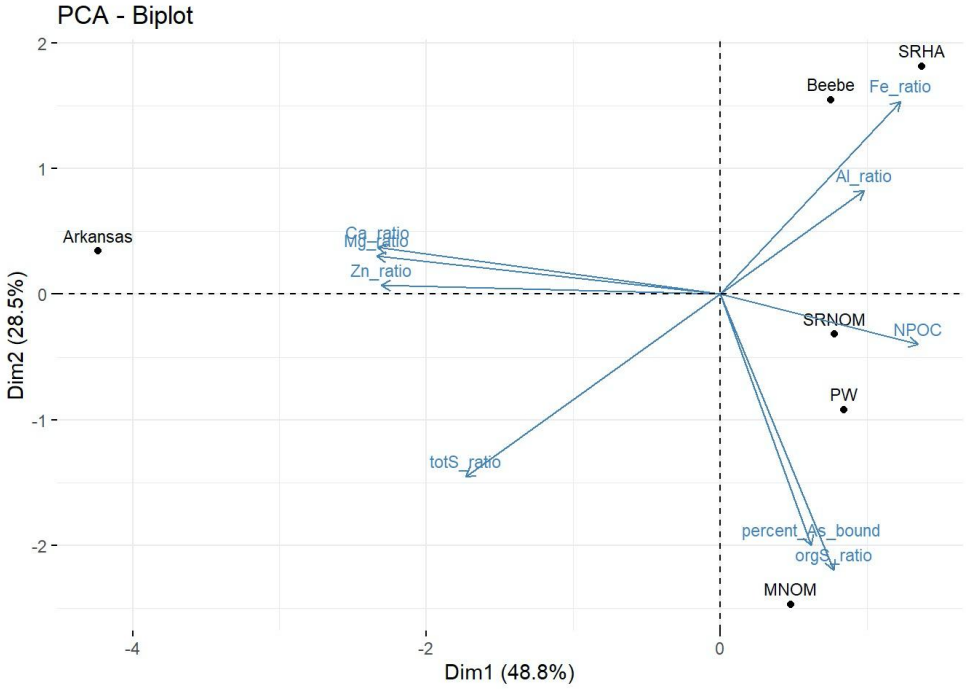

Figure S3: Principal Component Analysis (PCA) of the DOMs used in this study. Each point represents a single type of DOM. SW-1 was excluded from this PCA. Biplot vectors are overlaid according to the weight each characteristic influences each PC.

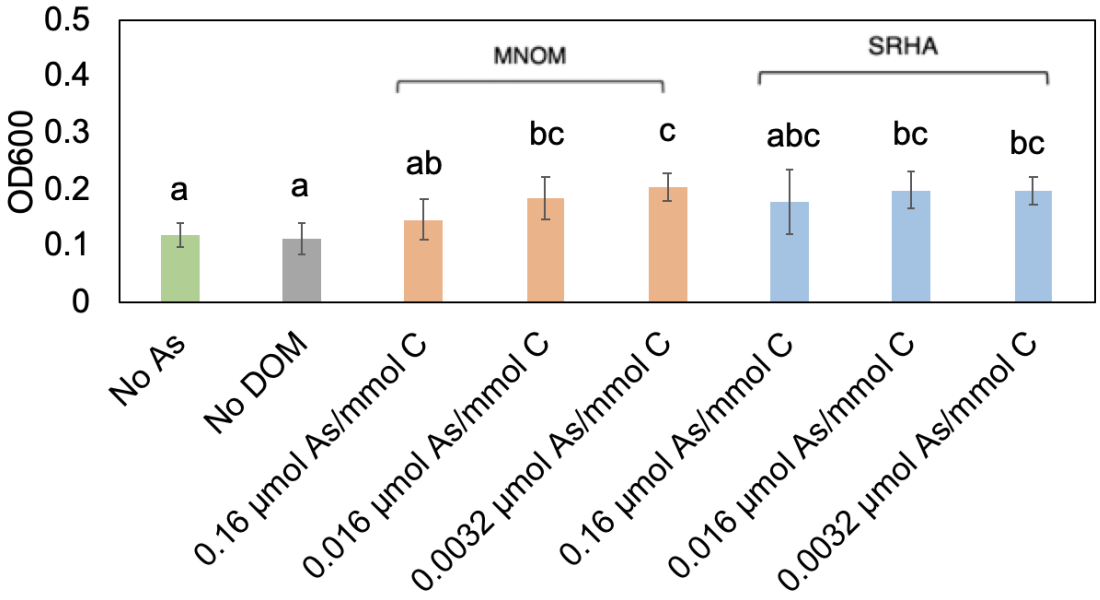

Figure S4: Optical Densities of the *E. coli* biosensor in different experimental conditions.

Table S1: Summary of As/DOC ratios in the soil solution from a review of As-DOM interactions. Modified from Table 2 in Aftabtalab et al. (2022).

DOC (mg/L)	DOC (mmol/L)	As (ug/L)	As (µmol/L)	As/DOC (µmol/mmol C)
3057	254.8	21.7	2.89E-01	1.14E-03
5509	459.1	118.4	1.58E+00	3.44E-03
230	19.2	6.4	8.53E-02	4.45E-03
119	9.9	3.8	5.07E-02	5.11E-03
2799	233.3	120.5	1.61E+00	6.89E-03
230	19.2	32.8	4.37E-01	2.28E-02
46.6	3.9	15.9	2.12E-01	5.46E-02
400	33.3	300	4.00E+00	1.20E-01
33	2.8	36	4.80E-01	1.75E-01
148	12.3	358	4.77E+00	3.87E-01
15	1.3	50.3	6.71E-01	5.37E-01
12.5	1.0	110	1.47E+00	1.41E+00
10.2	0.9	98.4	1.31E+00	1.54E+00
62.4	5.2	667.7	8.90E+00	1.71E+00
40	3.3	467	6.23E+00	1.87E+00
8.2	0.7	123	1.64E+00	2.40E+00

References

1. Maguffin, S. C.; Abu-Ali, L.; Tappero, R. V.; Pena, J.; Rohila, J. S.; McClung, A. M.; Reid, M. C., Influence of manganese abundances on iron and arsenic solubility in rice paddy soils. *Geochimica et Cosmochimica Acta* **2020,** *276*, 50-69.

2. Brezonik, P.; Arnold, W., *Water chemistry: an introduction to the chemistry of natural and engineered aquatic systems*. OUP USA: 2011.

3. Aftabtalab, A.; Rinklebe, J.; Shaheen, S. M.; Niazi, N. K.; Moreno-Jiménez, E.; Schaller, J.; Knorr, K.-H., Review on the interactions of arsenic, iron (oxy)(hydr) oxides, and dissolved organic matter in soils, sediments, and groundwater in a ternary system. *Chemosphere* **2022,** *286*, 131790.

APPENDIX B: SUPPLEMENTARY MATERIAL FOR CHAPTER 3

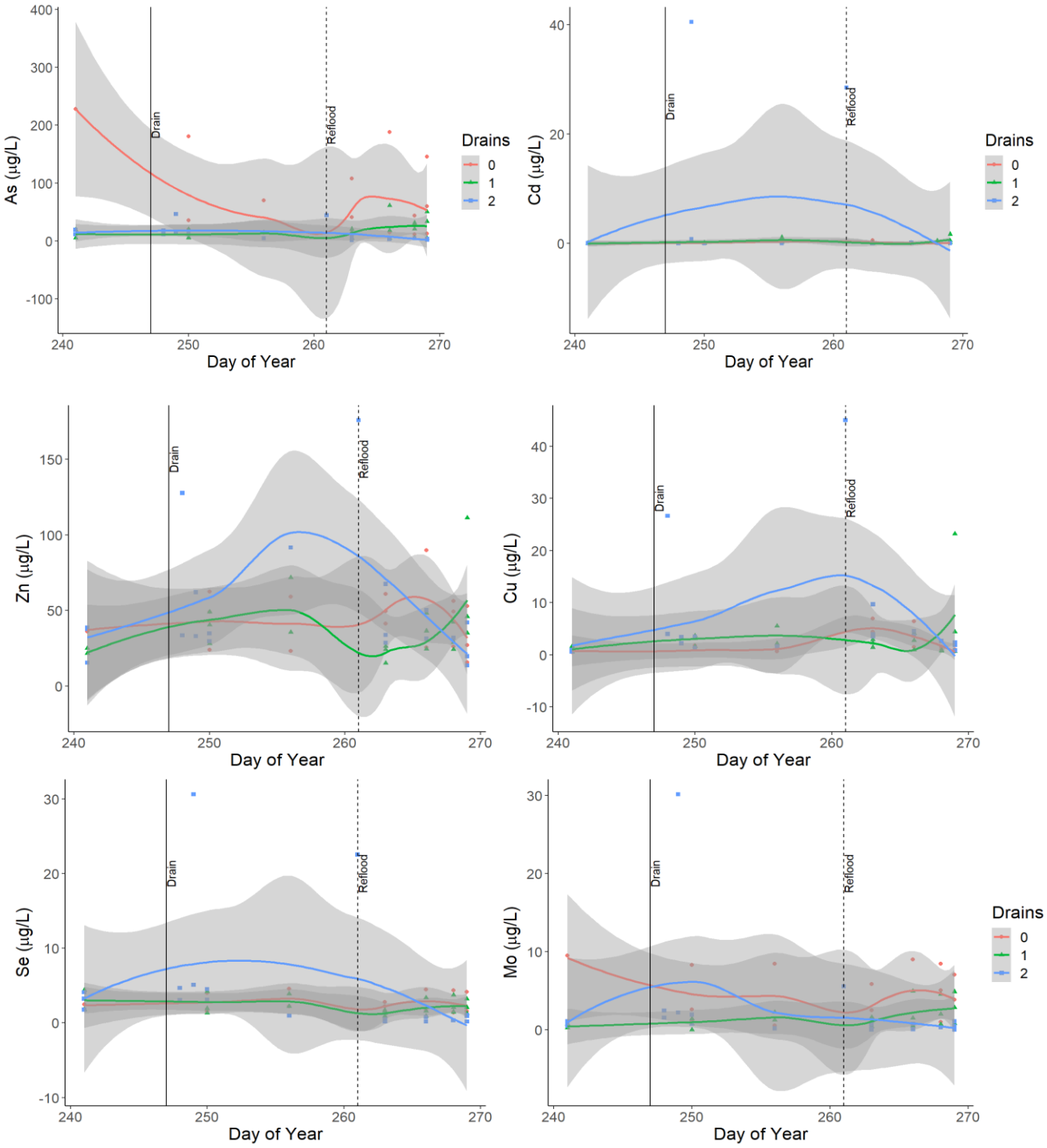

Figure S5: Pore water concentrations of As, Cd, Zn, Cu, Se, and Mo in the 2-drain rice paddy field in 2018. Lines represent a smooth model fit, and gray shades areas represent

95% confidence intervals. Solid and dotted lines represent the drain and reflood days, respectively.

APPENDIX C: SUPPLEMENTARY MATERIAL FOR CHAPTER 4

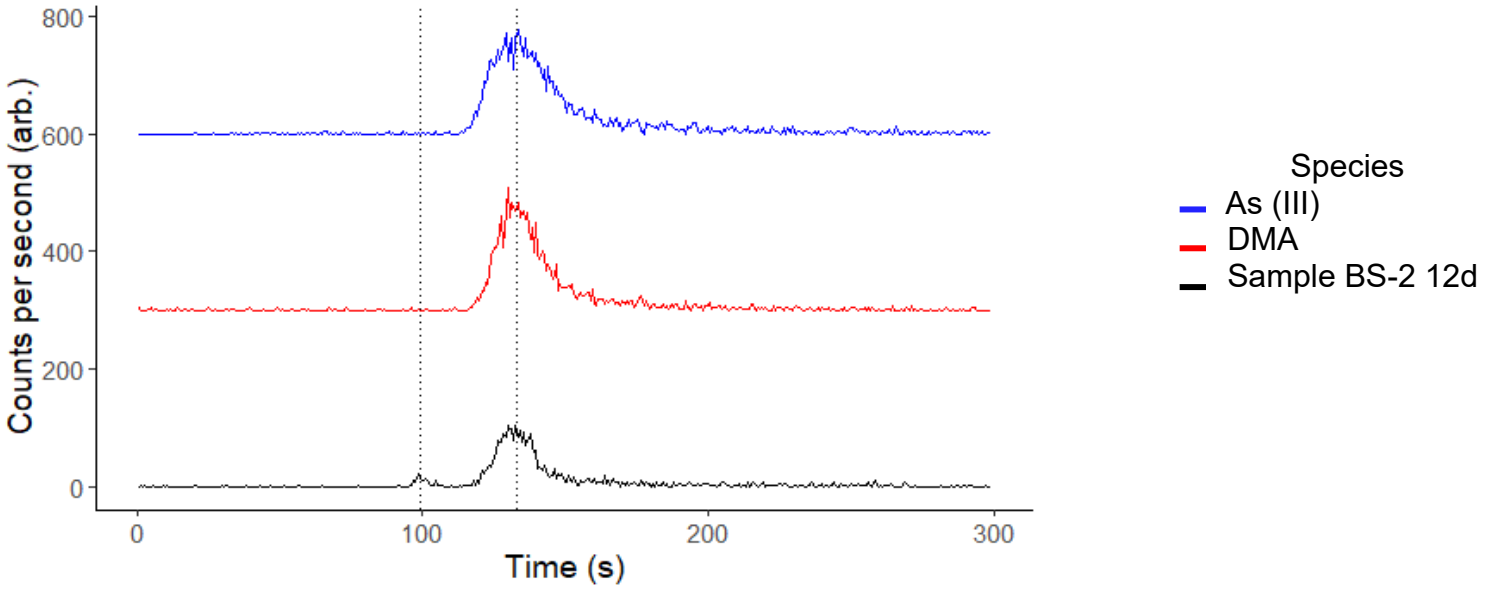

Figure S6: Chromatograms of unoxidized As(III) and DMA standards overlaid with sample BD-2 12d. Dotted lines show the peaks of the unidentified As species (~100 s) and As(III)/DMA (~135 s).